

UM-HSRI-81-19-4

STEERING AND SUSPENSION SYSTEMS

C.B. Winkler
P.S. Fancher

DESCRIPTIVE PARAMETERS USED IN ANALYZING THE BRAKING
AND HANDLING OF HEAVY TRUCKS

Volume 4

October 1981

Technical Report Documentation Page

1. Report No. UM-HSRI-81-19-4		2. Government Accession No.		3. Recipient's Catalog No.	
4. Title and Subtitle DESCRIPTIVE PARAMETERS USED IN ANALYZING THE BRAKING AND HANDLING OF HEAVY TRUCKS Steering and Suspension Systems - Vol. 4				5. Report Date October 1981	
				6. Performing Organization Code 361912	
7. Author(s) C.B. Winkler and P.S. Fancher				8. Performing Organization Report No. UM-HSRI-81-19-4	
9. Performing Organization Name and Address Highway Safety Research Institute The University of Michigan Huron Parkway & Baxter Road Ann Arbor, Michigan 48109				10. Work Unit No.	
				11. Contract or Grant No. MVMA Proj. 1196	
12. Sponsoring Agency Name and Address Motor Vehicle Manufacturers Association 300 New Center Building Detroit, Michigan 48202				13. Type of Report and Period Covered Final 7/1/78 - 4/15/81	
				14. Sponsoring Agency Code	
15. Supplementary Notes					
16. Abstract This volume is one of a set of five volumes being prepared under support from the Motor Vehicle Manufacturers Association. The set of volumes is entitled "Descriptive Parameters Used in Analyzing the Braking and Handling of Heavy Trucks." The volumes address the acquisition of data on (1) brakes, (2) inertial properties, (3) tires, (4) steering and suspension systems, and (5) antilock systems.					
17. Key Words Steering Systems, Suspension Systems, Inertial Properties, Tires, Brakes, Antilock Systems, Heavy Trucks				18. Distribution Statement UNLIMITED	
19. Security Classif. (of this report) NONE		20. Security Classif. (of this page) NONE		21. No. of Pages	22. Price

INTRODUCTION

The purpose of this volume is to provide a source of information concerning the mechanical properties of the steering and suspension systems employed on heavy trucks. The development of HSRI's current capabilities for measuring steering and suspension system properties was completed in a research project entitled "A Survey of Tandem Suspension Properties," sponsored by the Motor Vehicle Manufacturers Association (MVMA). In addition, a fixture for measuring the mechanical properties of leaf springs was developed in another study sponsored by MVMA. Test results obtained using both of the devices developed in these MVMA studies are presented in this document.

At the conclusion of these MVMA projects, the results presented in the progress reports were incorporated into two SAE papers (Numbers 800905 and 800906) entitled "Measurement and Representation of the Mechanical Properties of Truck Leaf Springs" and "A Test Facility for the Measurement of Heavy Vehicle Suspension Parameters." These SAE papers contain the best available descriptions of the test devices and their use. Also, pertinent data sets are included in these papers. Hence, copies of these papers have been included here.*

It is worth noting that spring characteristics (along with other parametric data) are obtained in the tests performed on the suspension test facility. Nevertheless, the leaf spring test device is useful if only the spring and not the entire suspension is available for testing. Furthermore, the spring tester is capable of stroking springs at frequencies up to 15 Hz, while the suspension test facility is essentially a quasi-static device. However, the frictional characteristics of typical leaf springs do not depend upon stroking frequency for frequencies less than 15 Hz (a finding demonstrated by using the leaf spring test fixture). Hence, the results from the suspension test facility are perfectly adequate for

*Additional copies of these papers are available from SAE as indicated in the enclosed papers.

characterizing the forces developed by leaf springs during braking and steering maneuvers.

The remainder of this volume contains three sources of data: (1) SAE Paper 800905 on leaf springs, (2) SAE Paper 800906 on the measurement of suspension parameters, and (3) additional sets of data on various suspensions as measured using the suspension test facility. The additional data sets (Item (3) above) are presented in the same format as that used in SAE Paper 800906. As more suspensions are studied using these same techniques, the resulting measurements may be appended directly to the data presented here.

SAE Technical Paper Series

800905

**Measurement and
Representation of the
Mechanical Properties of
Truck Leaf Springs**

**P.S. Fancher,
R.D. Ervin,
C.C. MacAdam, and
C.B. Winkler**

Highway Safety Research Institute
The Univ. of Michigan

**West Coast International Meeting
Los Angeles, California
August 11-14, 1980**



SOCIETY OF AUTOMOTIVE ENGINEERS, INC.
400 COMMONWEALTH DRIVE
WARRENDALE, PENNSYLVANIA 15096

The appearance of the code at the bottom of the first page of this paper indicates SAE's consent that copies of the paper may be made for personal or internal use, or for the personal or internal use of specific clients. This consent is given on the condition, however, that the copier pay the stated per article copy fee through the Copyright Clearance Center, Inc., Operations Center, P.O. Box 765, Schenectady, N.Y. 12301, for copying beyond that permitted by Sections 107 or 108 of the U.S. Copyright Law. This consent does not extend to other kinds of copying such as copying for general distribution, for advertising or promotional purposes, for creating new collective works, or for resale.

Papers published prior to 1978 may also be copied at a per paper fee of \$2.50 under the above stated conditions.

SAE routinely stocks printed papers for a period of three years following date of publication. Direct your orders to SAE Order Department.

To obtain quantity reprint rates, permission to reprint a technical paper or permission to use copyrighted SAE publications in other works, contact the SAE Publications Division.

Measurement and Representation of the Mechanical Properties of Truck Leaf Springs

P.S. Fancher,
R.D. Ervin,
C.C. MacAdam, and
C.B. Winkler

Highway Safety Research Institute
The Univ. of Michigan

THE PURPOSE OF THIS PAPER is to present findings from a research investigation into the force-versus-deflection characteristics of the leaf springs employed in commercial vehicle suspension systems.

Detailed knowledge of the mechanical properties of leaf springs is needed for analyzing the ride, braking, and directional performance of heavy vehicles. Prior to the research described herein, suspension tests have been employed in determining spring rate and friction parameters for use in vehicle dynamics simulations (1)*. Results from low frequency (quasi-static) tests of typical tandem suspensions have indicated that truck leaf springs are complicated force-producing mechanisms which may exhibit varying levels of (a) effective spring rate and (b) damping, coulomb friction, or hysteresis, depending upon the loading of the

spring and the amplitude of the oscillation studied (2). In essence, leaf springs are non-linear devices that dissipate energy during each cycle of oscillation. The objectives of the research reported herein have been to (1) measure the force-producing characteristics of several different types of leaf springs while exercising these springs at various amplitudes and frequencies of oscillation about nominal loading conditions and (2) develop means for representing the force-deflection characteristics of leaf springs in a form suitable for use in digital calculations (simulations) of the dynamic performance of commercial vehicles.

*Numbers in parentheses designate References at end of paper.

ABSTRACT

The force-versus-deflection properties of truck leaf springs are studied with respect to the influences of motion amplitude and frequency (0 to 15 Hz) upon hysteretic damping and effective spring rate. Presented test results indicate that the energy loss per cycle of motion of a leaf spring is independent of the frequency of cycling. Measurements showing the influence

of the amplitude of stroking are analyzed for five representative examples of currently employed leaf springs. A mathematical method for representing the force-versus-deflection characteristics of leaf springs is presented in a form suitable for use in digital simulations of vehicle dynamics.

TEST DEVICE

Figure 1 is a photograph of the test device used for measuring the static and dynamic properties of truck leaf springs. Each spring, including its associated shackle, slipper, torque rod, frame fastening hardware, etc., is mounted to the slotted layout plate shown in Figure 1. The versatility of the layout plate, permitting mounting of a great variety of

spring assemblies, is shown in the test arrangements of Figures 2 through 6.

The test apparatus loads the spring specimen using both air springs and a servo-controlled hydraulic actuator. The air springs provide for the preload (the nominal static load condition) while the servo actuator is devoted to the variation of load about the static value. By this scheme, a relatively small hydraulic device can be applied to the

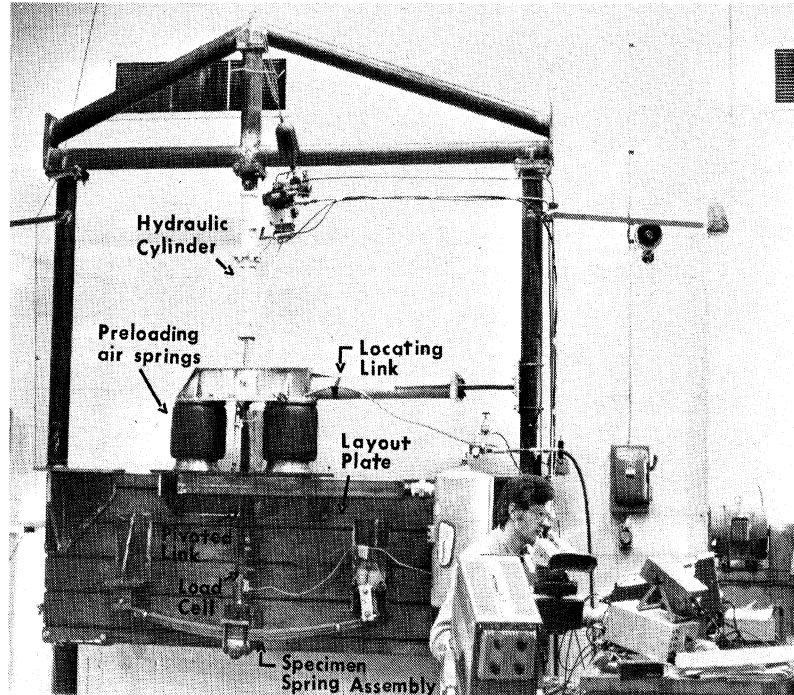


Fig. 1 - A device for measuring the mechanical properties of leaf springs

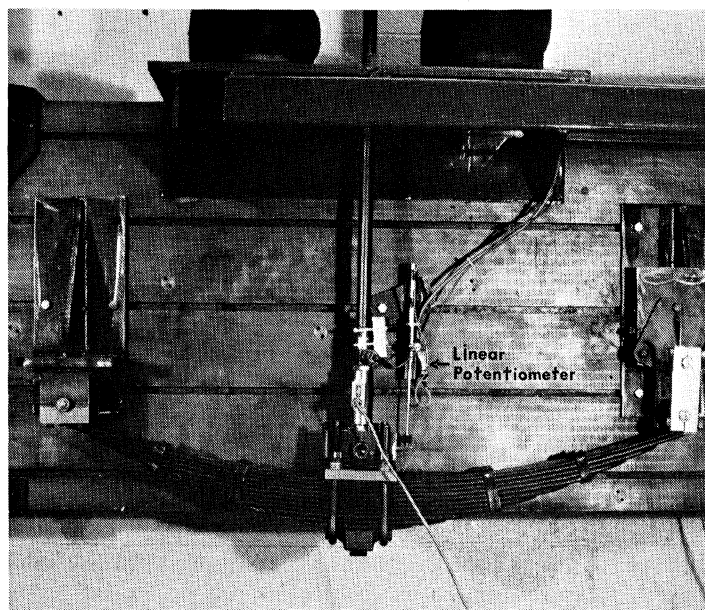


Fig. 2 - Multi-leaf spring, 12,000-lb axle rating

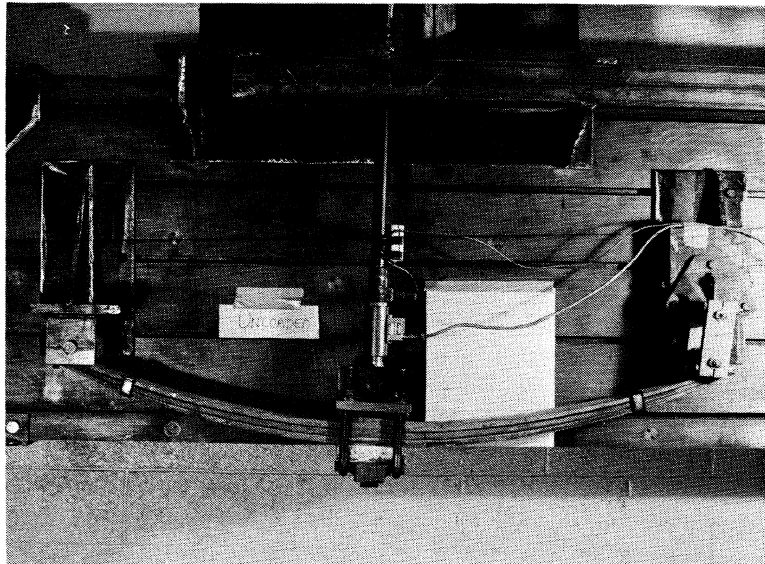


Fig. 3 - Tapered-leaf front spring, 12,000-lb axle rating

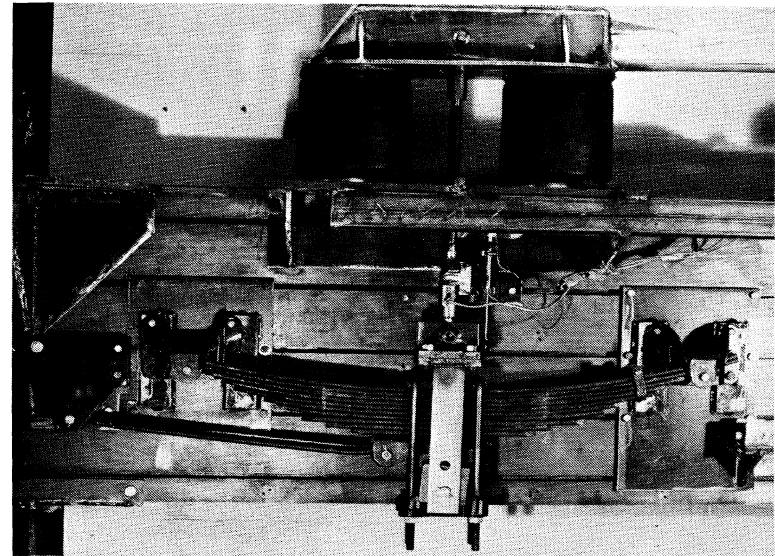


Fig. 4 - Multi-leaf rear spring with torque rod, 23,000-lb axle rating

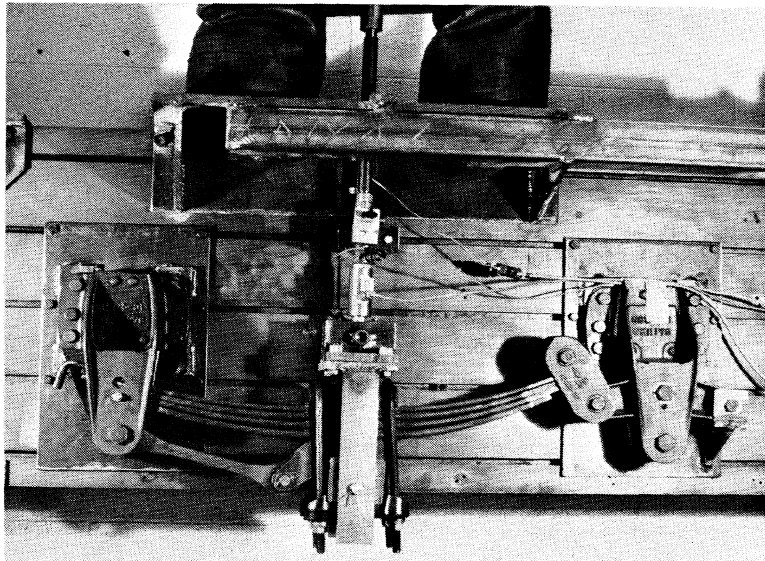


Fig. 5 - One spring from a four-spring suspension with torque rods

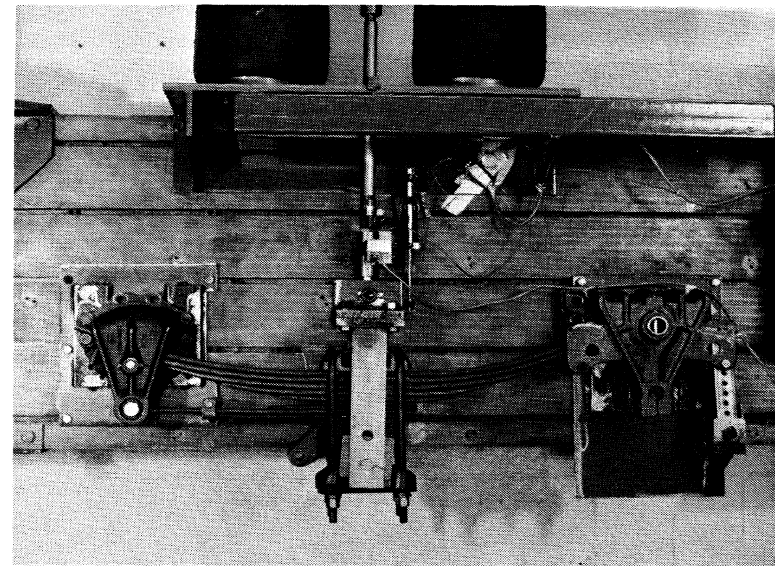


Fig. 6 - One spring from a four-spring suspension with torque leaves

dynamic investigation while the air springs permit attainment of full deflection travel of the springs.

The load is applied to the spring through a pivoted link which incorporates the load transducer. The spring is not kinematically constrained by this link, however, but rather is located fully by the elements comprising the actual spring constraints on a vehicle.

TEST PROCEDURES

In general, the procedure for testing a given spring consists of the following basic steps:

1. The necessary fixtures for mounting the spring in the test device are fabricated. As nearly as possible, the geometric location of the spring components is as in service.

2. The spring is stroked at various frequencies and amplitudes for each of two nominal static load conditions. The force-versus-displacement characteristics of the spring are then recorded while stroking about each static position. (A linear potentiometer is used to measure displacement of the spring with respect to its fixed mounts. See Figure 2.)

During preliminary testing in the study reported here, it was found that the "effective mass," M_e , of the spring will noticeably distort the force results at relatively high stroking accelerations. To correct for this mass effect, an accelerometer was used, measuring the acceleration, \ddot{z} , of the mid-point of the spring to permit the generation of an analog signal ($M_e\ddot{z}$). The effective mass of each spring was estimated using the weight of the total spring and clamping assembly and an adjustment which accounted for the distribution of deflection along the spring length according to an approximated mode shape. The ($M_e\ddot{z}$) signal was then subtracted from the total stroking force to produce a force deriving only from the elastic and frictional properties of the spring.

Shown in Figure 7 is an overlay of force-deflection loops representing (a) the composite force signal, including the mass effect at 15 Hz and (b) the simpler loop comprising only the elastic and damping components of the response signal. The "removal" of the inertial force component, $M_e\ddot{z}$, is rationalized with regard to the mathematical modeling of vehicles since the "effective mass" itself would be distributed between the sprung and unsprung mass elements of the vehicle. Thus, subtraction of the $M_e\ddot{z}$ component in the subject tests yields a spring characterization which applies directly to the definitions of component functions typically used in vehicle simulations.

RESULTS FOR REPRESENTATIVE LEAF SPRINGS

The spring testing device was used to measure the force-deflection properties of five

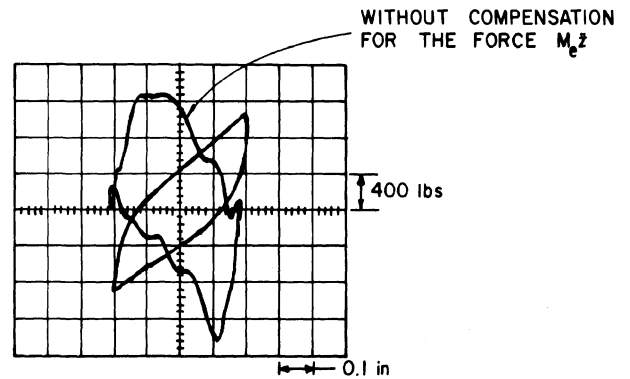


Fig. 7 - Influence of the inertial force

springs selected to be representative of a variety of applications. The springs tested were:

1. multi-leaf front spring (12,000 lb axle rating) (Fig. 2)
2. tapered leaf front spring (12,000 lb axle rating) (Fig. 3)
3. multi-leaf rear spring with torque rod (23,000 lb axle rating) (Fig. 4)
4. one spring from a four-spring suspension with torque rods and, also, incorporating shackle connections at the equalizer link and slipper connections at the opposing ends of each spring (Fig. 5)
5. one spring from a four-spring suspension with torque leaves (Fig. 6)

Figure 8 is an X-Y plot of force versus displacement for a 12,000-lb multi-leaf front spring. This plot is made at very low stroking rates (at which mass effects are negligible) and shows the overall envelope of the spring characteristics plus several small amplitude stroking cycles about three operating points. These data essentially define the damping and spring characteristics needed to represent the force-displacement characteristics of this spring. (Data defining the force versus displacement properties of the other four springs are presented in Appendix A.)

The data presented in Figure 8 derive from a low frequency (quasi-static) exercise over the operating range of the spring. To investigate changes in force-deflection characteristics caused by increasing the stroking frequencies, an oscilloscope and polaroid camera arrangement was used to record data at stroking frequencies of 0.5, 3, 6, 10, and 15 Hz. Typical recorded data for small amplitude (0.1-inch) stroking of the 12,000-lb multi-leaf front spring are presented in Figures 9a, b, c, and d. In these figures, the hysteresis loop obtained in one cycle at 0.5 Hz is superimposed upon the data obtained in one cycle at each of 3, 6, 10, and 15 Hz frequencies, respectively.

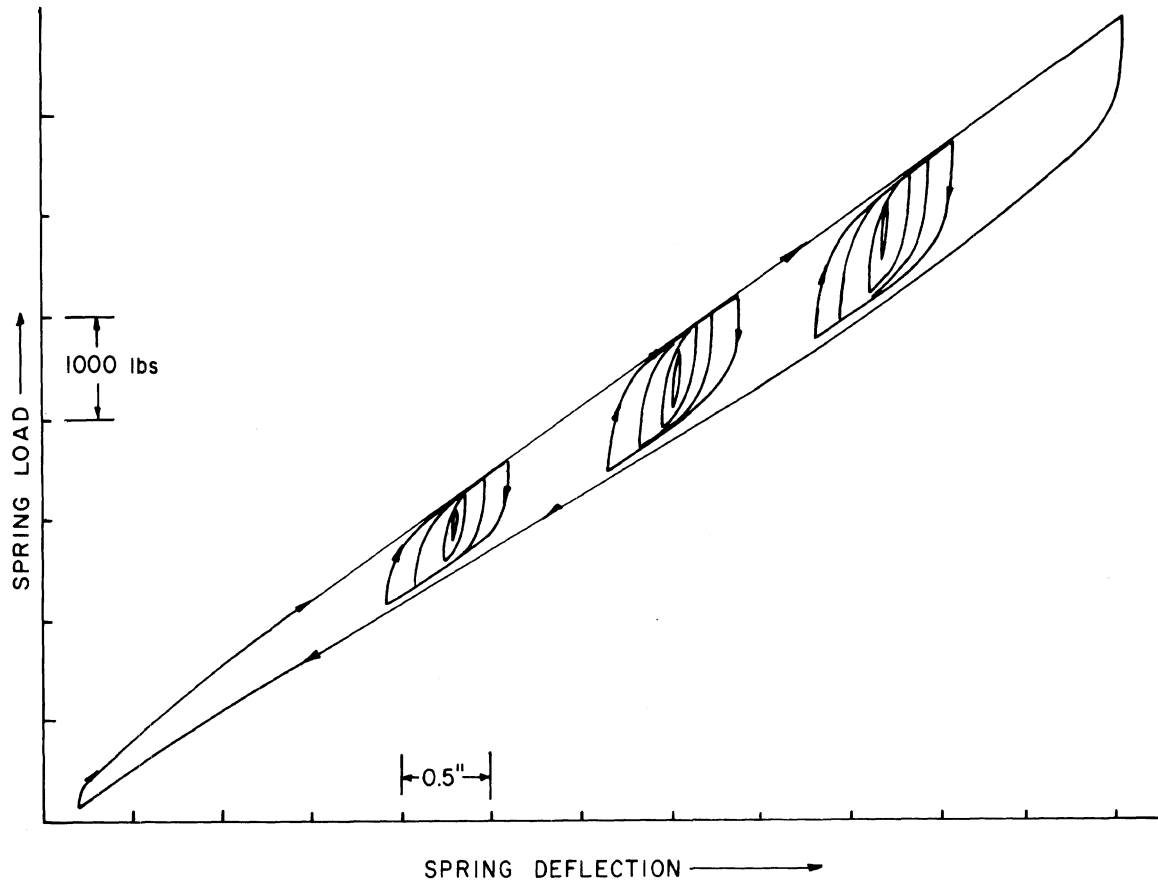


Fig. 8 - Multi-leaf front spring

Examination of Figures 9a through 9d indicates that the quasi-static force-deflection behavior, such as at 0.5 Hz, constitutes a good representation of the average or "smoothed" behavior up to 15 Hz. (The higher frequency "noise" seen superimposed on the 6, 10 and 15 Hz data in Figure 9 is presumed to derive from structural vibrations of the test machine.)

Data for larger amplitudes of stroking and for all five springs were gathered in this research program. Appendix B presents data for each of the five springs operated at two nominal loads. These data support a basic conclusion of this research, namely, that the force-producing properties of leaf springs are independent of frequency for oscillations occurring in the range from 0 to approximately 15 Hz.

Although the characteristics of these springs are not frequency-dependent, the data presented in Figure 8 and Appendix A clearly indicate that the force-deflection properties of truck leaf springs depend upon both the amplitude of motion and the nominal load. In order to quantify the effects of amplitude and nominal load, specialized definitions of an "average coulomb damping force, C_F " and an "effective spring rate, K_e " have been developed.

The average damping force, C_F , is based on the energy dissipated in a cycle of stroking

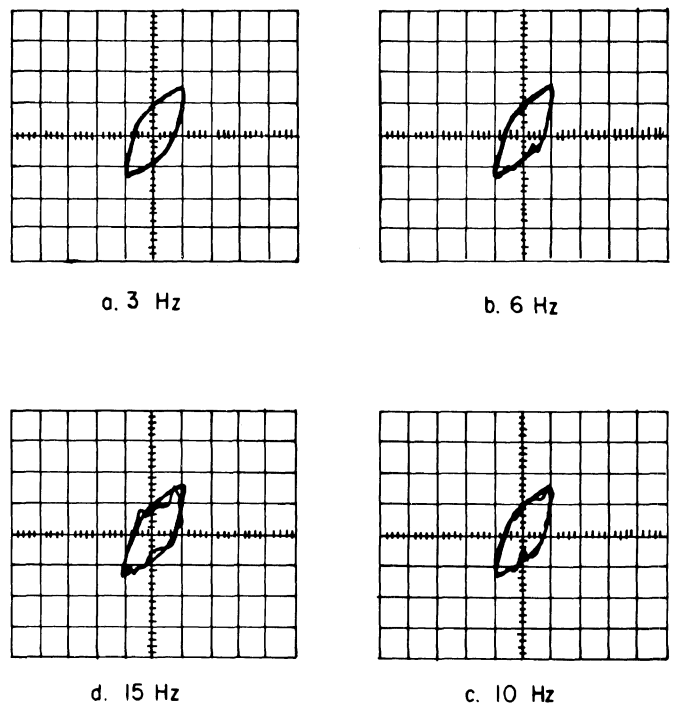


Fig. 9 - 12,000-lb multi-leaf front spring
 Nominal load: 4000 lb; Amplitude: 0.1 in (0.2 in peak to peak); Scales: vertical - 400 lb/large div., horizontal - 0.1 in/large div.

the spring. The total energy dissipated in a cycle is equal to the area, A , enclosed within the hysteresis loop generated in a plot of force versus displacement (see Fig. 10). A measure of the average damping force is determined by dividing the area of the hysteresis loop by the total spring motion during one cycle of stroking, viz., referring to Figure 10,

$$C_F = \frac{A}{4\delta}$$

where

δ = amplitude of the spring deflection
(peak-to-peak amplitude is 2δ)

For example, the area of the hysteresis loop shown in Figure 10 is determined by graphical integration to be approximately 268 in-lb (30 Nm) and the spring deflection amplitude, δ , is 0.2 in (0.5 cm). Accordingly, $C_F = 268/0.8 = 335$ lbs (1490 N).

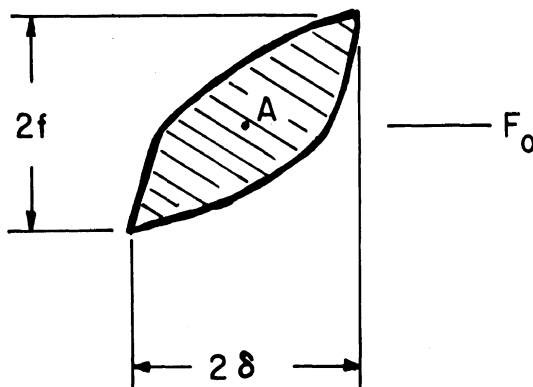
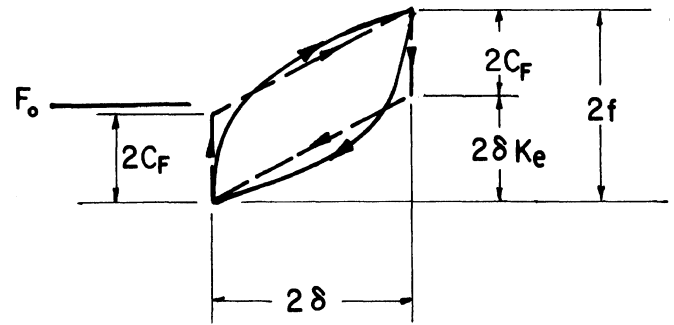


Fig. 10 - Hysteresis loop measurements for one cycle of stroking

Once the coulomb damping has been determined, the effective spring rate, K_e , can be estimated using the method illustrated in Figure 11. This method ensures that the approximation to the hysteresis loop (shown in the dashed line in Figure 11) will cover the same range of forces and deflections as the measured data.

In summary, the parameters C_F and K_e define an approximating hysteresis loop that (1) has the same energy dissipation per cycle as the leaf spring and (2) has the same amplitudes of force and deflection as the measured hysteresis loop.

Table 1 presents results for each of the five springs from tests at two nominal loads and three amplitudes of deflection. For each test condition, defined by a nominal load, F_0 , and a deflection amplitude, δ , the force amplitude, f , and the area, A , of the hysteresis loop are measured from the recorded data. The parameters C_F and K_e are then computed using the formulas shown in Figure 11.



$$A = (2C_F)(2\delta) \quad \text{or} \quad C_F = \frac{A}{4\delta}$$

$$2f = 2C_F + 2\delta K_e$$

$$\text{or} \\ K_e = \left(\frac{2f - 2C_F}{2\delta} \right)$$

Fig. 11 - Estimation of the effective spring rate (approximating hysteresis loop superimposed on the measured data)

The results recorded in Table 1 indicate that the coulomb friction, C_F , increases in magnitude as either nominal load or deflection amplitude is increased. Examination of the overall spring characteristics, as shown in Figure 8 and Appendix A, makes apparent that the average damping force (coulomb friction) should increase with increasing load or deflection, because hysteresis loops at either higher nominal load or greater deflection amplitude will have larger areas than hysteresis loops at smaller nominal loads or deflection amplitudes. The influence of nominal load on the value of coulomb friction depends upon the rate at which the upper and lower boundaries of the envelope of spring characteristics separate with increasing load. Clearly, widely separated boundaries of the envelope yield relatively large values of the parameter C_F .

The results presented in Table 1 indicate that the effective spring rate decreases as deflection amplitude increases. This "inverse" trend of K_e is necessary for the approximating hysteresis loop to have both the same force amplitude and area as the measured data.

The trends in C_F and K_e suggest that, for small amplitude oscillations, the higher prevailing value of spring rate and lower damping will favor the development of higher frequency, lightly damped resonances in the vehicle. In contrast, when oscillations develop at larger amplitudes, the lower prevailing spring rate and higher damping level will facilitate lower frequency and more heavily damped motions.

Figure 12 provides graphical comparisons between the effective spring rates for the two

Table 1

	Test Conditions		Direct Measurements		Computed Parameters	
	F _o lb.	δ in.	f lbs.	A lb-in	C _F lbs.	K _e lbs/in.
See Fig. 3	4000	.1	360	29.63	74	2860
	4000	.2	530	113.6	142	1940
	4000	.4	800	292.6	183	1543
	6000	.1	420	27.16	68	3520
	6000	.2	640	126.85	159	2405
	6000	.4	920	372.4	233	1718
See Fig. 2	4000	.1	580	108.52	271	3090
	4000	.2	720	267.7	335	1925
	4000	.4	942	567.2	355	1468
	6000	.1	730	132.1	330	4000
	6000	.2	920	320.9	401	2595
	6000	.4	1180	720	450	1825
See Fig. 5	1500	.05	350	14.03	70	5600
	1500	.1	625	44	110	5150
	1500	.2	1080	104.8	131	4745
	6000	.05	700	45.84	229	9420
	6000	.1	1020	102.9	257	7630
	6000	.2	1515	252.5	316	5995
See Fig. 4	2000	.05	365	29.43	147	4360
	2000	.1	515	74.06	185	3300
	2000	.2	730	170.2	213	2585
	6000	.05	585	50.91	255	6600
	6000	.1	835	140.2	351	4840
	6000	.2	1200	304.6	381	4095
See Fig. 6	2000	.05	580	59.08	295	5700
	2000	.1	800	151.4	379	4210
	2000	.2	1050	310.4	388	3310
	6000	.05	860	77.76	389	9420
	6000	.1	1200	202.6	507	6930
	6000	.2	1700	527.6	660	5200

Note: 1 lb ≡ 4.448 N.
1 in ≡ 2.54 cm.

front springs studied in this research investigation. As shown, these springs are very similar in effective spring rate at various loads and deflection amplitudes. The major difference between these springs for deflections in the range from 0 to 0.4 in occurs in the average damping per cycle. The results show that the multi-leaf spring dissipates almost twice as much energy as the taper leaf spring does under comparable conditions.

The two springs from different four-spring tandem suspensions are compared in Figure 13. The effective spring rates for these two springs are approximately equivalent, but, as in the case of the two front springs, these rear springs differ considerably in average damping per cycle.

The amount of damping per cycle that is best for a particular application is, of course, a total vehicle and roadway system problem,

depending upon factors such as resonances in the vehicle structure, tire and wheel imbalances, and the roughness of the road. In addition, spring characteristics can play an important role in analyzing vehicle performance in braking and/or handling maneuvers. Since the analysis of the test results has shown that leaf springs have rather unique force-deflection characteristics, a model of these springs suitable for representing their characteristics over wide ranges of loading, deflection amplitude, and random (or non-uniform) reversals of velocity is needed for use in generalized studies of vehicle dynamics. Accordingly, Equation (1) below has been devised to represent the characteristics of leaf springs (3):

$$F_i = F_{ENV_i} + \left(F_{i-1} - F_{ENV_i} \right) e^{-|\delta_i - \delta_{i-1}|/\beta} \quad (1)$$

where

- F_i is the suspension force at the current simulation time step
- F_{i-1} is the suspension force at the last simulation time step
- δ_i is the suspension deflection at the current simulation time step
- δ_{i-1} is the suspension deflection at the last simulation time step
- F_{ENV i} is the force corresponding to the upper and lower boundaries of the envelope of the measured spring characteristics at the deflection, δ_i.

and β is an input parameter used for describing the rate at which the suspension force within a hysteresis loop approaches the outer boundary of the envelope, F_{ENV}. Different values of β for increasing versus decreasing deflection may be specified.

For use in digital calculations (simulations), the upper and lower boundaries of the envelope of spring characteristics are entered into the computer code as functions (tables) of spring deflection. The "deflection constants," β, in the exponential term in Equation (1) are determined from test results. The deflection constants are selected so that the mathematical representation will closely match measured hysteresis loops. For example, the envelope of the multi-leaf front spring may be approximated by the following equations:

$$\text{For } \delta_i > \delta_{i-1} \\ F_{ENV} = 1300 \delta + 300 \quad , \quad \text{lbs}$$

$$\text{For } \delta_i < \delta_{i-1} \\ F_{ENV} = 1100 \delta - 100 \quad , \quad \text{lbs}$$

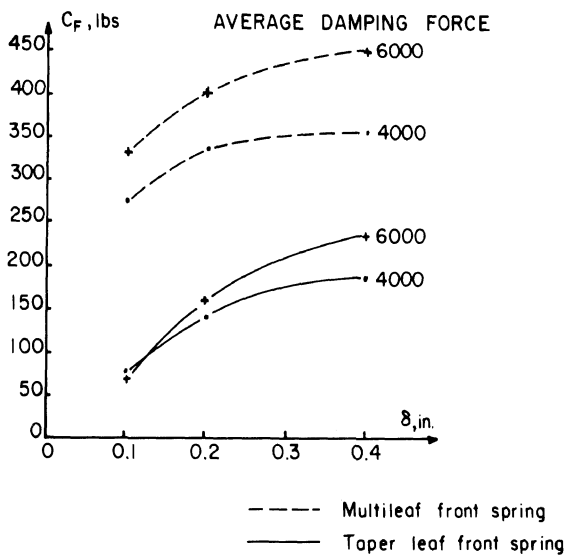


Fig. 12 - Comparison of two front springs

And the deflection constants chosen for this spring are (1) for $\delta_i > \delta_{i-1}$, $\beta = 0.080$ in and (2) for $\delta_i < \delta_{i-1}$, $\beta = 0.076$ in. Figure 14 shows the correspondence between the mathematical representation and the measured data for this spring.

Other springs, such as the rear springs, have variable rates requiring nonlinear functions or tables for representing their envelopes. Appendix C contains numerical results for the envelopes and deflection constants for each of the springs studied in this investigation.

Experience has shown that the exponential form used in Equation (1) does an excellent job of matching test results. Nevertheless, other mathematical functions could be used if necessary to represent a particular spring.

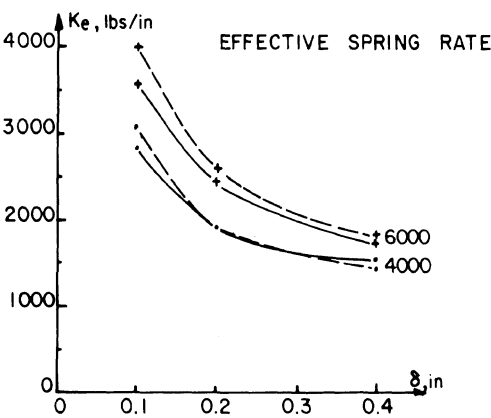


Fig. 13 - Comparison of two rear springs from comparable four-spring tandem suspensions

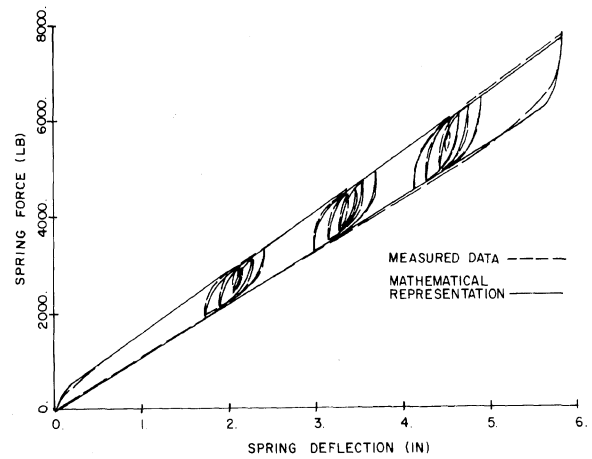


Fig. 14 - Comparison between measured and calculated results

SUMMARY AND CONCLUSIONS

The force-deflection characteristics of leaf springs have been investigated in order to provide a detailed understanding of the influences of (1) the frequency of stroking, (2) the amplitude of stroking, and (3) the nominal static load on the spring rate and energy dissipation properties of truck leaf springs. Measurements of five commercially available leaf springs were made at five frequencies of stroking (0.5, 3.0, 6.0, 10.0, and 15.0 Hz) for three amplitudes of stroking at two static loads. The test results indicate that (1) the frequency of stroking over the range from 0 to 15 Hz has no influence on the spring rate and energy dissipation properties of truck leaf springs and (2) truck leaf springs are highly nonlinear devices for which (a) the average damping force in a cycle of stroking increases with increases in either the amplitude of stroking or the nominal static load

and (b) the effective spring rate decreases if either the amplitude of stroking is increased or the nominal static load is decreased.

Since truck leaf springs are complicated nonlinear devices, involving hysteretic damping, their representation in detailed analyses of vehicle dynamics studies of ride, braking, or handling is not easily accomplished using linear approximations or simplified models. Accordingly, a mathematical method for representing the force-deflection properties of truck leaf springs has been presented and discussed herein.

REFERENCES

1. R.W. Murphy, J.E. Bernard, and C.B. Winkler, "A Computer-Based Mathematical Method for Predicting the Braking Performance of Trucks and Tractor-Trailers." Phase I Report:

Motor Truck Braking and Handling Performance Study, Highway Safety Research Institute, University of Michigan, Ann Arbor, September 15, 1972.

2. P.S. Fancher, Jr., "Pitching and Bouncing Dynamics Excited During Antilock Braking of a Heavy Truck." Proceedings, 5th VSD-2nd IUTAM Symposium, Vienna, Austria, September 19-23, 1977, pp. 203-221.

3. C.C. MacAdam, "Computer Simulation and Parameter Sensitivity Study of a Commercial Vehicle During Antiskid Braking." 6th VSD-3rd IUTAM Symposium, Berlin, Germany, September 1979.

APPENDIX A

Figures A-1 through A-4 plus Figure 8 illustrate the overall force versus deflection characteristics of the leaf springs examined in this research investigation.

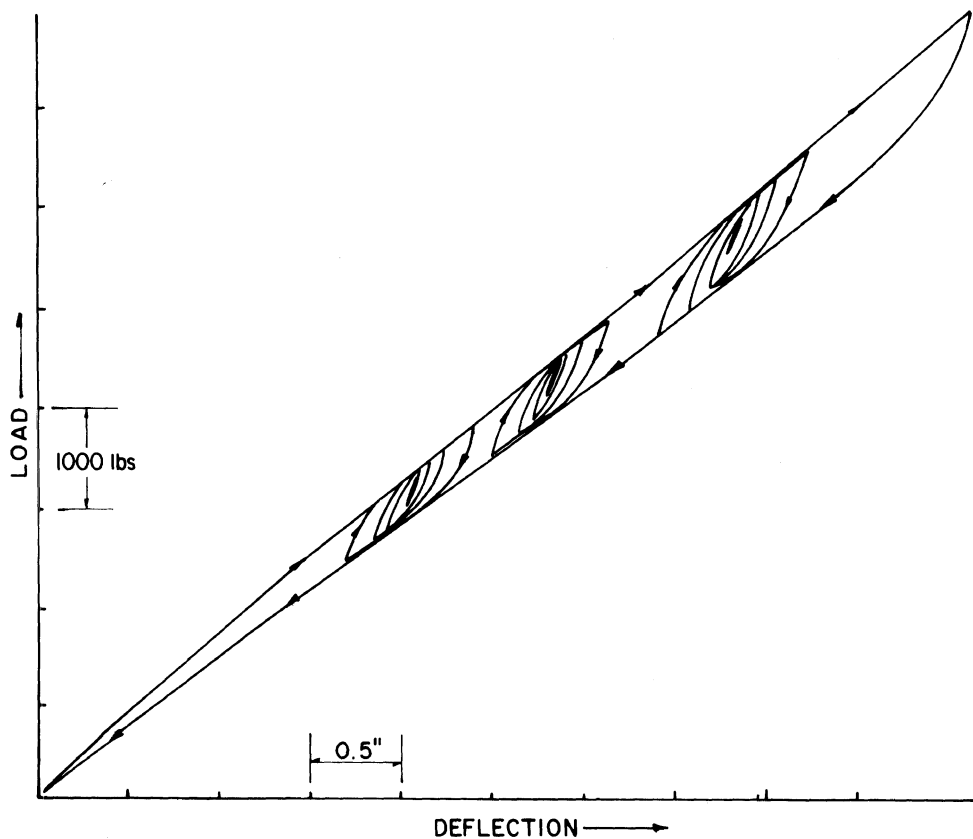


Fig. A-1 - Tapered-leaf front spring

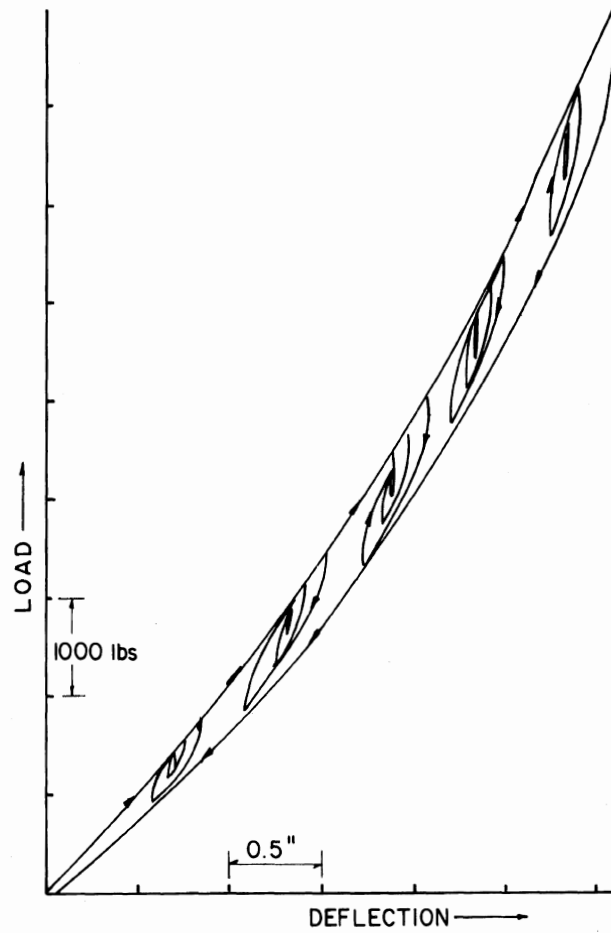


Fig. A-2 - Multi-leaf rear spring (see Fig. 4)

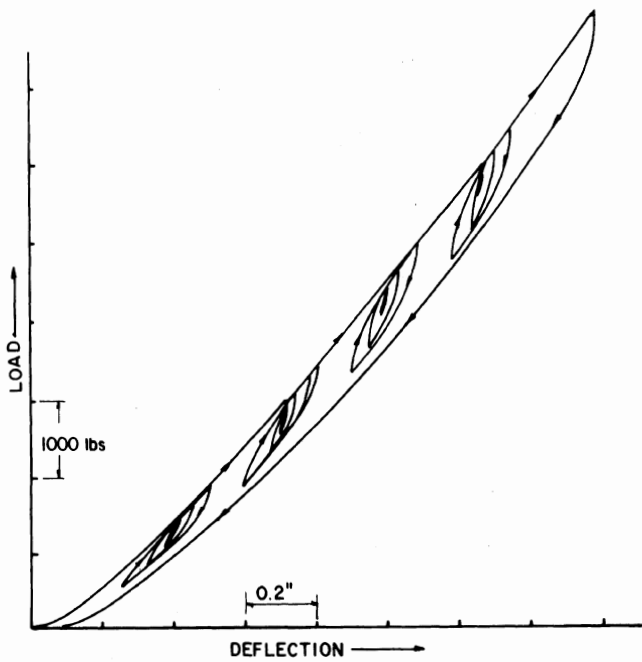


Fig. A-3 - One spring from a four-spring suspension with torque rods (see Fig. 5)

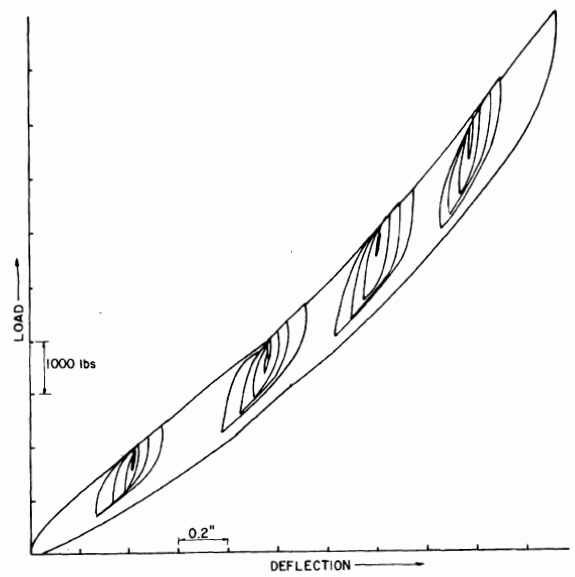


Fig. A-4 - One spring from a four-spring suspension with torque leaves (see Fig. 6)

APPENDIX B

The figures in this appendix (B-1 through B-5) provide comparisons between test results obtained at 0.5 and 6.0 Hz. Four sets of data (at two amplitudes of deflection and two nominal loads) are presented for each of the springs

tested. Although the data measured at 6.0 Hz contain high frequency fluctuations, examination of the data presented in this appendix indicates that the force-deflection characteristics measured at 6.0 Hz are practically the same as the results obtained at 0.5 Hz.

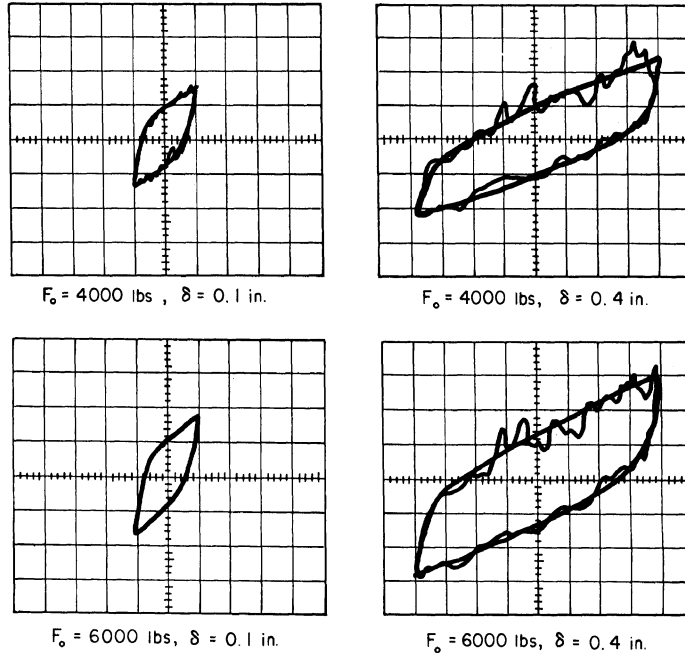


Fig. B-1 - Multi-leaf front spring

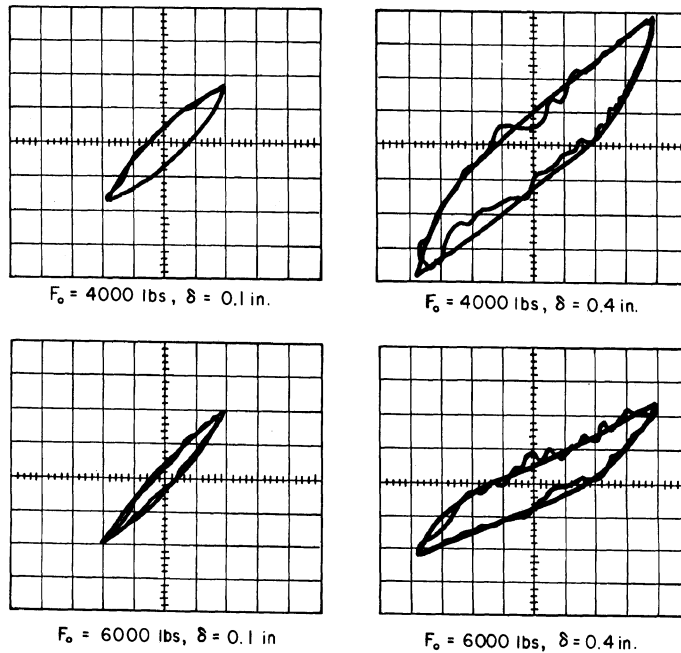


Fig. B-2 - Tapered-leaf front spring

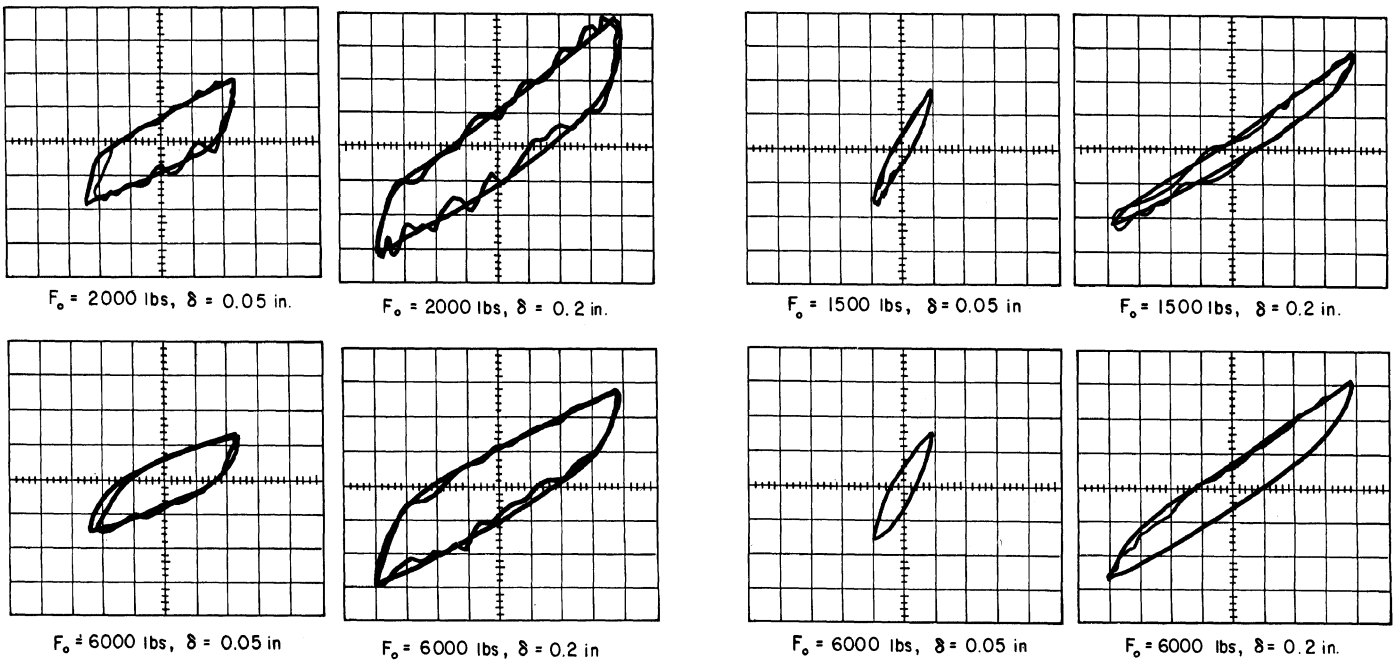


Fig. B-3 - Multi-leaf rear spring (23,000-lb axle rating)

Fig. B-4 - One spring from a four-spring suspension (see Fig. 5)

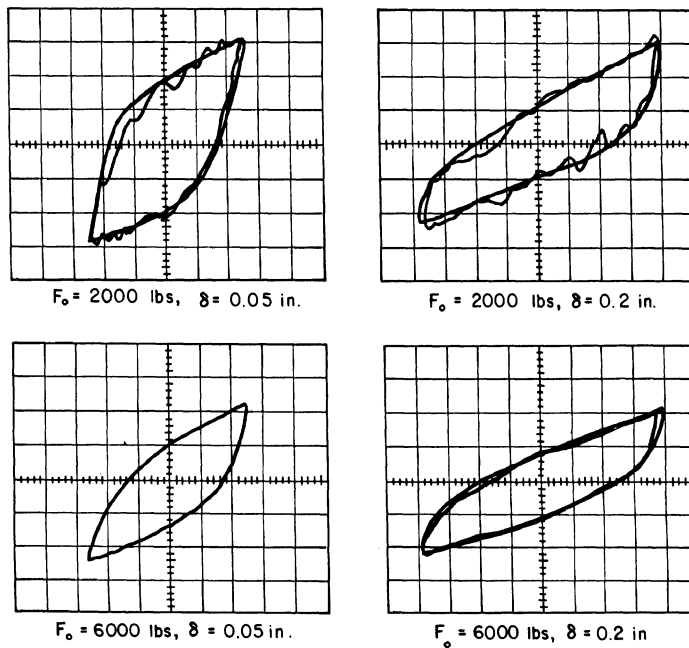


Fig. B-5 - One spring from a four-spring suspension (see Fig. 6)

APPENDIX C

This appendix contains numerical results describing the envelopes and deflection constants for each of the springs studied in this investigation. The notation associated with Equation (1) is used in presenting these numerical results.

1. Multi-leaf front spring (Fig. 2)

For $\delta_i > \delta_{i-1}$

$$F_{ENV} = 1300 \delta + 300 \quad , \quad \text{lbs}$$

$$\beta = 0.08 \text{ in}$$

For $\delta_i < \delta_{i-1}$

$$F_{ENV} = 1100 \delta - 100 \quad , \quad \text{lbs}$$

$$\beta = 0.076 \text{ in}$$

2. Tapered leaf front spring (Fig. 3)

For $\delta_i > \delta_{i-1}$

$$F_{ENV} = 1475 \delta + 300 \quad , \quad \text{lbs}$$

$$\beta = 0.0139 \delta + 0.02 \quad , \quad \text{in}$$

(Note that β has been made a function of δ to improve the accuracy of the fit to the experimental results.)

For $\delta_i < \delta_{i-1}$

$$F_{ENV} = 1358 \delta + 100 \quad , \quad \text{lbs}$$

$$\beta = 0.0133 \delta + 0.019 \quad , \quad \text{in}$$

3. Multi-leaf rear spring (Fig. 4)

(Note that for the rear springs the envelopes are sufficiently nonlinear to warrant the use of tabular functions to describe them.)

For $\delta_i > \delta_{i-1}$

δ , in	F_{ENV} , lbs
0.0	0.0
0.4	800
0.8	1700
1.2	2700
1.6	3790
2.0	4900
2.4	6370
2.8	8040
3.0	8890
3.1	9300

$$\beta = 0.0374 - 0.0062 \delta \text{ in}$$

For $\delta_i < \delta_{i-1}$

δ , in	F_{ENV} , lbs
0.0	0.0
0.4	520
0.8	1240
1.2	2050
1.6	3000
2.0	4100
2.4	5450
2.8	6980
3.0	7750
3.1	8130

$$\beta = 0.02 \text{ in}$$

4. One spring from a four-spring suspension with torque rods (Fig. 5)

For $\delta_i > \delta_{i-1}$

δ , in	F_{ENV} , lbs
0.0	0.0
0.2	610
0.4	1480
0.6	2450
0.8	3450
1.0	4500
1.2	5600
1.4	6800
1.6	8100
1.8	9450

$$\beta = 0.02 \text{ in}$$

For $\delta_i < \delta_{i-1}$

δ , in	F_{ENV} , lbs
0.0	-50.0
0.2	260
0.4	980
0.6	1780
0.8	2700
1.0	3650
1.2	4660
1.4	5830
1.6	7140
1.8	8300

$$\beta = 0.021 \text{ in}$$

5. One spring from a four-spring suspension with torque leaves (Fig. 6)

For $\delta_i > \delta_{i-1}$

δ , in	F_{ENV} , lbs
0.0	0
0.1	740
0.3	1500
0.6	2630
0.9	3800
1.2	5000
1.5	6520
1.8	8280
2.0	9400
2.2	10500

$\beta = 0.02$ in

For $\delta_i < \delta_{i-1}$

δ , in	F_{ENV} , lbs
0.0	0.0
0.1	250
0.3	750
0.6	1550
0.9	2600
1.2	3750
1.5	5090
1.8	6700
2.0	7890
2.2	9050

$\beta = 0.02$ in

This paper is subject to revision. Statements and opinions advanced in papers or discussion are the author's and are his responsibility, not the Society's; however, the paper has been edited by SAE for uniform styling and format. Discussion will be printed with the paper if it is published in SAE Transactions.



Society of Automotive Engineers, Inc.
400 COMMONWEALTH DRIVE, WARRENDALE, PA 15096

For permission to publish this paper in full or in part, contact the SAE Publications Division.

Persons wishing to submit papers to be considered for presentation or publication through SAE should send the manuscript or a 300 word abstract of a proposed manuscript to: Secretary, Engineering Activity Board, SAE.

16 page booklet.

Printed in U.S.A.

SAE Technical Paper Series

800906

**A Test Facility for the
Measurement of Heavy
Vehicle Suspension Parameters**

**Christopher B. Winkler and
Michael Hagan**

Highway Safety Research Institute
The Univ. of Michigan

**West Coast International Meeting
Los Angeles, California
August 11-14, 1980**



SOCIETY OF AUTOMOTIVE ENGINEERS, INC.
400 COMMONWEALTH DRIVE
WARRENDALE, PENNSYLVANIA 15096

The appearance of the code at the bottom of the first page of this paper indicates SAE's consent that copies of the paper may be made for personal or internal use, or for the personal or internal use of specific clients. This consent is given on the condition, however, that the copier pay the stated per article copy fee through the Copyright Clearance Center, Inc., Operations Center, P.O. Box 765, Schenectady, N.Y. 12301, for copying beyond that permitted by Sections 107 or 108 of the U.S. Copyright Law. This consent does not extend to other kinds of copying such as copying for general distribution, for advertising or promotional purposes, for creating new collective works, or for resale.

Papers published prior to 1978 may also be copied at a per paper fee of \$2.50 under the above stated conditions.

SAE routinely stocks printed papers for a period of three years following date of publication. Direct your orders to SAE Order Department.

To obtain quantity reprint rates, permission to reprint a technical paper or permission to use copyrighted SAE publications in other works, contact the SAE Publications Division.

A Test Facility for the Measurement of Heavy Vehicle Suspension Parameters

**Christopher B. Winkler and
Michael Hagan**

Highway Safety Research Institute
The Univ. of Michigan

ALTHOUGH IT IS WELL understood that the suspension properties of heavy vehicles have a first-order effect on the handling, braking and ride performance of these vehicles, facilities capable of the comprehensive measurement of these properties are notably rare. The few measurements of heavy vehicle suspension properties which are found in the literature (1, 2, 3, 4)* generally derive from facilities which are limited in scope, relatively inefficient in terms of required effort, and often decidedly temporary by nature.

In recognition of this state of affairs, the Highway Safety Research Institute, under the sponsorship of the Motor Vehicle Manufacturers Association, Ad Hoc Committee on Heavy Truck Braking and Handling, undertook the design and construction of a permanent facility for the measurement of heavy vehicle suspension properties. The facility was completed in June of 1979.

In general terms, the facility is capable of measuring virtually all the compliance, kinematic and coulomb friction properties of

heavy vehicle suspension and steering systems as they react to vertical force, roll moment, lateral force, brake force, and aligning moment. The facility can accept single-axle and tandem-axle suspensions (maximum tandem spread 180 cm., 70 inches) of all common, on-highway track widths. Suspensions may be tested in their normal configuration, i.e., mounted on a vehicle, or as mounted on an abbreviated frame section. All measurements are performed at steady-state or quasi-steady-state; that is, the facility is not intended for dynamic testing.

In the first part of this paper, a detailed description of the test facility and its elements is presented. The second part describes test methodology and certain generic qualities of a limited number of measurements made to date (based in part on measurements made previously to the development of this facility).

*Numbers in parentheses designate References at end of paper.

ABSTRACT

A new facility for the measurement of the compliance, kinematic and coulomb friction properties of heavy vehicle suspensions is described. The facility may test single or tandem and front or rear suspensions. Test pro-

cedures for measurement of vertical and roll rates, kinematic and compliant steer effects are presented. Qualitative findings are discussed and example data is appended.

A summary completes the text. The more detailed description of certain of the machine elements, and specific suspension data, are presented in the Appendices.

THE FACILITY

The HSRI Heavy Vehicle Suspension Testing Facility is a permanently installed laboratory device intended for the measurement of all compliance, kinematic and coulomb friction properties of heavy vehicle suspension and steering systems presently of interest. The facility, shown schematically in the roll plane view in Figure 1, has these major mechanical systems:

(1) a static structure, (2) a movable table, and (3) four wheel pad assemblies.

The static structure includes a foundation structure which forms a .91 meter (3 ft) deep pit, and an overhead static structure (Fig. 2), which is used to secure the vehicle frame during rear suspension testing (Fig. 3).

A large, rigid table with a surface measuring 3.05 meters (10 ft) in the lateral direction and 2.29 meters (90 in) in the longitudinal direction simulates the ground and is movable in the vertical and roll directions. This table is divided approximately in half in the lateral direction. During tandem suspension testing, the table halves are rigidly coupled and move in

concert, each half supporting one axle. For single-axle testing, one table half is held in the down position and the other is used to exercise the suspension. In the case of front suspension testing, the overhead frame is removed to accommodate the vehicle cab, and the immobilized table half is used as a tie-down structure for the front-end of the vehicle.

Each table half is motivated by a pair of hydraulic cylinders, one cylinder located under each of four wheel positions. The action of these cylinders produces the vertical (Fig. 4) and roll (Fig. 5) motions of the table and suspension. These cylinders are controlled by an electrohydraulic servo system. Various modes of table control will be detailed below. The table is restrained from all other motions by two identical four-bar linkages (one per table half) which are located in, and anchored to, the pit structure (Fig. 6). The linkages are designed such that the point at which they attach to the table is located on the simulated ground plane and moves on nearly a pure vertical path over the length of the table stroke. Vertical table stroke is 25.4 cm (10 in). Roll stroke varies depending on the average vertical position and is otherwise limited by the 10-inch cylinder stroke. Maximum roll stroke is ± 5.7 degrees.

The wheel pad assemblies (Figs. 7 and 8) are a key element of the facility in that (1)

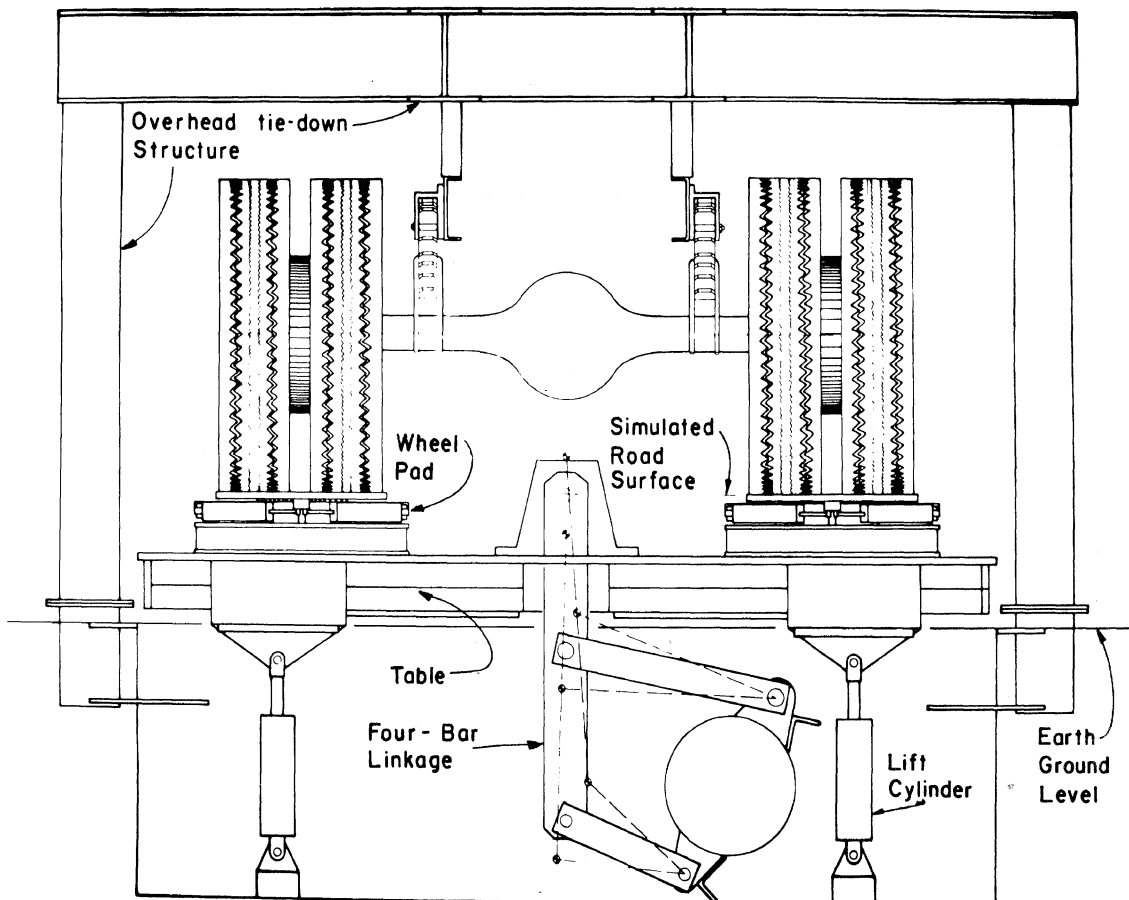


Fig. 1 - Heavy vehicle suspension test facility schematic

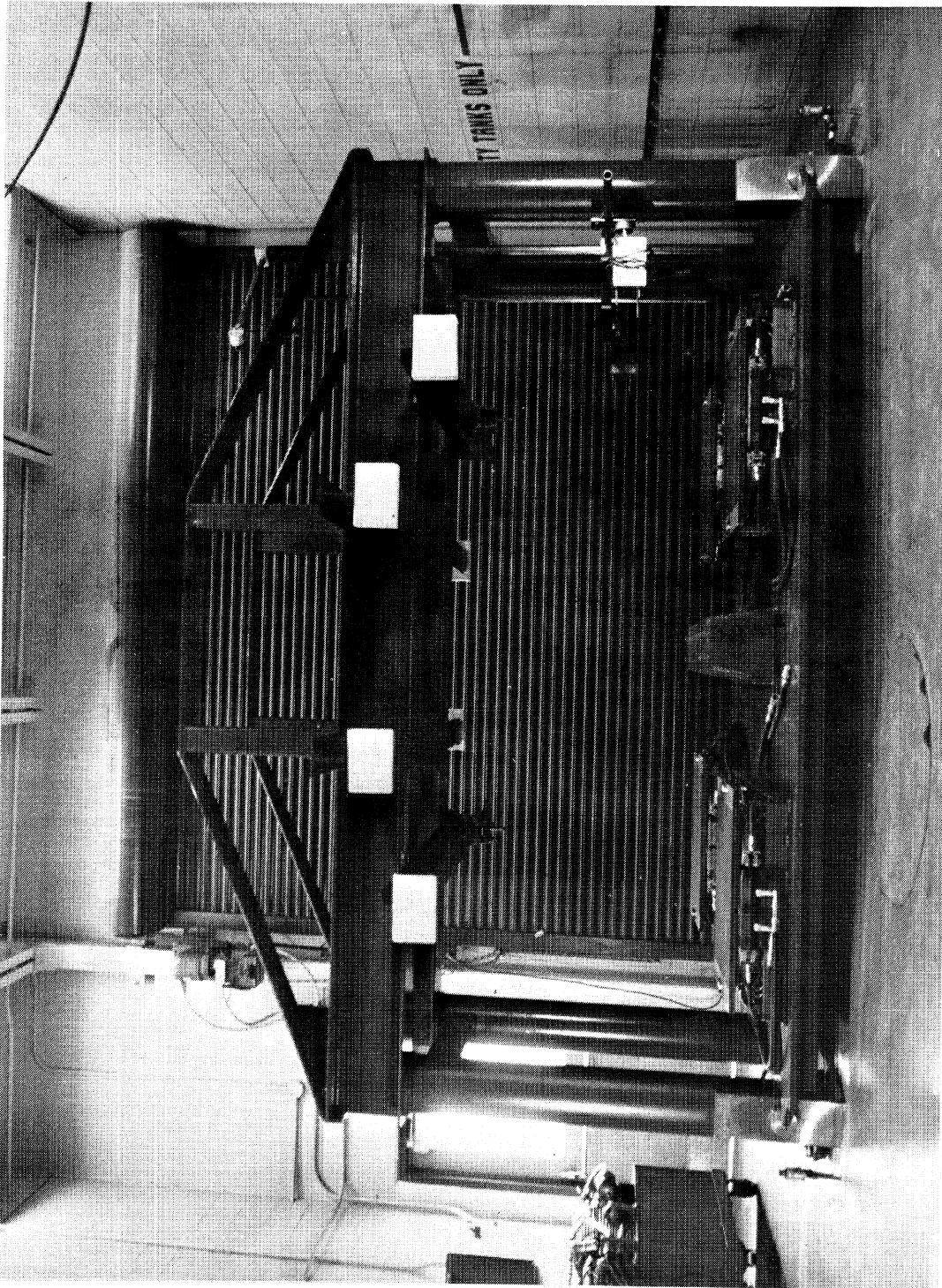


Fig. 2 - The facility

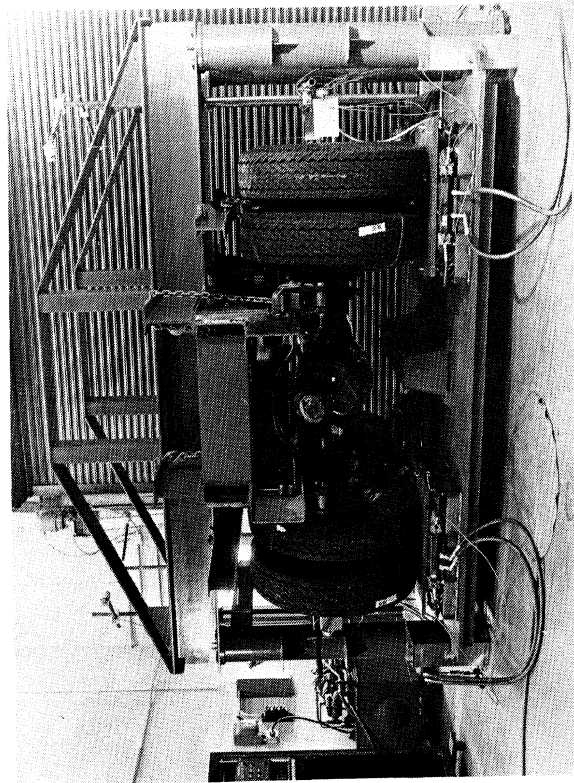


Fig. 3 - The facility with a tandem suspension mounted

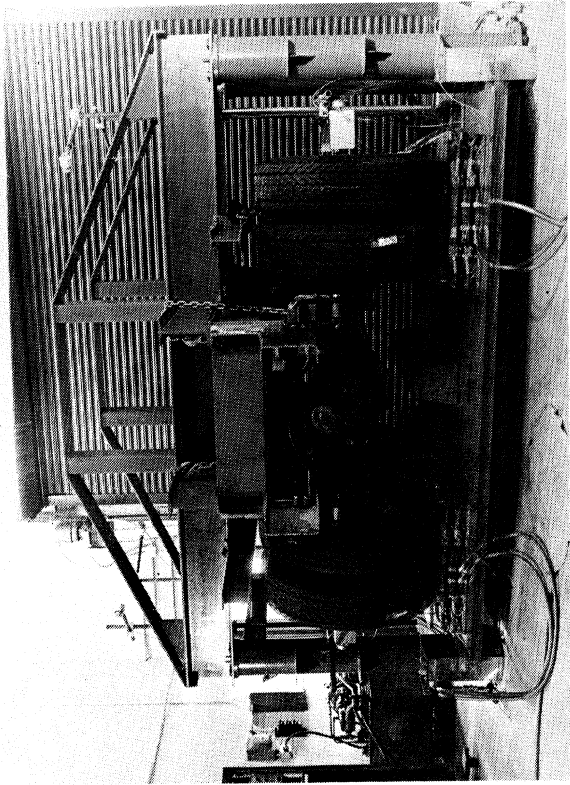


Fig. 4 - Double exposure: vertical motion

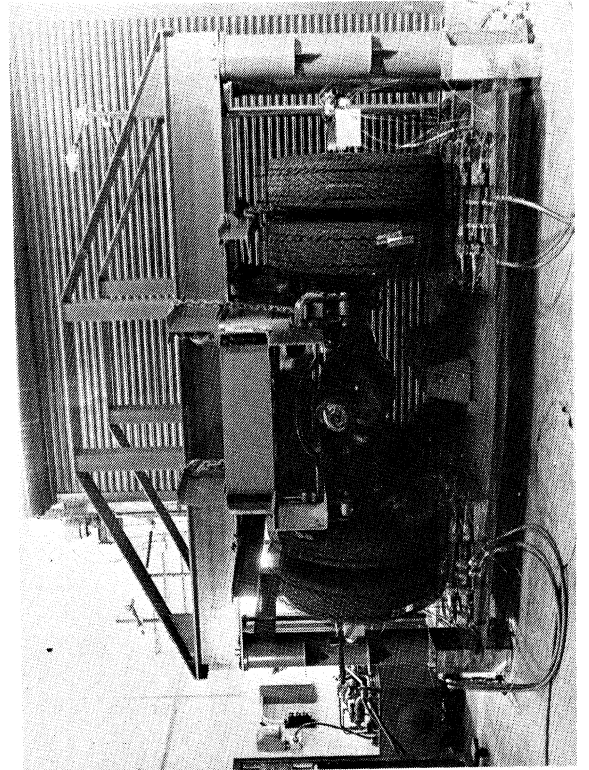


Fig. 5 - Double exposure: roll motion

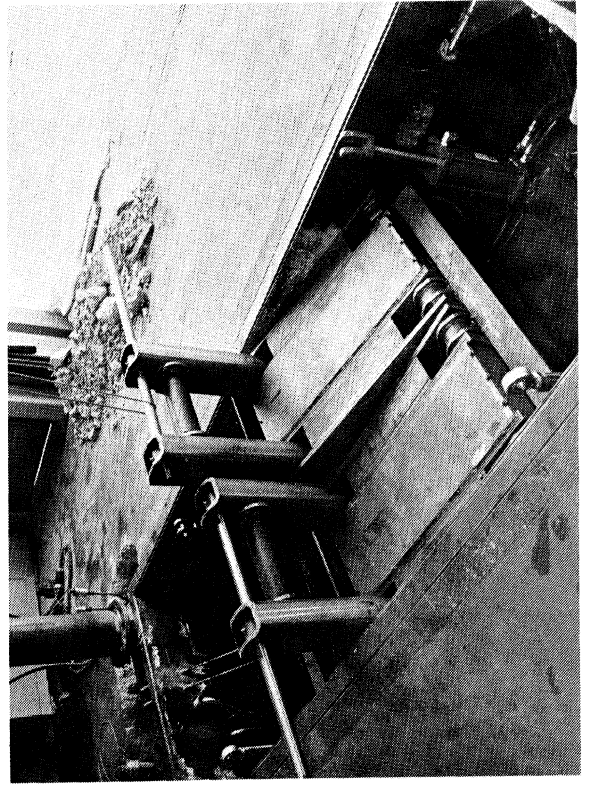


Fig. 6 - The linkages mounted in the pit

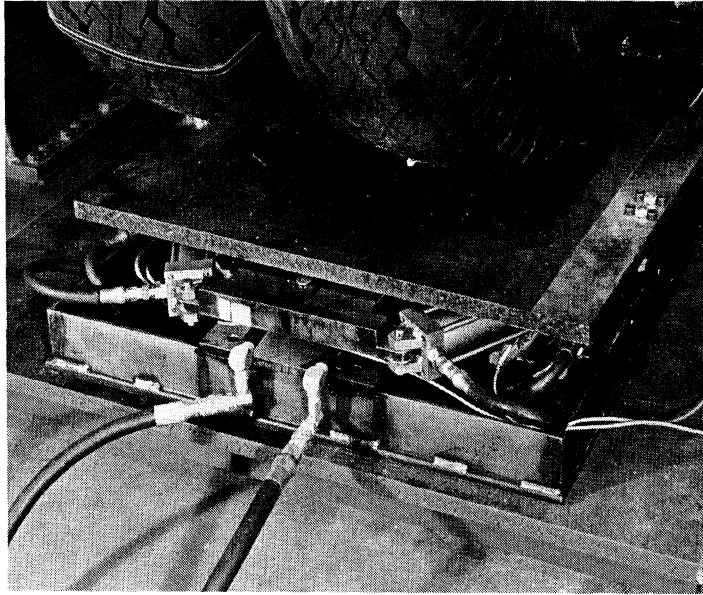


Fig. 7 - A wheel pad

they provide control of the tire-road shear forces and moment which are applied to the tires and, hence, to the suspension, and (2) they house all of the force transducer elements of the system.

As shown in Figure 8, a wheel pad assembly is composed of several serially assembled parts, viz.:

- 1) Base frame
- 2) Load cell/flexure group
- 3) Lower bearing plate
- 4) Four shear plane hydraulic cylinders
- 5) Upper bearing/ground plane plate

The upper and lower bearing plates are separated by a circular field of approximately 2,500 1/4-inch ball bearings. These two plates and the ball field constitute the shear plane bearing.

The hydraulic cylinders of each wheel pad are controlled by two electrohydraulic servo control systems. These two systems combine to provide precise control of aligning moment (M_z) and one component of shear force (F_h), i.e., the force in the h-direction as shown in Figure 8. The cylinder assembly is designed such that the component of shear force at right angles to the controlled force (that is, in the j-direction) is always minimized. (See Appendix A.)

Each of the four wheel pads simply sits on the surface of the table* so that the pads may

be located to accept any tandem spacing and track dimensions which can generally be accommodated by the table dimensions. Further, the wheel pads may be rotated such that the h-direction of the pads can be aligned with either the longitudinal or lateral directions of the suspension. In this way, the controlled shear force, F_h , may be representative of either brake force or lateral force, respectively.

The load cell/flexure assembly transduces a matrix of forces which, through appropriate calculations, are reduced to the four tire-road forces and moments of interest, viz., F_z , F_h , M_z , and M_j . This transducer assembly is fixed

*Shear plane reactions at the table/wheel pad interface are supported by an aggressive "frictional" coupling. A self-adhering sandpaper (3M Safety Walk™) material is applied to both the upper surface of the table and the bottom surfaces of the wheel pads. These sandpaper surfaces "interlock" to produce an apparent friction coefficient well in excess of unity. The sandpaper surface is also applied to the "ground plane" surface of the upper bearing plate to provide an aggressive surface at the tire-road interface. The friction coefficient at this interface is approximately 3/4.

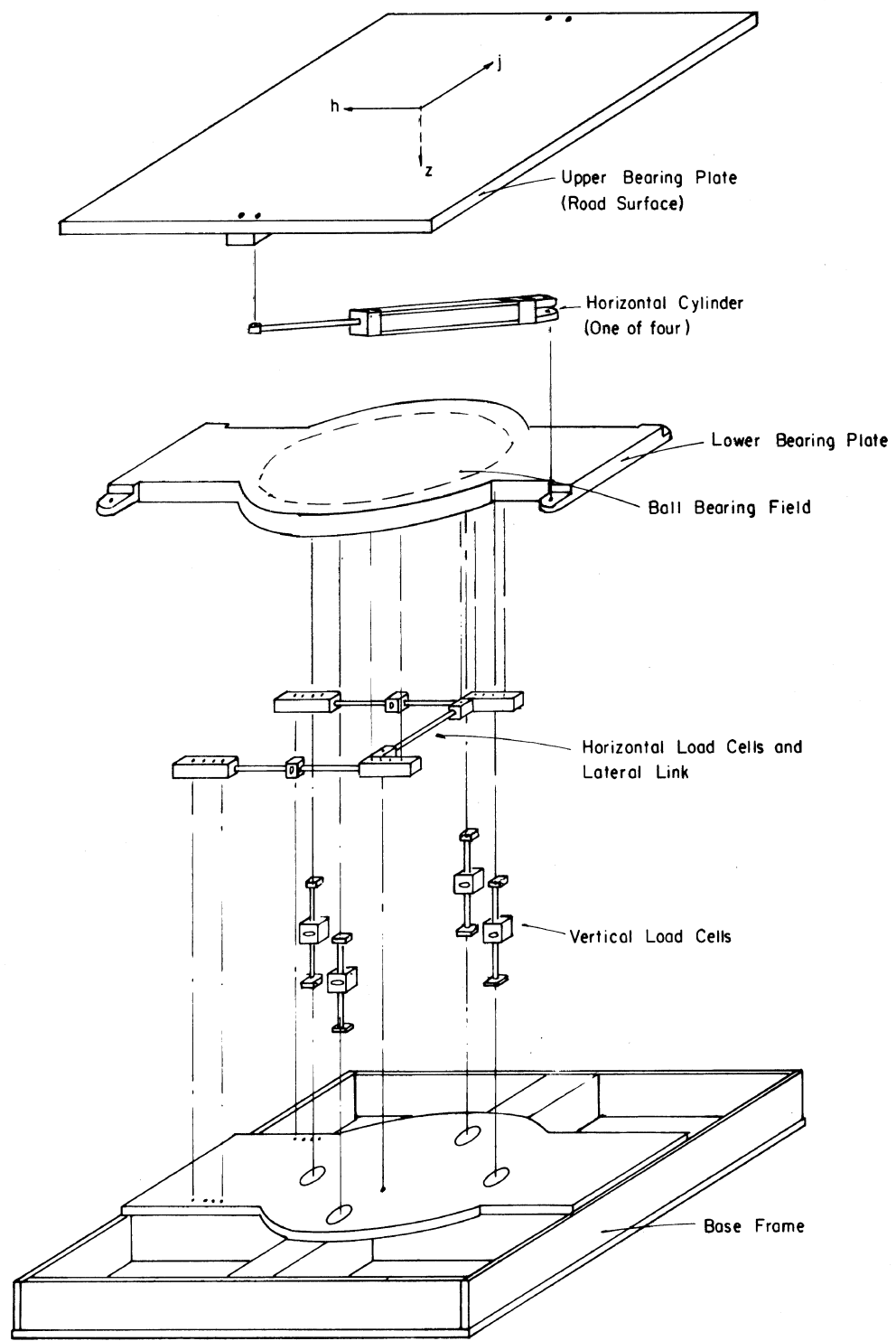


Fig. 8 - The elements of the wheel pads

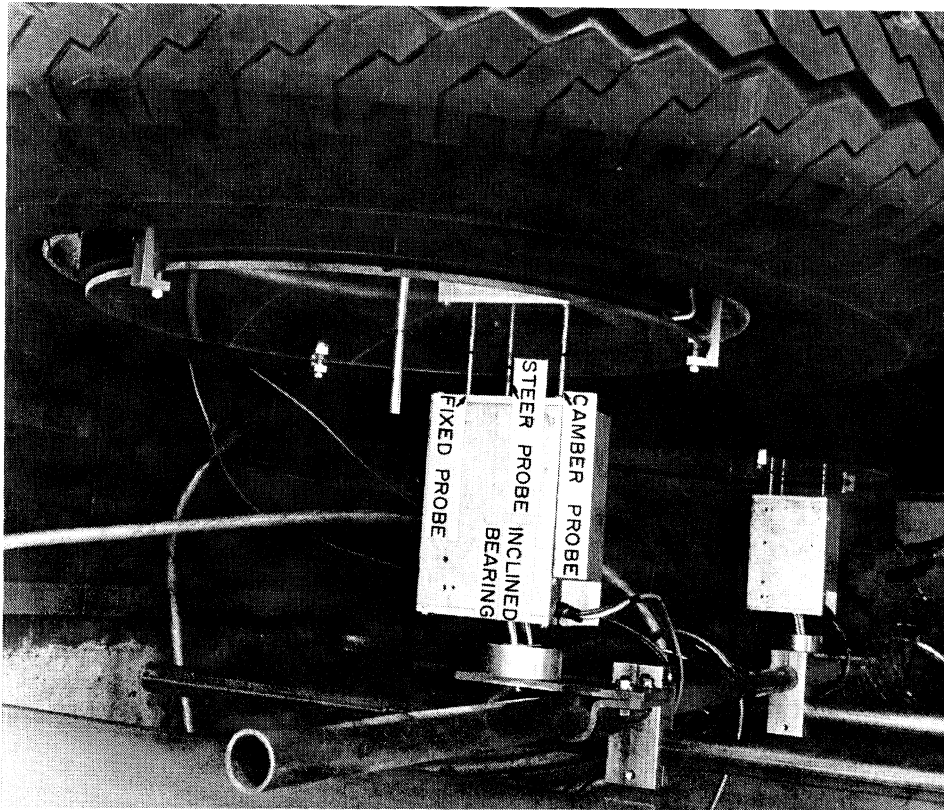


Fig. 9 - The wheel angle transducer

in the base frame of the wheel pad so that, regardless of suspension or steering system deflections, the transducer axis system remains fixed in the "ground" (table).

With the exception of flexible hydraulic lines, the load cell/flexure assembly represents the only force path between ground (table) and suspension (i.e., the shear plane bearing and force transducers are not parallel force paths) such that the frictional quality of the shear plane bearing is not an issue with respect to the accuracy of the transduced forces. (See Appendix B.)

The maximum capability of the facility in terms of loads applied to the suspension are essentially a function of the transducer capability. Limits on controlled load inputs at each wheel pad are:

Vertical Load:	90,000 N (20,000 lbs)
Shear Force:	27,000 N (6,000 lbs)
Aligning Moment:	2,275 N (20,000 in-lbs)

In addition to the major mechanical elements discussed above, the deflection transducers and the electronic control and data gathering system remain as important elements of the facility.

All deflection transduction is accomplished by potentiometric devices. The table is equipped with two potentiometers which essentially transduce the vertical position of the left and right ends of the table. These signals are used

directly in servo control of the table position and are ultimately reduced to produce vertical motion and roll angle data. Transduction of vertical and roll motions of the suspension axles is accomplished in analogous fashion. String-pots located high above the frame (Fig. 3) transduce the vertical motion of "axle center pointers" located on each wheel (Fig. 9).

Angular deflections of each wheel (steer and camber angles) are measured with the transducer assembly shown in Figure 9. The frame of the assembly rides on a linear bearing which is inclined at 15 degrees from horizontal. Thus, the one of the three probes which is fixed to the transducer is caused to bear on the flat surface plate (a mirror) which is mounted on the wheel parallel to the wheel plane. In this way, the transducer frame remains a fixed distance from the wheel regardless of lateral translation of the wheel. Steer and camber motions of the wheel, however, cause the other two probes, i.e., the steer and camber probes, to deflect relative to the transducer frame. By means of parallelogram linkage (of which the mirror surface is one element), these motions are converted to potentiometric signals which are proportional to the angular deflection of interest.

Other data channels are available which can be used in the measurement of longitudinal or lateral axle deflection, or steering-wheel position or torque.

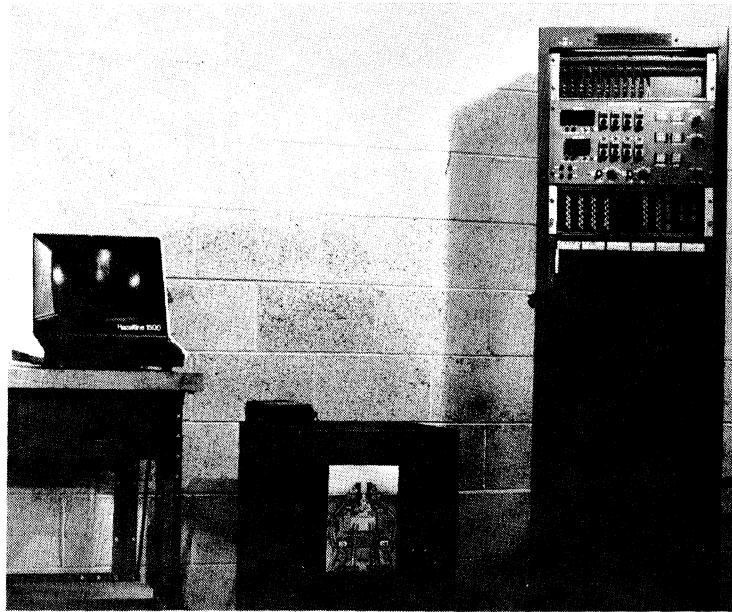


Fig. 10 - Data collection and control electronics

The data collection and control electronics (Fig. 10) consist of analog signal conditioning and servo control circuitry plus a microcomputer and associated interface circuitry. A block diagram of the electronics is shown in Figure 11.

The low-level signals from the transducers are amplified and scaled by the analog signal conditioning unit.

The analog unit also provides for zero and gain calibration functions and for loop closure, as well as the appropriate compensation within the various servo systems. Additionally, direct output of the primary and derived (i.e., calculated as a function of primary signals) analog data signals is available through a ten-by-sixty patchboard. Via this patchboard, the operator can route any of the 60 available data channels to any one of ten output display channels. Two of these output channels are connected to digital panel meters while all may be connected to an X-Y recorder, strip chart, or other analog display device. This enables the operator to

monitor the analog circuitry and provides a real-time output of machine activity.

The 41 raw data channels are also connected to a microprocessor via a 12-bit A/D converter. The microcomputer provides the primary data collection, control, and display functions. The operator interfaces with the machine through a video terminal. All pertinent test parameters (vehicle geometric data, scale factors, test identification, etc.) are entered and stored in memory. The microcomputer can also display the current values of any or all of the primary data channels (in engineering units) as well as those of a variety of derived data. The operator can also select which channels are to be collected, for ultimate storage on magnetic tape, in a particular test. During a test, the microcomputer digitizes the selected data and sends the data, along with stored geometric parameters and scale factors, to a PDP 11/45 minicomputer where all data is stored on tape. While digitizing the data, the microcomputer also generates the servo commands that control

the table and/or pads. At this time, these commands are limited to ramp waveforms. The operator enters, in engineering units, the value to be ramped to and the time rate of the ramp.

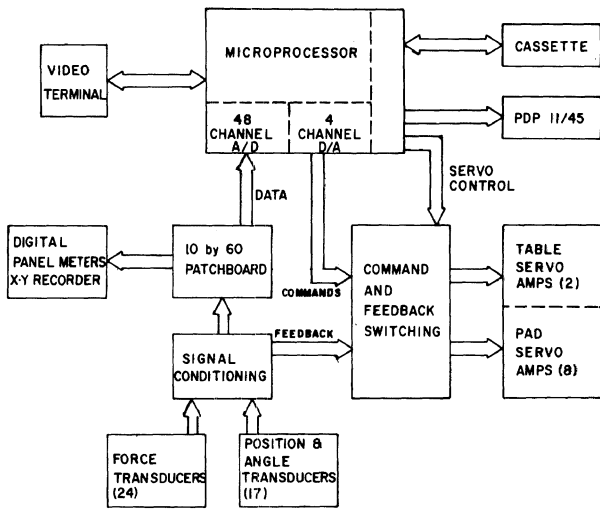


Fig. 11 - Block diagram of electronics

As has been mentioned in the above discussion, all motivation for exercising the subject suspension derives from electrohydraulic servo control systems. These systems control the vertical and roll motion of the table and the generation of shear force (F_h) and moment (M_z) by the wheel pads.

There are three separate modes by which table motion can be controlled, namely:

- 1) table position control mode
- 2) axle position control mode
- 3) wheel load control mode

A simplified schematic diagram of the table control system is shown in Figure 12. In each mode, the appropriate table motions are generated to provide the desired response of the control variables implied by the mode name. That is, when operating in the table position mode, the operator has direct control of the vertical and roll positions of the table. In the axle position mode, table motions are generated which produce the desired positioning of the axles, vertically and in roll. Similarly, in the wheel load mode, the table is caused to move in a manner which creates the desired values of total suspension load and roll moment. (In each of the latter two modes, control can be generated in accordance to the average experience of the two axles of a tandem suspension or in accordance with either the forward or aft axle only.)

The process of switching from one table control mode to another is controlled by the microcomputer. As this process begins, the computer samples and checks the existing values of the signals which will be used as feedback in the mode about to be activated. At the time that mode switching occurs, these sampled values

are put out on the appropriate D/A converter command lines. At the same time, the feedback paths in the servo circuitry are switched to the new mode feedback. This process enables a smooth transition between modes without disturbing the table position. The operator inputs a simple command at the terminal to initiate the switching process.

Control of the wheel pad motions has only one mode based on force and moment feedback. Thus, the control scheme for each pad is very similar to that of the table force control mode and the operator has direct control of the application of F_h and M_z .

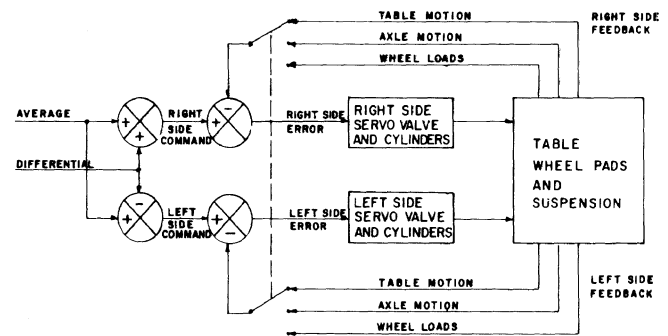


Fig. 12 - Simplified diagram of table control system

TEST METHODOLOGY

The series of tests which HSRI conducts on heavy vehicle suspensions includes measurements of the following suspension properties:

- Spring Rate
- Roll Rate
- Roll Steer
- Roll Center Height
- Bounce Steer
- Aligning Moment Compliance Steer
- Lateral Force Compliance Steer
- Brake Force Compliance Steer
- (For tandem suspensions only)
 - Interaxle Load Distribution
 - Interaxle Load Transfer

Many heavy vehicle suspensions exhibit a significant coulomb friction-related hysteresis with respect to many of the above parameters. These hysteretic effects are also measured during testing. In the following paragraphs, a brief review of test methodology employed to determine each of the above parameters will be presented. Certain qualitative findings deriving from tests conducted with this, and previously used facilities are also discussed. Specific examples of test results are presented in Appendix C. Although repeated references to Appendix C are avoided in the following text, the reader may find it helpful to refer to the example data frequently.

SPRING RATE - Measurement of the suspension vertical spring rates is conducted with the table in the axle position control mode and with the shear plane force and moments commanded to zero. In this mode, the axle is caused to move in a purely vertical manner (no roll component) relative to the vehicle frame. Thus, force-deflection data related to vertical spring rate and hysteretic properties can be gathered. Vertical load and overturning moment data is gathered at each wheel, as is vertical deflection data. This data may be reduced to produce vertical force-deflection curves for individual springs and/or average characteristics. As shown in Figure 13, data is gathered during large and small amplitude deflection cycles so that hysteretic characteristics as well as spring rate may be comprehensively determined.

Figure 13 is representative of the quality of force-deflection data gathered from leaf spring suspensions. The average of the up-going and down-going, large deflection data (that is, the upper and lower "outer" boundaries of the data, respectively) is indicative of the nominal spring rate. The half-spacing (measured along the ordinate of the graph) between these boundaries indicates the nominal coulomb friction level. The increased spacing of these boundaries at higher vertical loads is typical and reflects the increasing normal load at the frictional interface.

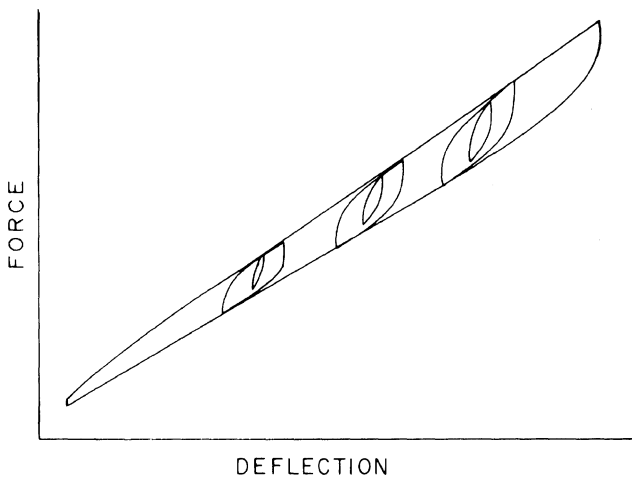


Fig. 13 - Typical force-deflection quality of multi-leaf spring suspensions

The small deflection behavior, indicated by the smaller "internal loops," is representative of the small deflection behavior of multi-leaf springs. Typically, in small deflection cycles, multi-leaf springs exhibit the rounded, exponential-like approach to the large deflection boundaries that is shown in Figure 13. In contrast, single tapered-leaf springs are characterized by a linear approach to the large deflection boundaries (Fig. 14). It is hypothe-

sized that multi-leaf springs provide a large number of local coulomb friction regions on the inter-leaf interfaces which apparently saturate ("break away") at different force levels, thus producing the "rounding" effect. On the other hand, single tapered leaves have but one or two friction fields at the spring/slipper interface which saturate in one step. For these springs, the small deflection spring rate, then, is the rate of a leaf spring whose two ends are "frozen" at a fixed distance from one another.

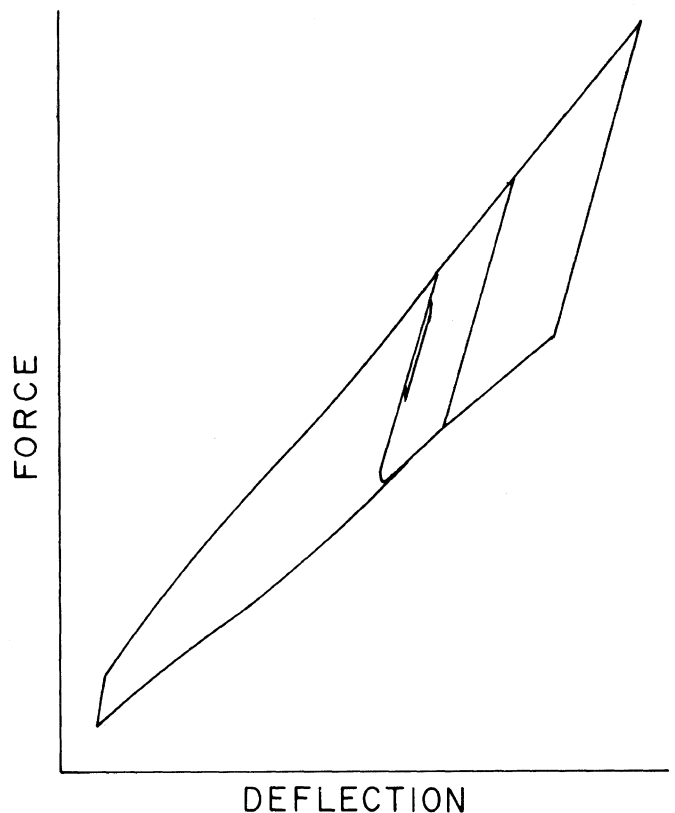


Fig. 14 - Typical force-deflection quality of single-leaf spring suspensions

Reference (5) discusses leaf spring behavior and testing, and describes a mathematical model developed to accurately reflect the measured spring rate and hysteretic properties of leaf springs.

ROLL RATE - It has been found that calculation of heavy vehicle suspension roll rate (and roll hysteretic properties) based solely on vertical force-deflection data and the appropriate geometric considerations may be inadequate. One obvious reason for this is that mechanisms providing auxiliary roll stiffness may be deliberately added to the suspension. Less obviously, it also appears that, for leaf-spring suspensions, the longitudinal twisting of the individual springs (see Fig. 15) which must occur when the axle rolls relative to the

frame may introduce significant levels of auxiliary roll stiffness (particularly if the leaf spring ends are mounted in fixed bushings rather than on slippers). Mechanisms also appear to exist which alter the hysteretic properties—possibly the redistribution of inter-leaf contact pressures due to longitudinal spring twisting. Consequently, suspensions are tested to obtain a direct measure of roll rate.

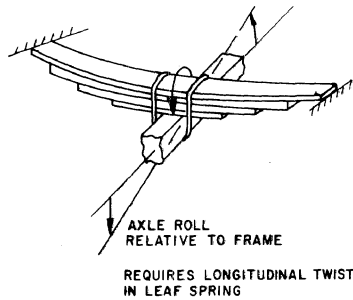


Fig. 15 - Axle roll motions require longitudinal twisting of the leaf spring

Roll rate testing is conducted with the table in the wheel load control mode and with the shear plane force and moment commanded to zero. Total suspension load is brought to the desired level and held constant during the test. Data is gathered while the table is rolled in order to apply a roll moment to the suspension. (That is, vertical load is transferred from one side of the suspension to the other while the total load is held constant.) Vertical load, overturning moment, and axle deflection data is gathered as in spring rate testing. The test procedure is repeated at a variety of vertical load conditions of interest.

ROLL STEER - Roll steer measurements are conducted in the same manner as are roll rate measurements. Indeed, by adding steer angle data from each wheel to the data records, both measurements are made during one operation. Data from roll steer measurements are presented as a graph of steer angle versus roll angle. Roll steer data is difficult to typify for the following reasons:

1) Roll steer data may or may not exhibit a hysteretic relationship between steer and roll angles.

2) Roll steer data exhibits varying degrees of linearity at a given vertical load level, i.e., the roll steer coefficient (slope of the steer angle/roll angle data) may be constant or vary with the amount of roll.

3) Roll steer coefficient may be strongly related to the total vertical suspension load, in some cases changing polarity with load.

4) For front suspensions, roll steer coefficient may be strongly related to the nominal steer angle, again, in some cases showing polarity reversals.

5) For tandem suspensions, the roll steer behavior of the individual axles can be substantially different.

ROLL CENTER - There are two methods available by which to determine the roll center(s) of a suspension. One is based on the kinematic or the deflection experience of the axle(s) during a roll experience, while the other depends on statics, that is, the force and moment equilibriums of the suspensions during quasi-static roll.

Considering the kinematic method first: As in the other roll-related experiments described previously, the suspension is rolled by the application of a roll moment superimposed on the desired, constant vertical load (in the absence of tire shear forces and moment). While the roll motion occurs, measurements of the axle roll angle and lateral translation are made. The relative rate of change of these measurements are reduced through kinematic analysis to determine the roll center position for the axle.

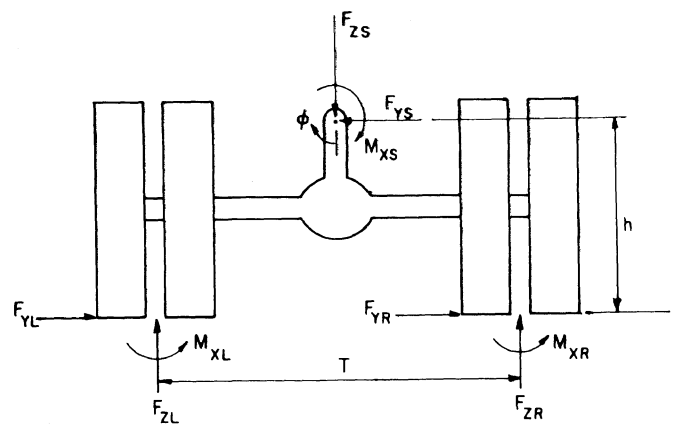


Fig. 16 - Axle free-body with idealized spring reactions

In theory, the static equilibrium method is nearly as straightforward as the kinematic method. In practice, however, the presence of substantial amounts of coulomb friction in the heavy vehicle suspension complicates the method.

Figure 15 presents the pitch plane free-body diagram of an axle in which the suspension reactions have been idealized into lateral and vertical forces acting through the roll center and a roll moment. Clearly, three static equilibrium equations may be written for the axle (lateral force, vertical force and roll moment), however, these equations will contain four unknowns, viz., F_{ys} , F_{zs} , M_{xs} , and h (all other variables are directly measurable). The additional information by which the number of unknowns may be reduced to three may be obtained through the measurement of the roll angle, ϕ , and the subsequent determination of

M_{XS} from ϕ through the use of the previously determined relationship between these variables (i.e., the roll rate data). The complication derives from the fact that the M_{XS} to ϕ relationship may be substantially hysteretic. In this case, the initial conditions of the experiment must be carefully controlled so that it is well established where the experiment is being conducted with respect to the roll rate "hysteresis loop." The procedure used is as follows:

1) With the table in force control mode, the desired vertical load on the suspension is established, and the vertical loads, side-to-side, are equal.

2) With vertical loads held constant, lateral shear forces are now applied by the wheel pads. They are applied in a direction which causes the axle to roll to a small positive angle.

3) With lateral force held constant, force control is used to transfer vertical load side-to-side on the suspension such that the suspension rolls to a large positive displacement. Vertical load is then returned to an equal side-to-side condition, again establishing a small positive roll angle.

These three steps establish an initial condition for the experiment wherein the roll moment developed by the suspension springs is assumed to be in accordance with the negative-going (roll angle) outer-boundary of the roll rate hysteresis loop. (Reference example roll rate data of Appendix C.)

4) The lateral forces applied by the wheel pads are now commanded to ramp from their existing positive value to a similar negative value. During this time, data describing lateral force, overturning moment and vertical force (although vertical force is held constant through the action of the table servo control) is collected from each wheel pad. Axle roll angle data is also collected, which data is later used to determine suspension roll moment.

5) Steps (3) and (4) are now repeated with all polarities reversed. Through solution of the static equilibrium equations, the data is used to determine the roll center height, h .

These two methods have been found to produce measurements of roll center height which agree fairly well. Measurements made by the static-equilibrium method, however, generally exhibit more scatter and show poorer agreement with theoretical expectations. Presumably, these results are due to the difficulties presented by the hysteretic qualities of the suspensions.

As would be expected, leaf-spring suspensions (which generally do not employ any laterally oriented links) have been found to exhibit roll center heights very near to the average height of the leaf-spring ends (that is, at the slipper/spring interface height on rear sus-

pensions and at the average spring bushing height on front suspensions).

BOUNCE STEER - The front wheels of heavy vehicles can exhibit a steer response to pure bounce motions of the suspension due to the asymmetric kinematics of their steering systems.

This behavior is measured by deflecting the axle vertically (in axle position control mode) in the absence of tire shear forces and moment, while collecting data describing steer angle of both wheels and vertical axle position. The experiment may be conducted at a variety of axle roll angles and nominal steer angles in order to determine the influence of these parameters.

During this experiment, as with virtually all experiments conducted on front suspensions, the steering wheel must be constrained at a fixed position. Further, steering system lash should be eliminated when examining front suspension kinematic steer effects (roll steer as well as bounce steer). The system may be carefully adjusted to eliminate lash, or, in some cases, a small, constant aligning moment may be applied during the experiment in order to eliminate lash through preloading.

COMPLIANCE STEER TO ALIGNING MOMENT, BRAKE FORCE AND LATERAL FORCE - Measurements of compliance steer behavior relative to all three of the tire shear force reactions are conducted in essentially the same manner. The facility is operated in the axle position control mode in order that the axle may be held in a fixed position during the test. This insures that the kinematic steer effects (roll and bounce steer) do not contaminate the data being collected.

With the desired axle position (vertical and roll) established and held fixed, the shear force or moment of interest is applied through the action of the wheel pads, and the resulting wheel steer deflections are measured.

In determining the compliance steer reaction to shear forces, accurate location of the wheel pads can be of critical importance. The pads must be located such that the line of action of the applied force passes through the contact patch center. If this is not the case, then the application of force also results in the application of an aligning moment and the resulting measurements will be in error accordingly.

As can be expected, due to the presence of the steering system, compliance steers are generally found to be more significant on front suspensions than on rear suspensions.

INTERAXLE LOAD DISTRIBUTION - Virtually all tandem suspensions are designed with some mechanism whose purpose is to equalize the vertical load carried by the two axles of the suspensions. Such mechanisms include the walking beam, on walking-beam suspensions, the load leveler on four-leaf suspensions, and

interaxle air lines on air suspensions. The primary goal of these mechanisms is to maintain desirable axle loading while traversing uneven surfaces (such as construction site terrain, driveway entrances, etc.)

Although these mechanisms are meant to equalize axle loading, in some cases it has been found that the distribution of vertical load is rather sensitive to the relative pitch angle between the vehicle frame and the ground plane. This sensitivity is examined by conducting vertical loading cycles at fixed frame pitch angles of 0, -1, and -2 degrees (i.e., pitch "forward"). The tests are conducted in load control mode with the wheel pad reactions commanded to zero. Pitch angles are attained through shimming the vehicle frame relative to the tie-down structure. Vertical load data is gathered at each wheel and front and rear axle loads are compared.

Particularly with four-spring suspensions, it has been found that the front axle may support substantially more load as the pitch angle becomes more negative.

INTERAXLE LOAD TRANSFER - It is well known that the same mechanisms which are intended to equalize tandem-axle vertical loading under conditions of free running, generally result in the redistribution of vertical load during the braking process. This interaxle load transfer phenomenon may also be sensitive to frame pitch as well as total vertical load. In a tandem suspension test series, the following procedure is conducted at several conditions of vertical load and pitch angle.

The table is placed in vertical load control and the desired level of gross suspension load is maintained constant during the experiment. The wheel pads are commanded to apply brake force, ramping from zero to the desired level and returning to zero. Brake force may be applied equally at all wheels or on any combination, as desired. Data is gathered describing the forces applied and the resulting vertical loads.

As expected, four-spring suspensions tested are found to transfer load from the front axle onto the rear axle during the application of brake force. Interestingly, the magnitude of interaxle load transfer has also been found to decrease with increasing negative pitch angle.

SUMMARY

This paper reports on a new and unique facility for the measurement of the compliance, kinematic, and coulomb friction properties of heavy vehicle suspensions. A general description of the facility and its major, functional elements has been presented. Various test methods have been discussed and a review of qualitative findings to date was given. Detailed descriptions of machine elements, and

specific suspension data is presented in appendices.

REFERENCES

1. R. W. Murphy, J.E. Bernard, and C.B. Winkler, "A Computer-Based Mathematical Method for Predicting the Braking Performance of Trucks and Tractor-Trailers." Phase I Report: Motor Truck Braking and Handling Performance Study, Highway Safety Research Institute, University of Michigan, September 15, 1972.
2. J.E. Bernard, C.B. Winkler, and P.S. Fancher, "A Computer-Based Mathematical Method for Predicting the Directional Response of Trucks and Tractor-Trailers." Phase II Technical Report: Motor Truck Braking and Handling Performance Study, Highway Safety Research Institute, University of Michigan, June 1, 1973.
3. R.D. Ervin, C.B. Winkler, J.E. Bernard, R.K. Gupta, "Effects of Tire Properties on Truck and Bus Handling." Final Report on Contract DOT-HS-4-00943, Highway Safety Research Institute, University of Michigan, Report No. UM-HSRI-76-11, December 1976.
4. C.B. Winkler, "Measurement of Inertial Properties and Suspension Parameters of Heavy Highway Vehicles." SAE Paper No. 730182, January 1973.
5. P.S. Fancher, R.D. Ervin, C.C. MacAdam, and C.B. Winkler, "Measurement and Representation of Truck Leaf Springs." SAE Paper to be presented February 1980.
6. A.L. Nedley and W.J. Wilson, "A New Laboratory Facility for Measuring Vehicle Parameters Affecting Understeer and Brake Steer." SAE Paper No. 720473, May 1972.

APPENDIX A - WHEEL PAD ACTUATION

The purpose of the wheel pad actuation system is to provide

- 1) application of a controlled tire shear force in the h direction (F_h),
- 2) application of a controlled tire aligning moment (M_z), and
- 3) minimization of the rectilinear tire shear force (F_j) regardless of wheel motions and loads.

To accomplish these goals, an electrohydraulic servo actuation system was designed. The system employs two servo loops, each using two hydraulic cylinders plumbed in a "push-pull" arrangement. Each cylinder pair is driven by an electrohydraulic servo valve. Feedback derives from two strain-gauged load cells. A simplified system schematic appears in Figure A-1.

The schematic indicates that the force and moment signals (CF_h and CM_z) are operated on to produce the commands (C_1 and C_2) which are equivalent to the desired forces at the load cells.

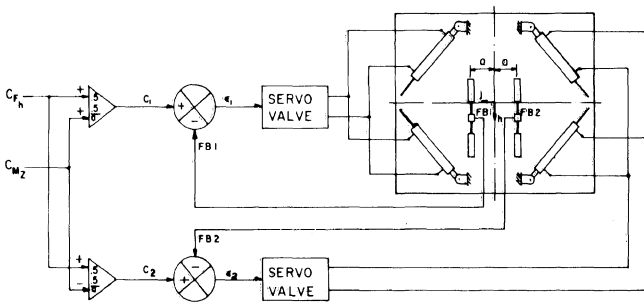


Fig. A-1 - Simplified schematic diagram of the wheel pad control system

These commands are combined with the appropriate load cell feedback signals to produce the error signals (ϵ_1 and ϵ_2) which drive the servo valves, and ultimately, the actuation cylinders. Thus, it is the operation of the servo system which insures control of F_h and M_z . (See Appendix B for an explanation of the load cell transducer system.)

It is the geometry of the actuator cylinders and the "push-pull" plumbing arrangement of cylinder pairs which insures the minimizing of F_j . Perhaps the most convenient method of illustrating the advantage of the "push-pull" cylinder pairing is through comparison with a single cylinder actuation system. Consider Figure A-2 which compares the behavior of a wheel pad actuated by a two-cylinder system with the behavior of a wheel pad actuated by two "push-pull" cylinder pairs. (In Figure A-2, the "push-pull" cylinder pairs are shown to be aligned when the pad is in its neutral position. This is done to simplify the following discussion. The points which will be made generally hold for the actual cylinder geometry shown in Figure A-1.)

Figure A-2a illustrates that, when the wheel pad is in a centered position, the application of F_h (or M_z) does not result in the generation of any F_j , because all cylinders are aligned in the h direction and, therefore, can exert no force in the j direction. However, Figure A-2b shows that, if the wheel pad is displaced in the j direction, then a non-zero F_j results. For the two-cylinder arrangement, the j displacement of the pad results in:

$$F_j = (F_{C_1} + F_{C_2}) \sin \theta = F_h \tan \theta \quad (A.1)$$

That is, F_j is equal to the sum of the cylinder force components in the j direction, which, given that $F_h = (F_{C_1} + F_{C_2}) \cos \theta$, implies that $F_j = F_h \tan \theta$.

For the four-cylinder arrangement, F_j is again equal to the sum of the cylinder components in the j direction, i.e.,

$$F_j = (F_{C_1} + F_{C_2} - F_{C_3} - F_{C_4}) \sin \theta \quad (A.2)$$

In this case, however, the j components of F_{C_3} and F_{C_4} have the opposite direction of those of F_{C_1} and F_{C_2} . Thus, the four components tend to cancel one another.

The resulting F_j is not reduced to zero, but is attenuated by the factor $a/(2A-a)$ where A is the cylinder bore area and a is the cylinder rod area. That is,

$$F_j = \frac{a}{2A-a} F_h \sin \theta \quad (A.3)$$

That is, if cylinders 1 and 3 of the four-cylinder wheel pad of Figure A-2b are actuated by a pressure, P_1 , and cylinders 2 and 4 are actuated by a pressure, P_2 , then:

$$F_{C_1} = A P_1 \quad (A.4a)$$

$$F_{C_2} = A P_2 \quad (A.4b)$$

$$F_{C_3} = (A-a) P_1 \quad (A.4c)$$

$$F_{C_4} = (A-a) P_2 \quad (A.4d)$$

and

$$F_h = (F_{C_1} + F_{C_2} + F_{C_3} + F_{C_4}) \cos \theta \quad (A.5)$$

$$F_j = (F_{C_1} + F_{C_2} - F_{C_3} - F_{C_4}) \sin \theta \quad (A.6)$$

Equations (A.4), (A.5), and (A.6) can be solved to obtain Equation (A.3).

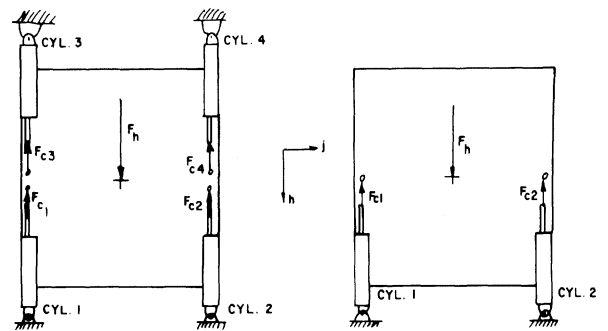


Fig. A-2a - In the centered position, two- and four-cylinder arrangements produce zero F_j

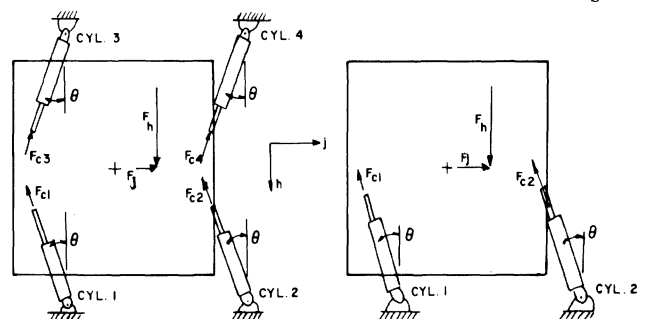


Fig. A-2b - In an off-center position, the two-cylinder arrangement produces a larger F_j component

Table A-1

Pad Displacement			F_j Sensitivity			
Inches, h Direction	Inches, j Direction	Degrees, z Direction	Pounds, F_j per Pound F_h		Pounds, F_j per in-lb M_z	
			4-Cyl.	2-Cyl.	4-Cyl.	2-Cyl.
0	0	0	0	0	0	0
2	0	0	0	0	-.005	0
0	2	0	.003	.143	.001	0
2	2	0	.005	.167	-.004	0
0	0	4	.020	.002	0	0
2	0	4	.030	.003	-.005	0
0	2	4	.021	.146	.001	-.001
2	2	4	.033	.171	-.004	-.001

For the cylinders used in the wheel pads of this facility, the factor $a/(2A-a) = .05$. Thus, it can be seen that the use of two "push-pull" cylinder pairs can generally reduce the value of the unwanted F_j force to about 5% of the F_j force which results from a simple two-cylinder arrangement under conditions of lateral pad displacement.

The four-cylinder arrangement is not so advantageous when the pad takes on a non-zero rotational position. Generally, both the two- and four-cylinder arrangements will produce a small F_j when generating F_h , essentially because the cylinders do not all assume the same angular displacements. In this case, the four-cylinder arrangement produces larger values of F_j . However, the sensitivity of the four-cylinder arrangement under angular displacement conditions remains substantially smaller (approximately 20%) than the sensitivity of the two-cylinder arrangement under comparable lateral displacement conditions.

The angular arrangement of cylinders actually used in the test facility alters these sensitivities somewhat, but provides a more space-efficient wheel pad package. Table A-1 provides a comparison of F_j sensitivities calculated for the actual geometry of the wheel pad of the facility and compares them to those of a two-cylinder actuation system. The table indicates that:

-A two-cylinder mechanism produces a rather large F_j force under conditions of large j displacement while generating an F_h force.

-The four-cylinder mechanism produces a small to moderate F_j force under conditions of large angular displacement while generating an F_h force.

-Neither system produces significant F_j forces under any displacement condition while generating aligning moment.

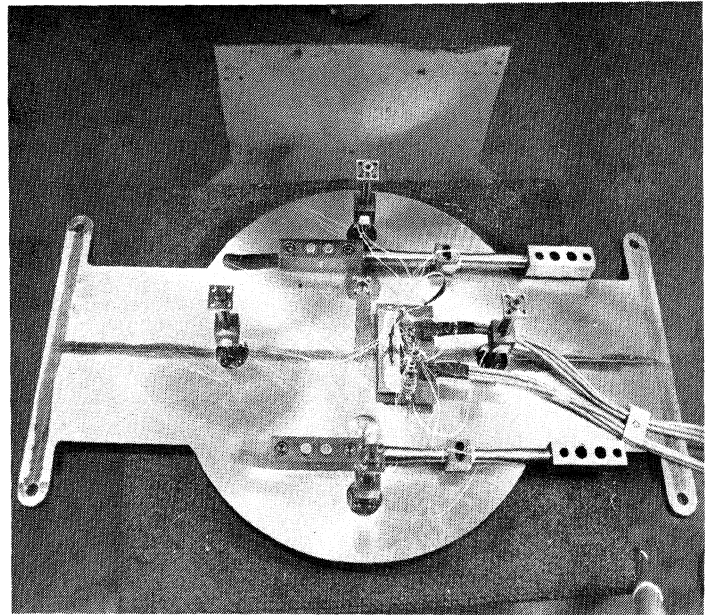


Fig. B-1 - A load cell/flexure group

APPENDIX B - WHEEL PAD FORCE TRANSDUCTION

As shown in Figure 8 of the text, the wheel pad assemblies each contain six discrete load cell/flexure members plus a lateral constraint, flexure link. Thus, the four wheel pad assemblies house the four transduction systems for the suspension test facility.

Figure B-1 shows a set of six load cell/flexures installed on the underside of a lower bearing plate. Each of the six elements is strain gauged to transduce the tensile/compressive load oriented in its own longitudinal direction while being relatively insensitive to other loads. Further, each element has a longitudinal-to-lateral-stiffness ratio on the order of 1000:1. These factors, plus the precise, rectangular orientation of the elements ensures good isolation of the appropriate

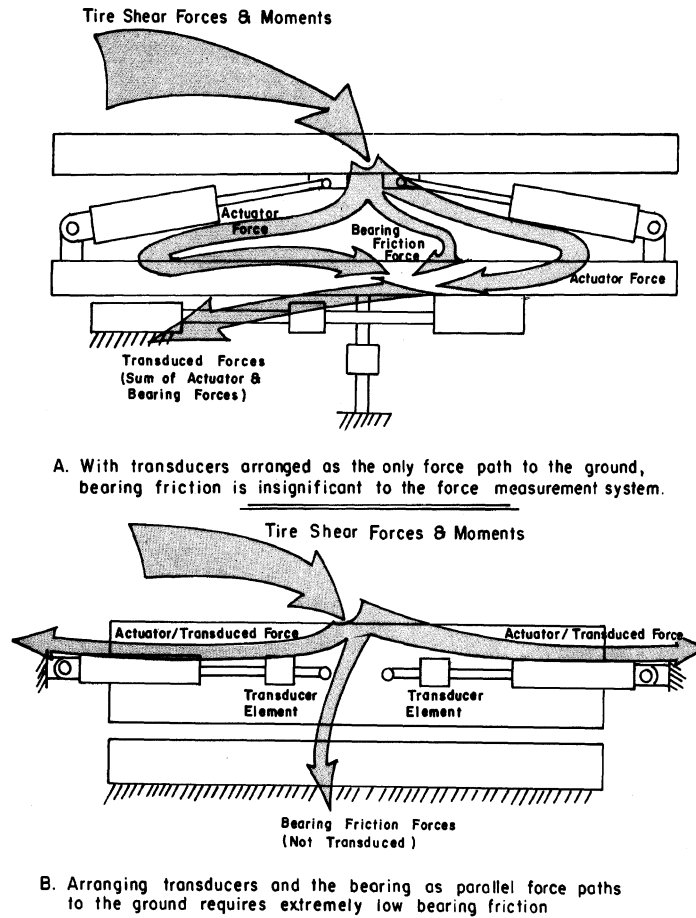


Fig. B-2 - Force flow through the bearing and transducers

forces and moments (force couples) and results in a minimum of cross-talk in the system.

It is of significance that the entire force transduction system is fixed in the base frame of the wheel pad, i.e., there are no elements located in the movable upper bearing plate. Thus, the transduced shear forces remain purely lateral (or longitudinal) with respect to the sprung mass regardless of the motion induced by the wheel pad actuation system.

The location of the transducer system also ensures that the transduced forces are equivalent to the tire-road interface forces regardless of the frictional quality of the wheel pad bearing. (This fact allowed the use of a simple ball bearing rather than a hydro-static fluid bearing as used by HSRI and others (6) in facilities of similar purpose.) That is, in the subject facility, the actuation cylinder forces and the bearing frictional forces are, of course, in parallel,

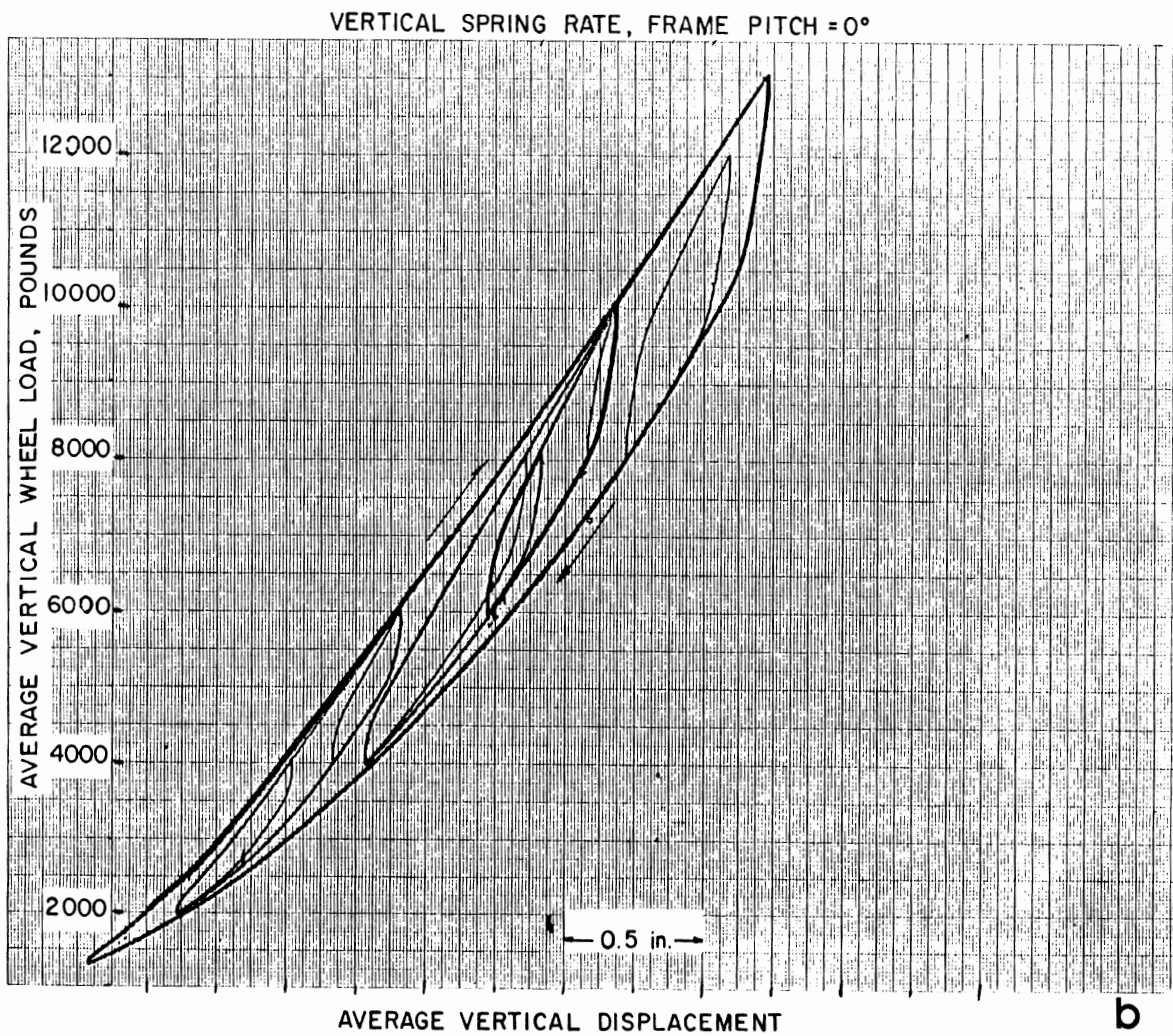
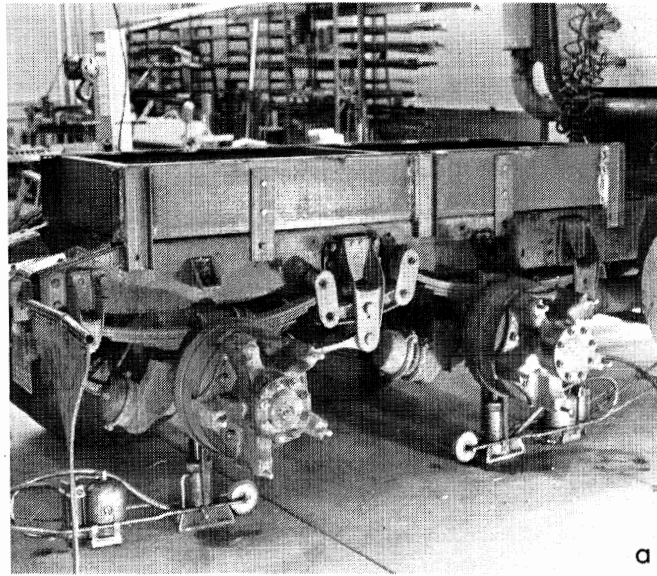
but they are recombined in the lower bearing plate prior to passing through the transducers. Thus, the load cell assembly represents the only significant force path to ground*, rather than being in parallel with the bearing interface. Figure B-2 illustrates the point.

APPENDIX C - TWO PRELIMINARY DATA SETS

Note: This data was collected prior to the completion of a digital data acquisition system. Consequently, roll moment data must be considered to be approximate. Errors will exist in the roll moment data due to the absence of overturning moment measurements at individual wheel pads.

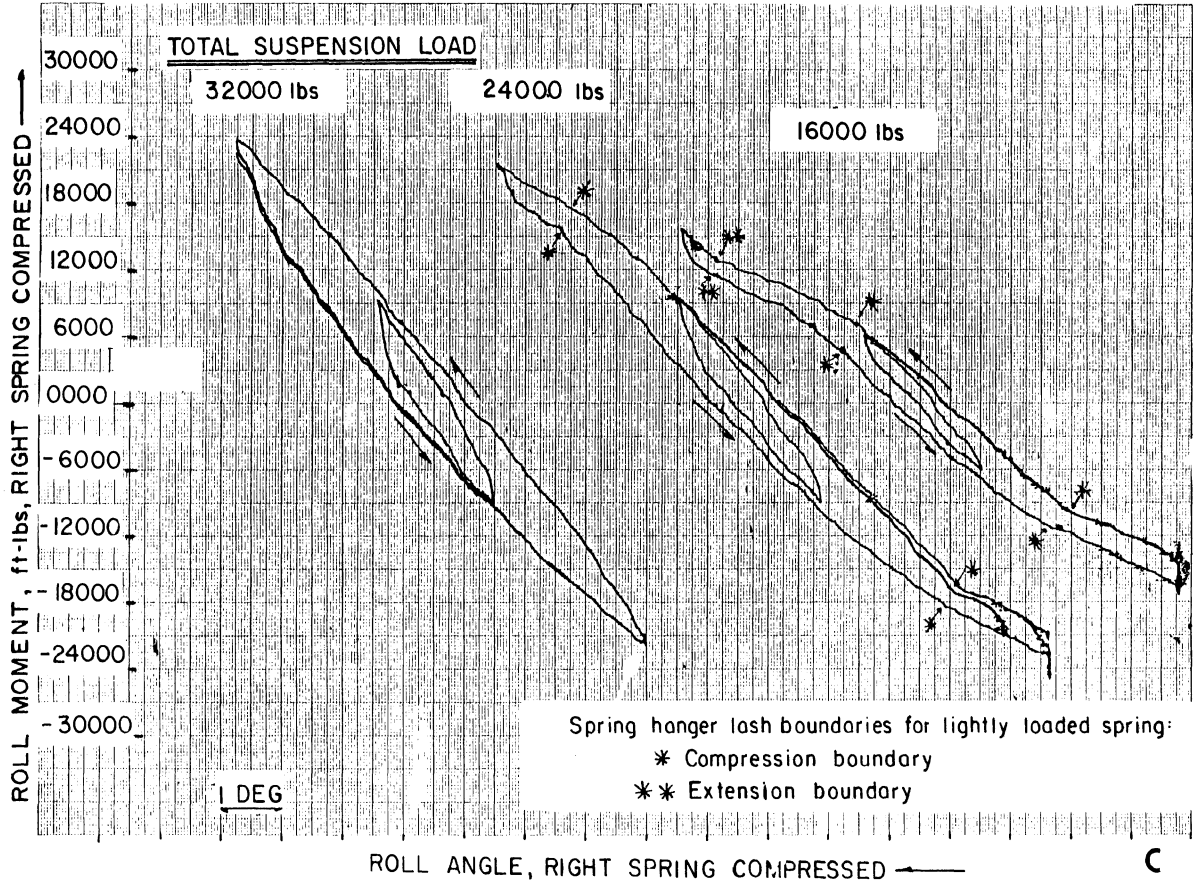
*Flexible hydraulic lines do represent a parallel force path to ground.

Fig. C-1 - Test suspension #1

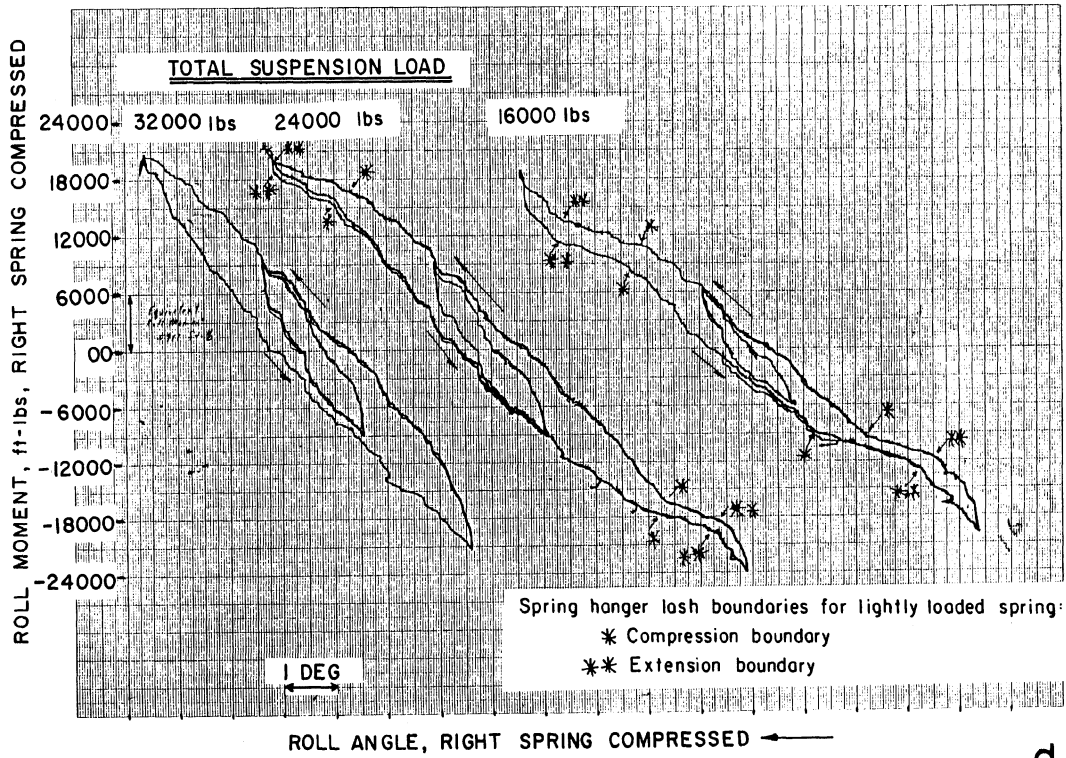


b

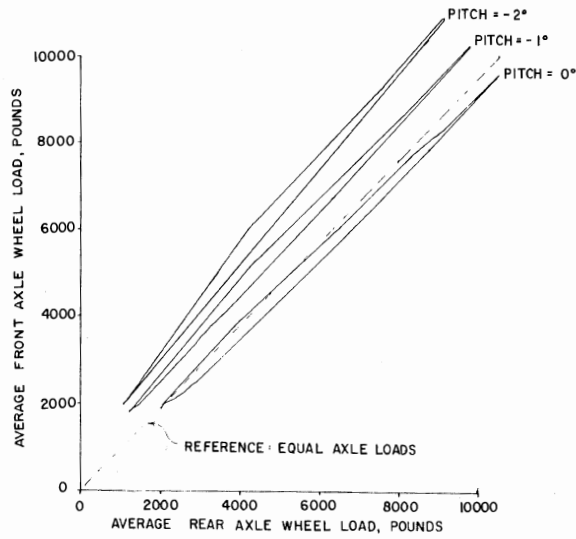
ROLL RATE, FRONT AXLE, FRAME PITCH = 0° (Measurement simultaneous with rear axle)



ROLL RATE, REAR AXLE, FRAME PITCH = 0° (Measurement simultaneous with front axle)

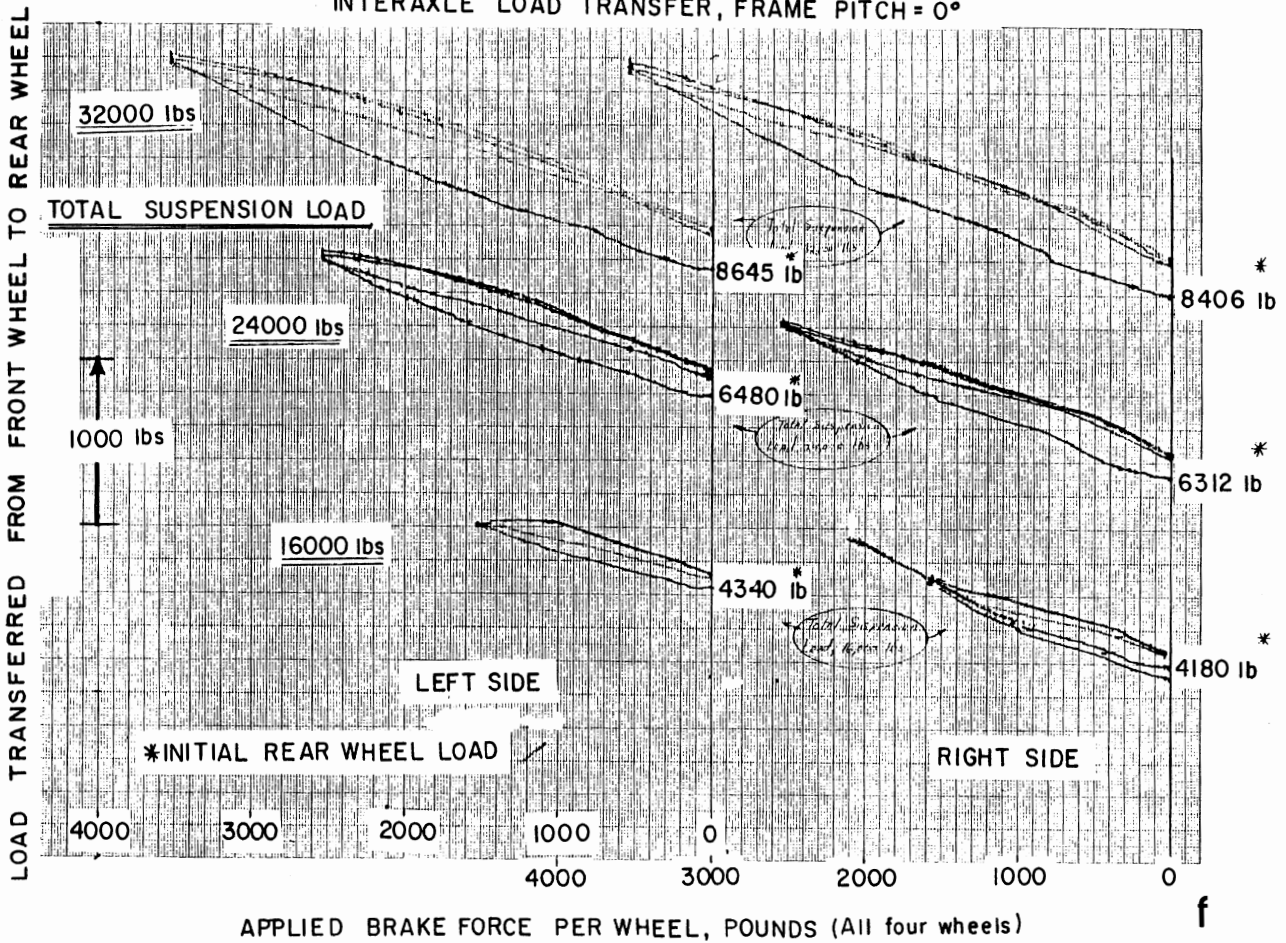


INTERAXLE LOAD DISTRIBUTION AS A FUNCTION OF FRAME PITCH. BRAKE FORCE = 0 lbs.

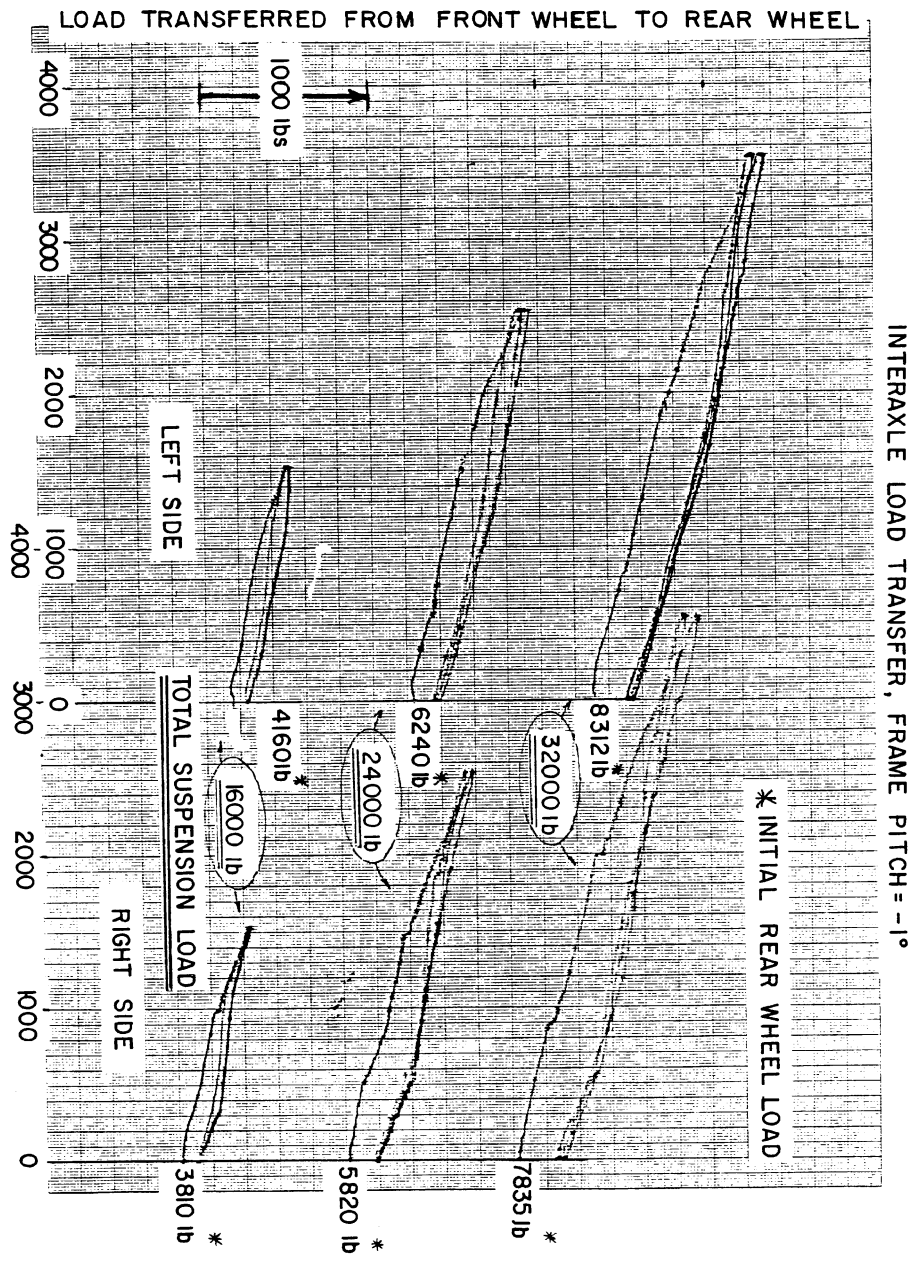


e

INTERAXLE LOAD TRANSFER, FRAME PITCH = 0°

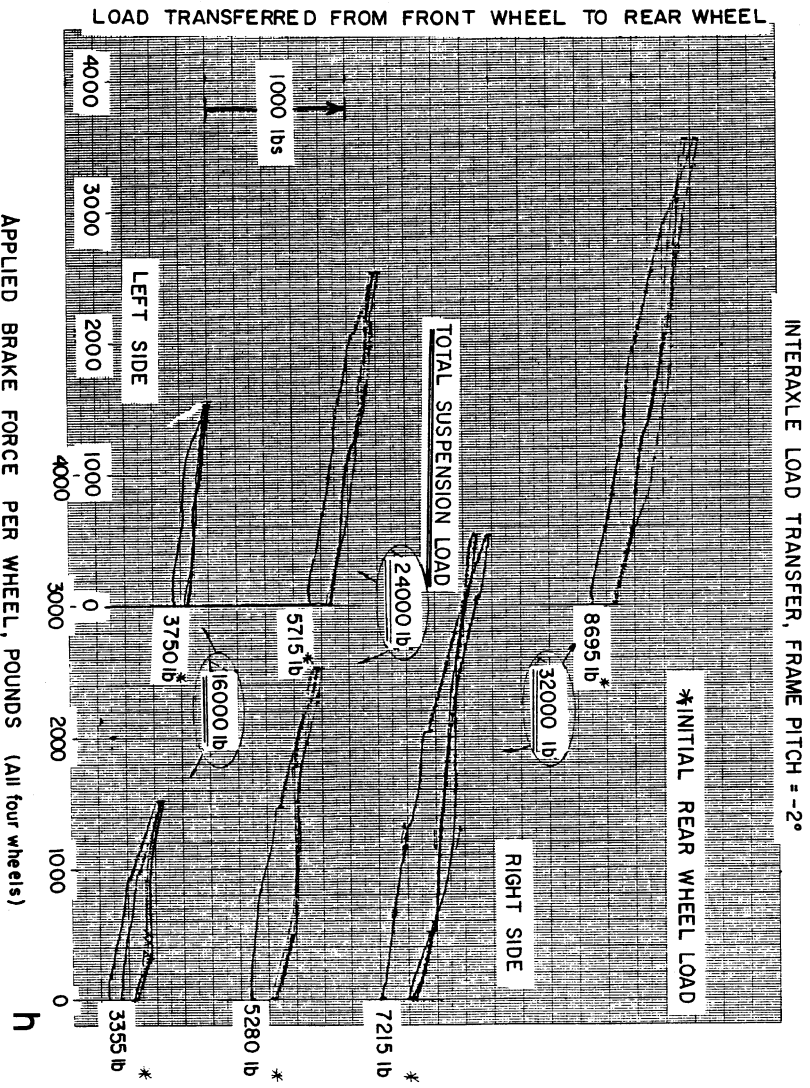


f



APPLIED BRAKE FORCE PER WHEEL, POUNDS (All four wheels)

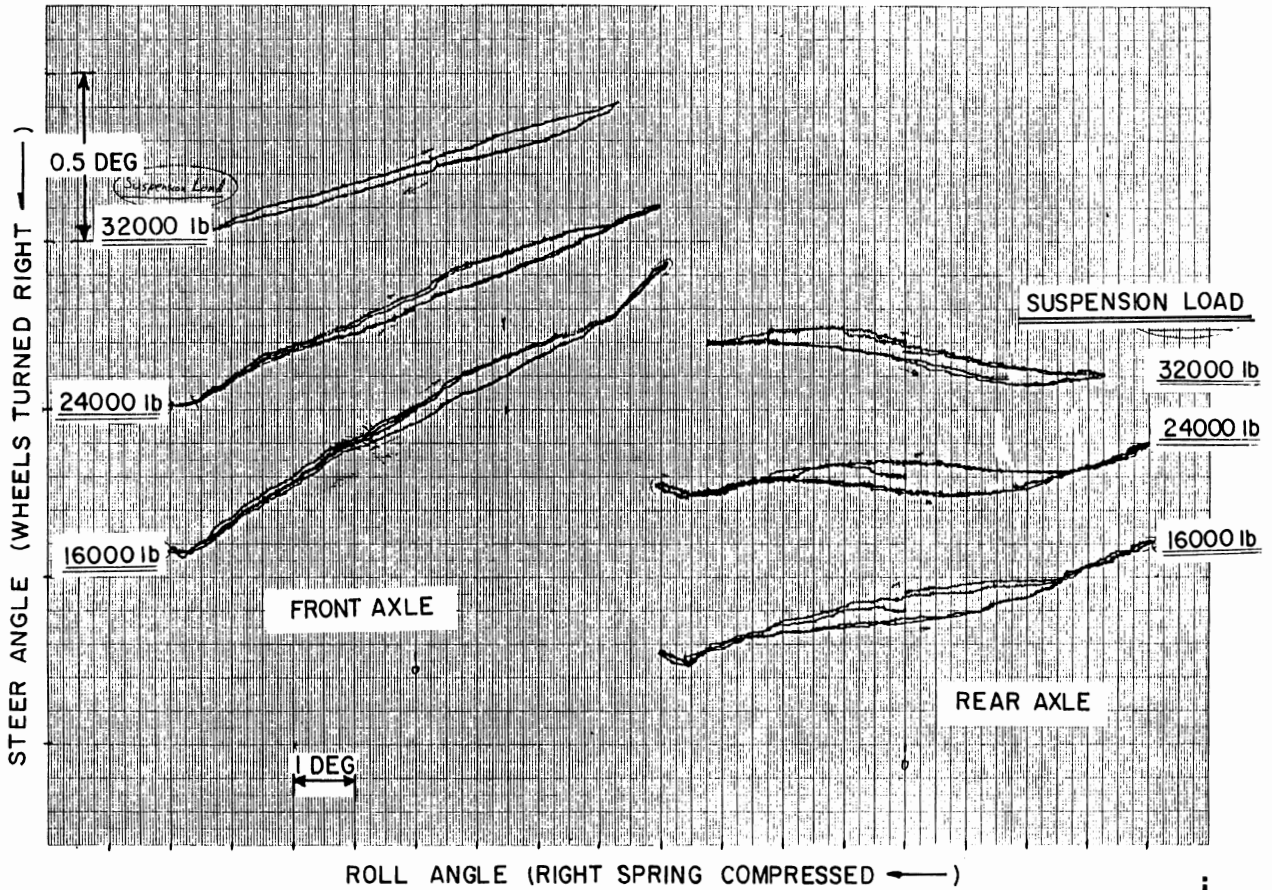
g



APPLIED BRAKE FORCE PER WHEEL, POUNDS (All four wheels)

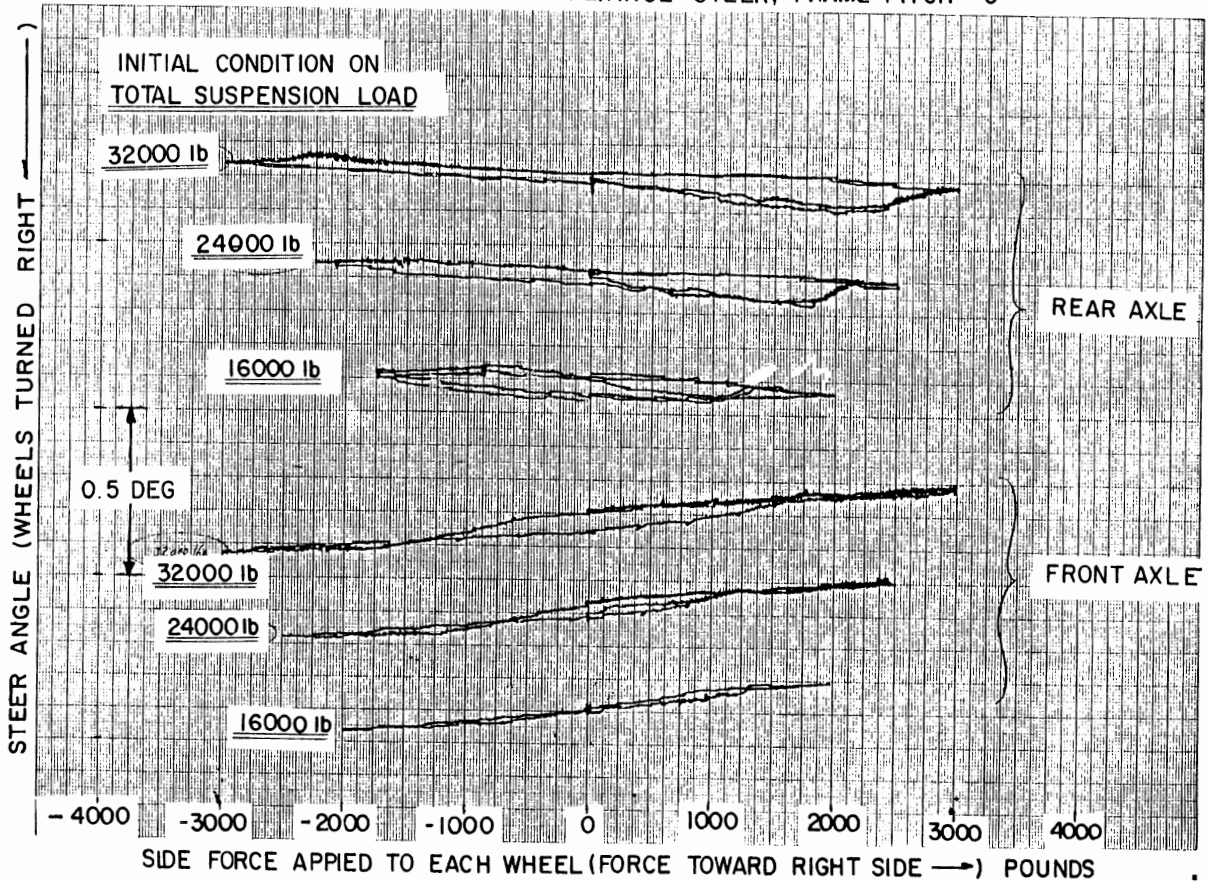
h

ROLL STEER, FRAME PITCH = 0°



i

LATERAL FORCE COMPLIANCE STEER, FRAME PITCH = 0°



j

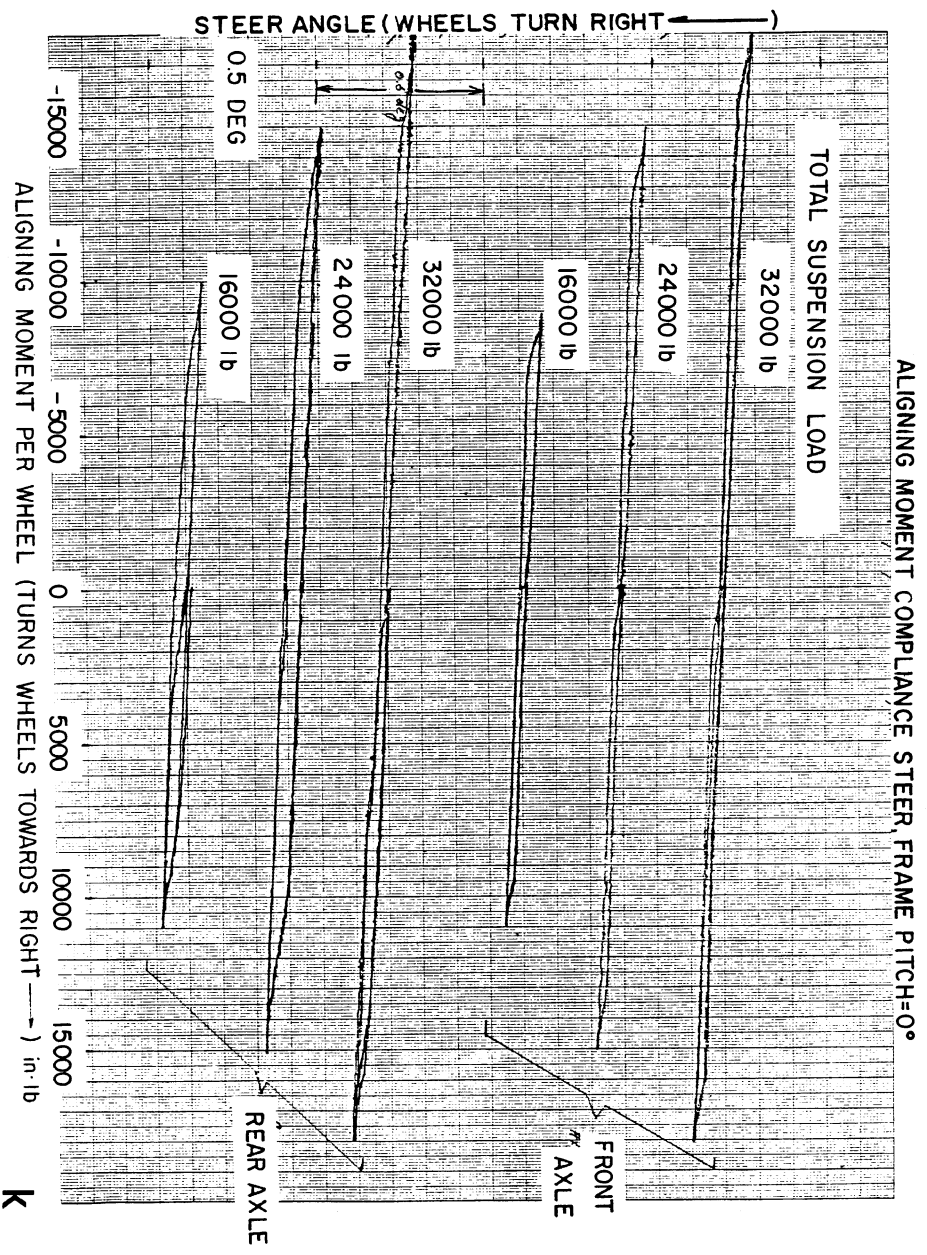
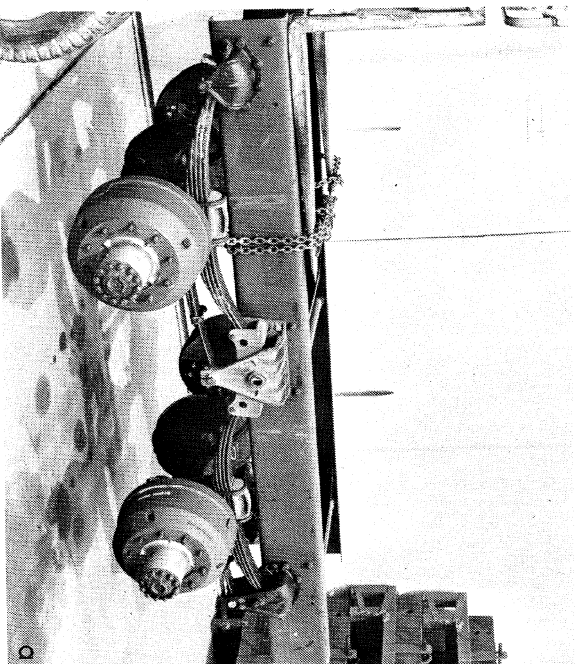
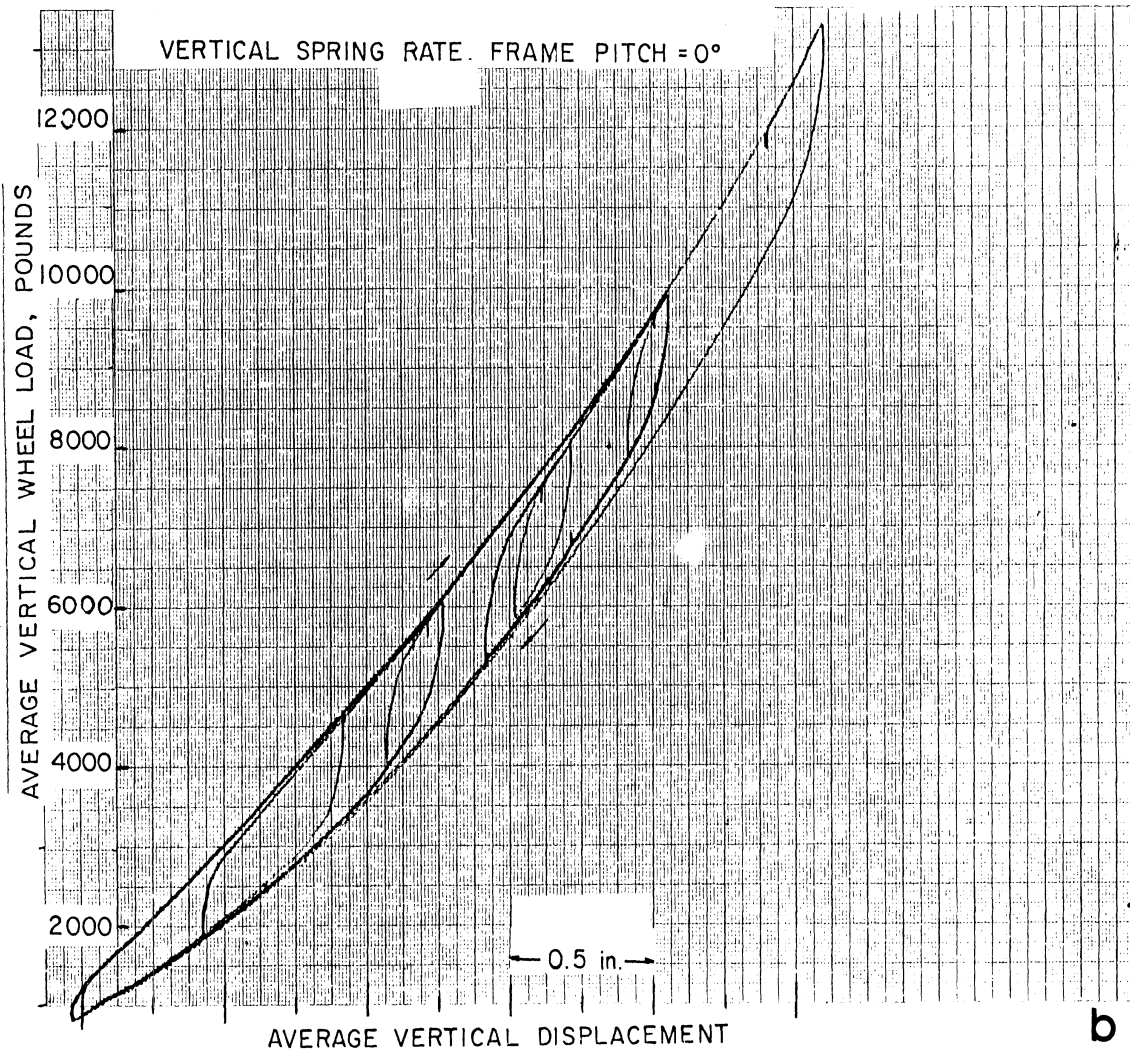
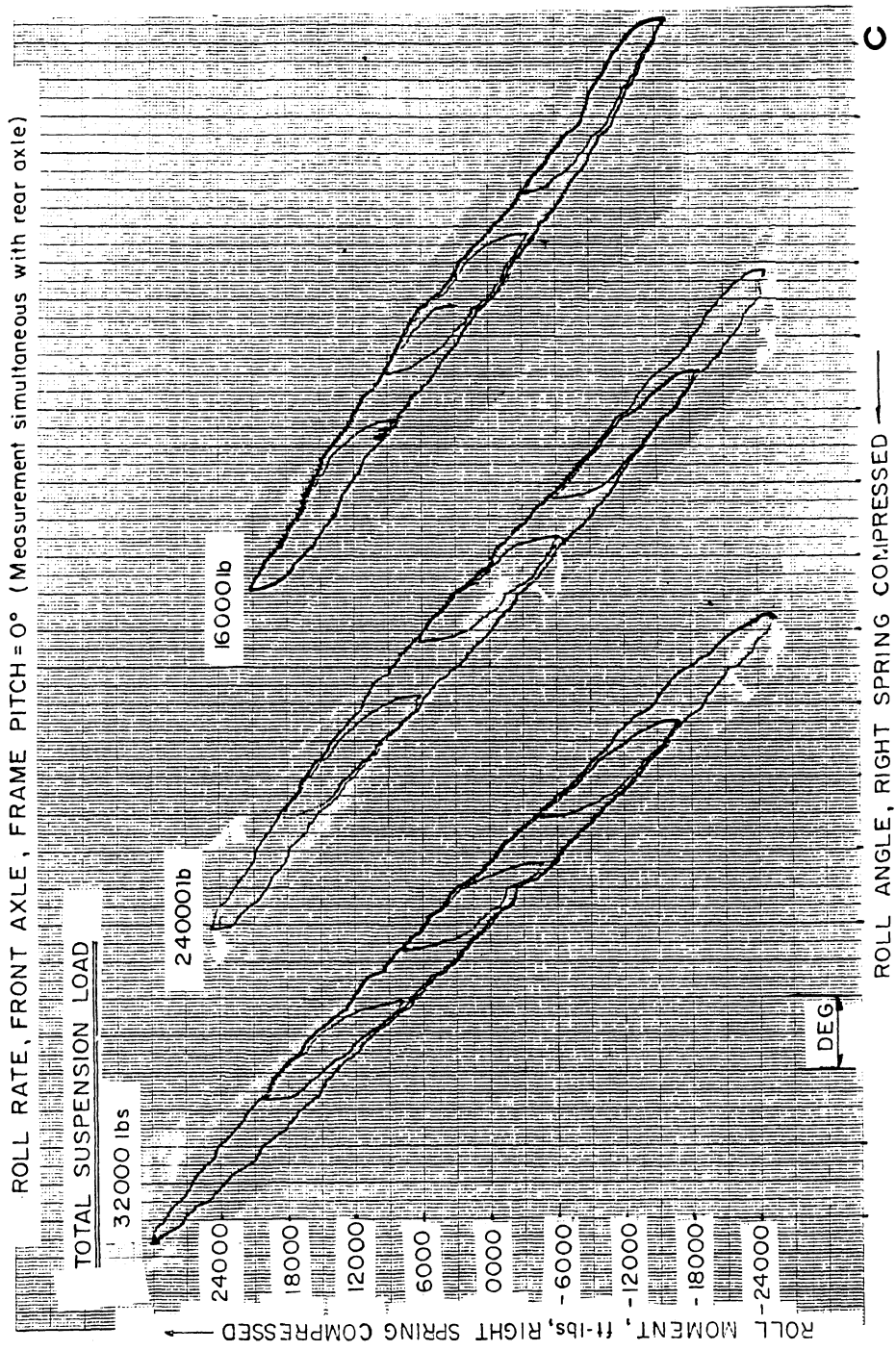


Fig. C-2 - Test suspension #2

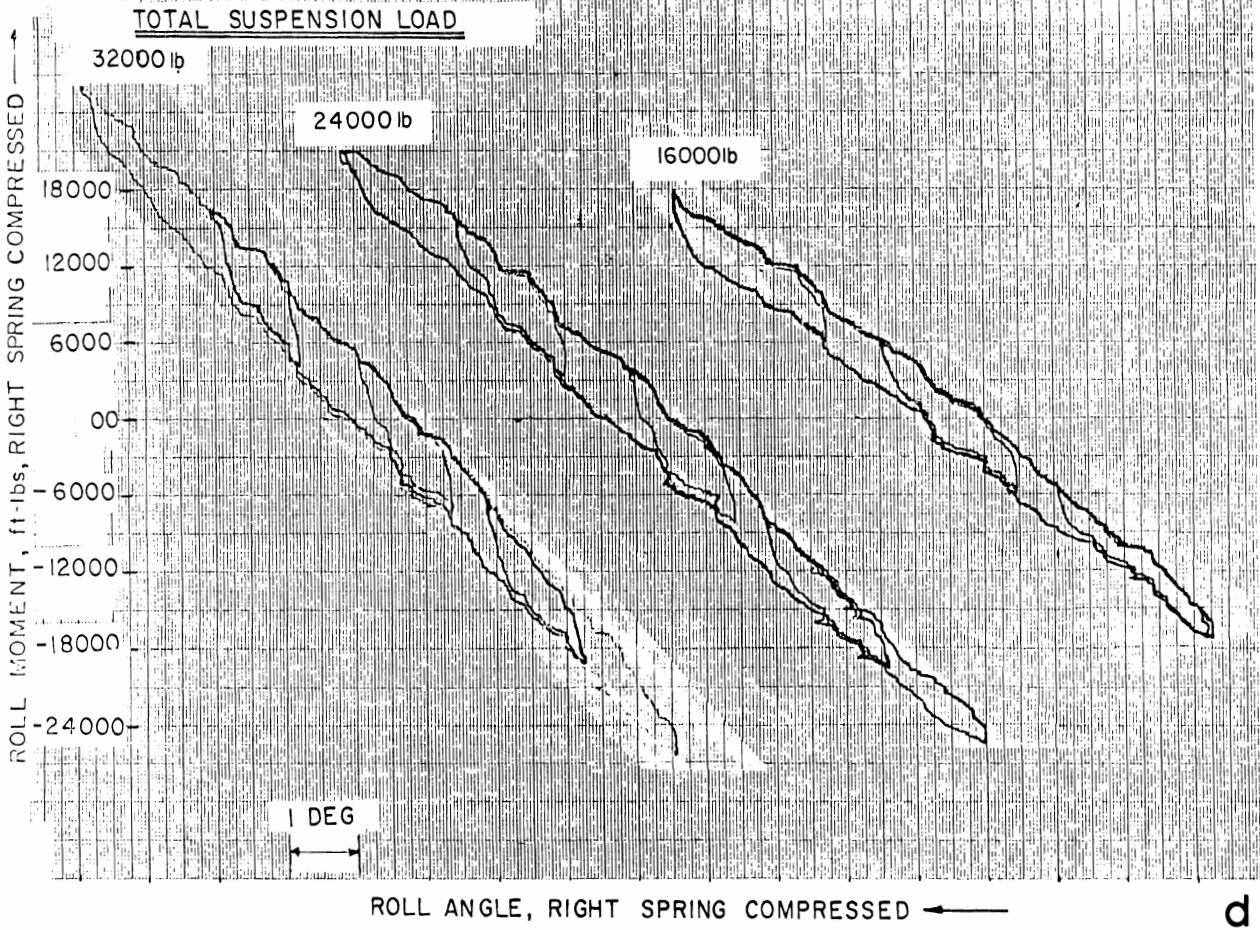


Q



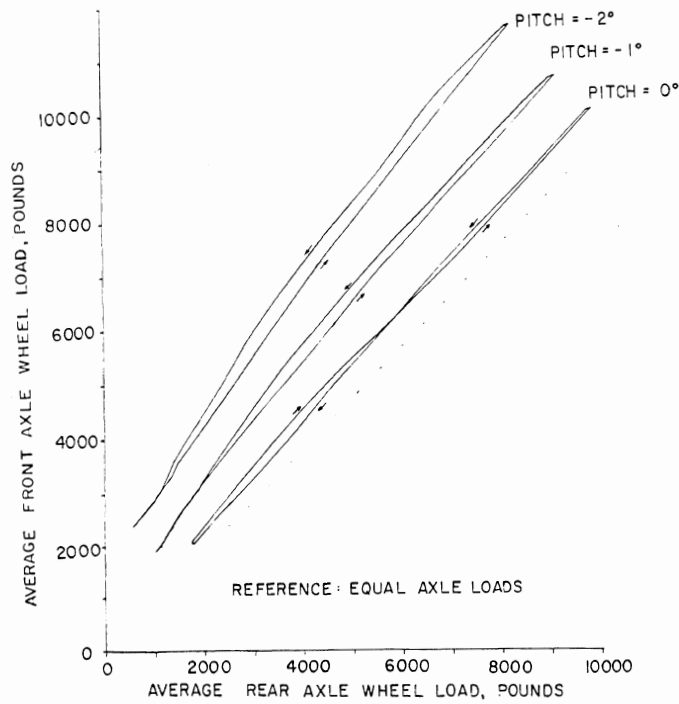


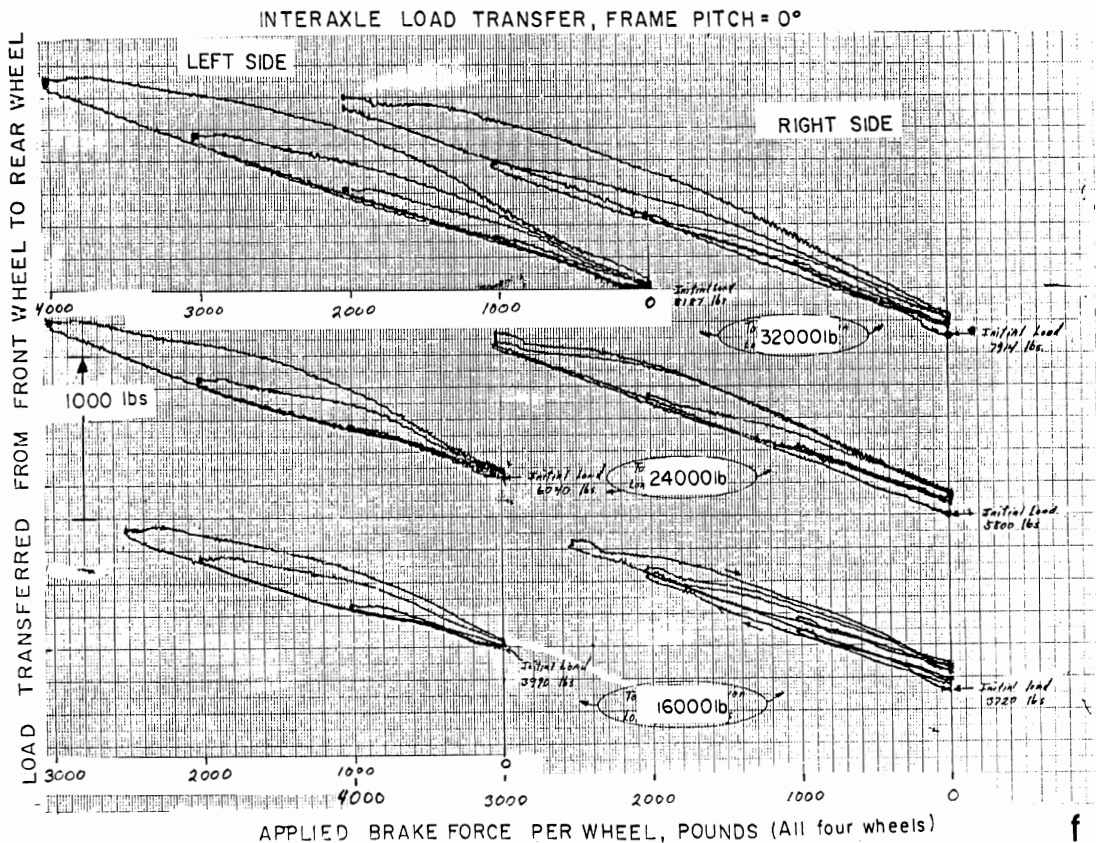
ROLL RATE, REAR AXLE, FRAME PITCH = 0° (Measurement simultaneous with front axle)



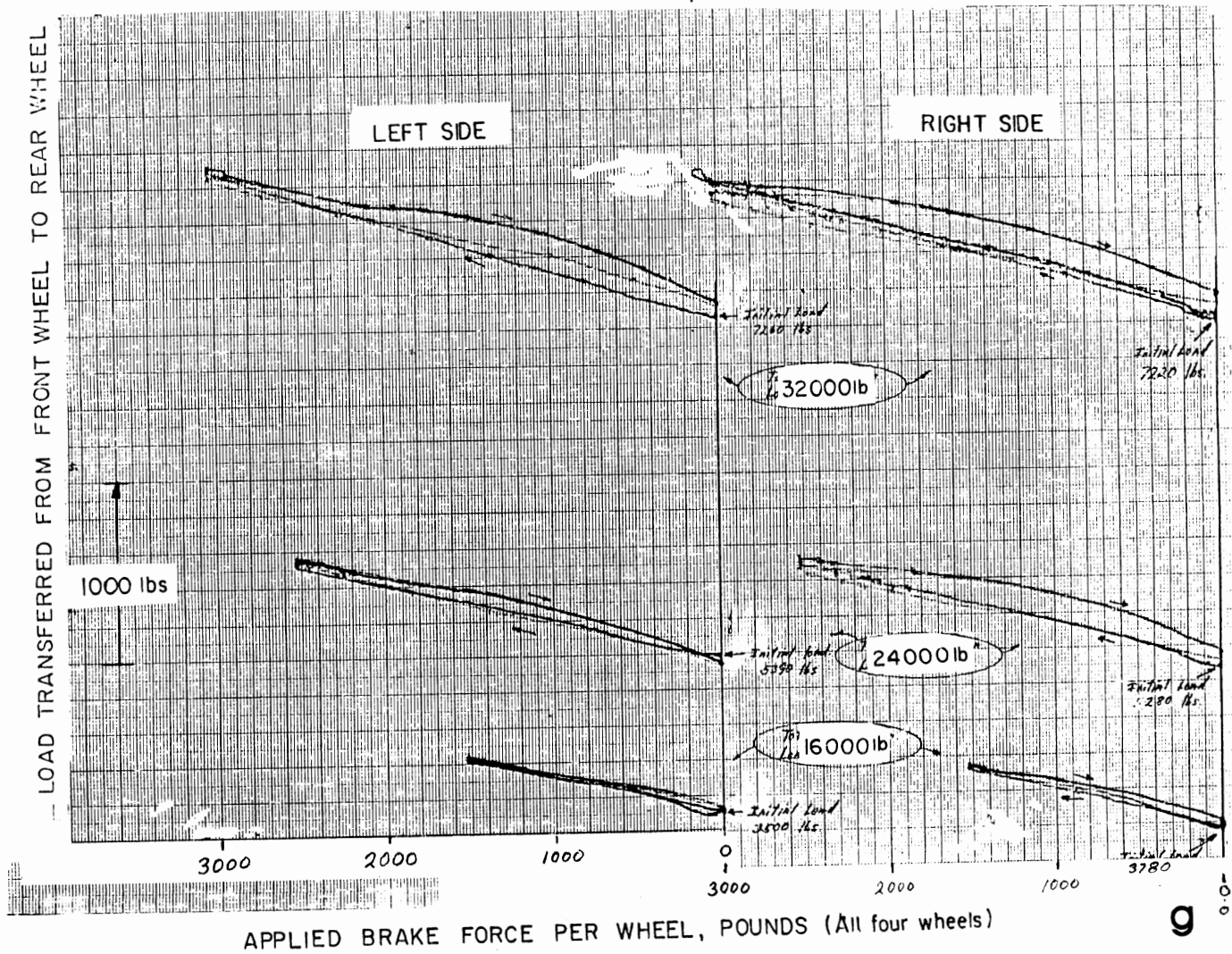
INTERAXLE LOAD DISTRIBUTION AS A FUNCTION OF FRAME PITCH.

BRAKE FORCE = 0 lbs.

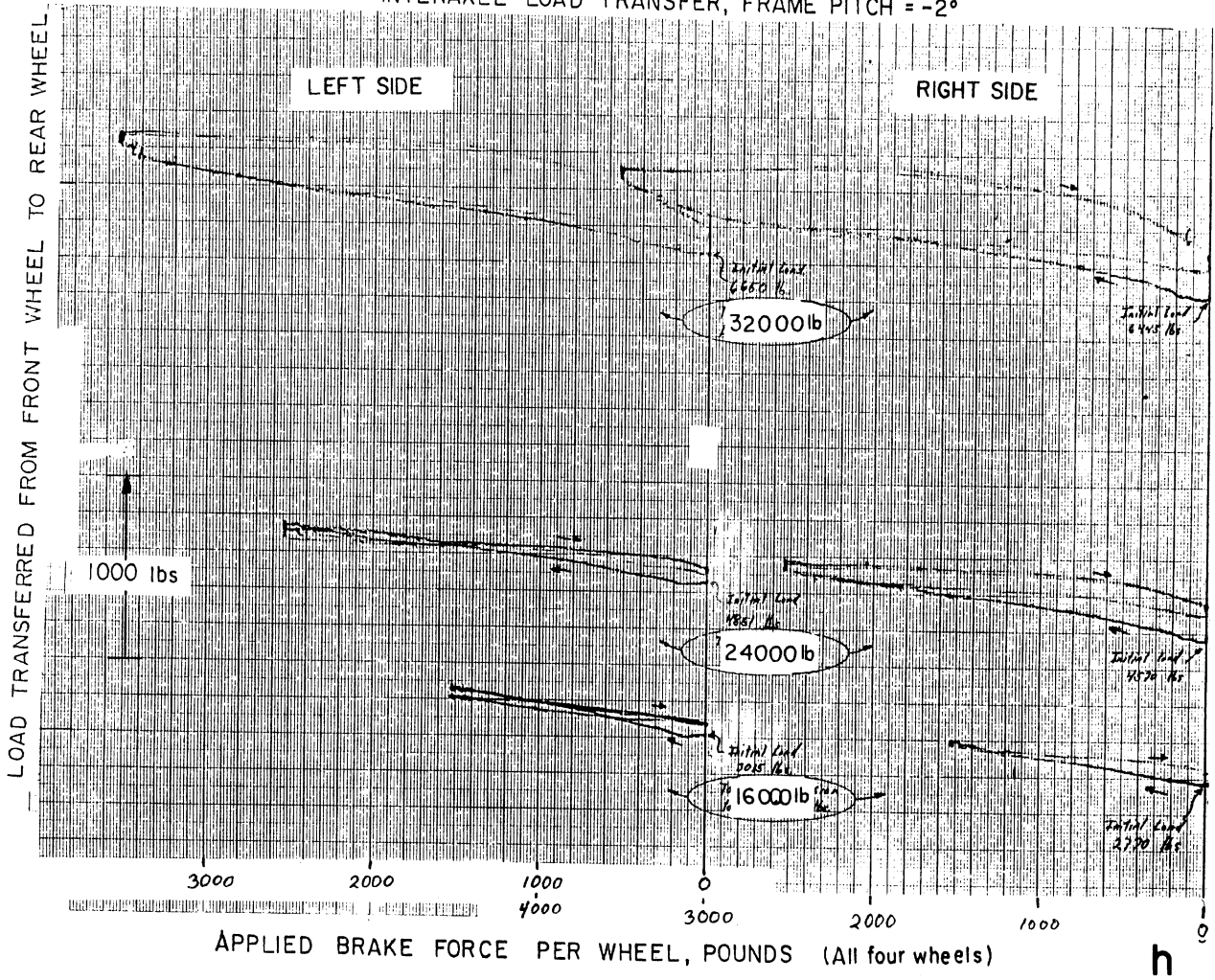


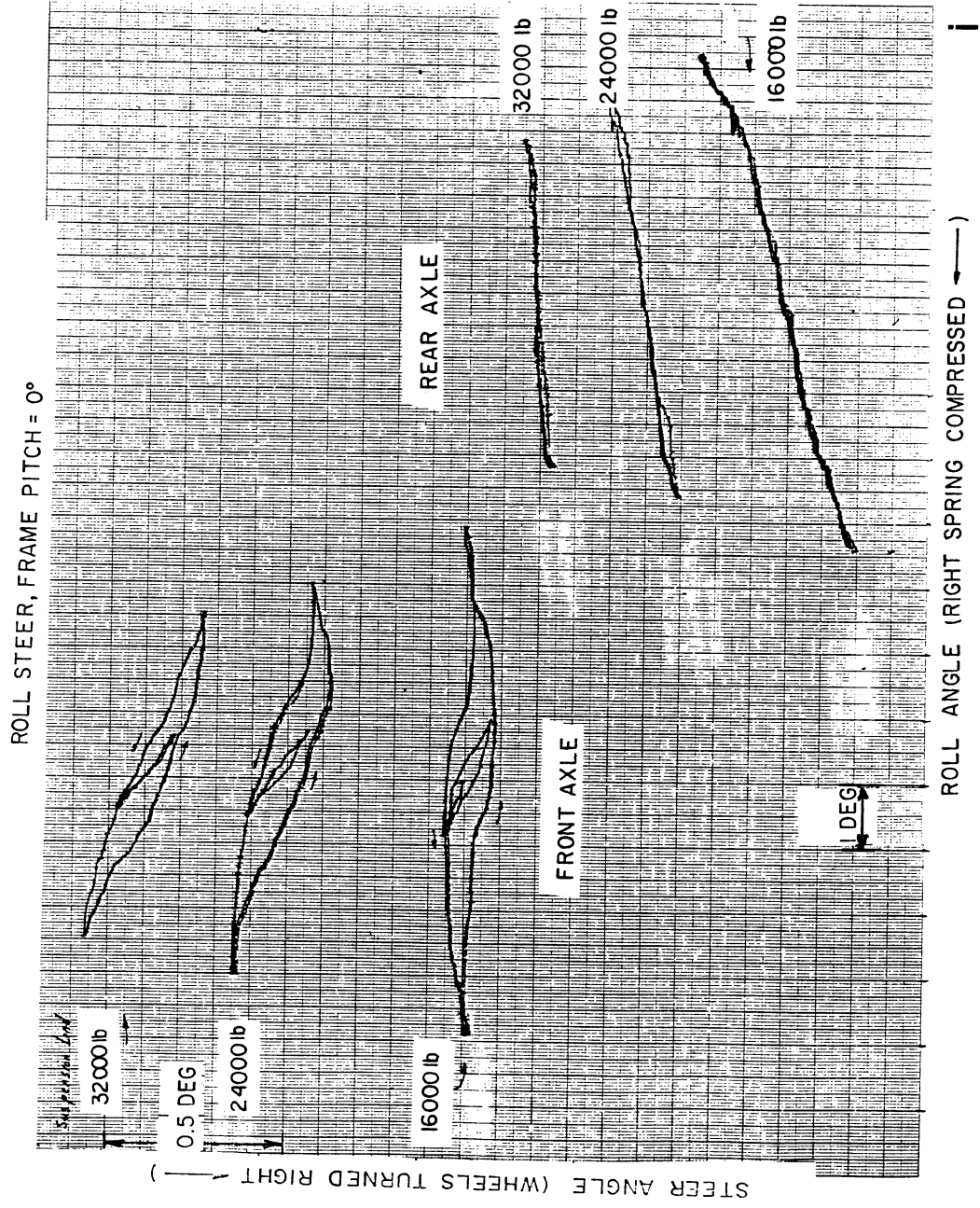


INTERAXLE LOAD TRANSFER, FRAME PITCH = -1°

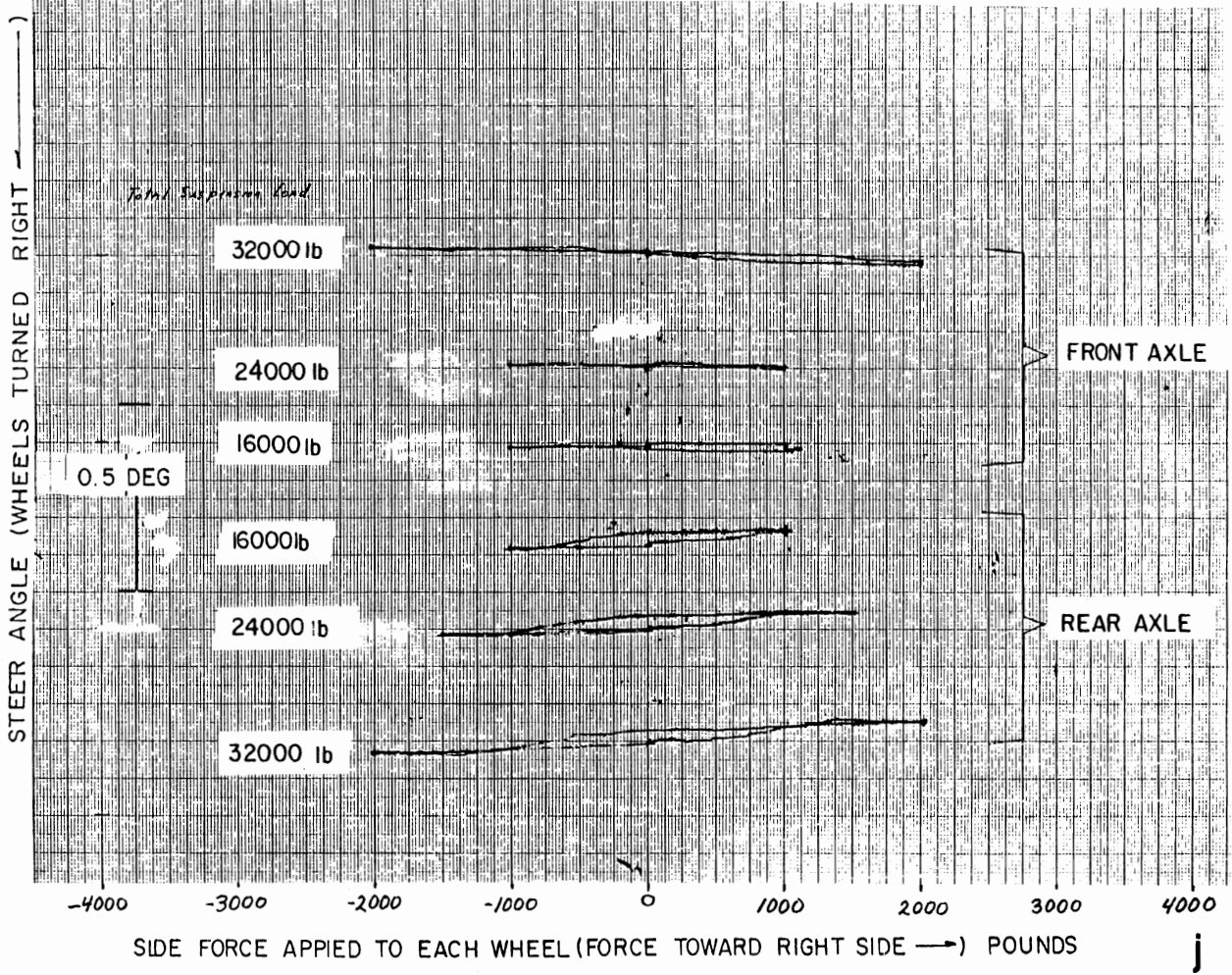


INTERAXLE LOAD TRANSFER, FRAME PITCH = -2°





LATERAL FORCE COMPLIANCE STEER, FRAME PITCH = 0°





This paper is subject to revision. Statements and opinions advanced in papers or discussion are the author's and are his responsibility, not the Society's; however, the paper has been edited by SAE for uniform styling and format. Discussion will be printed with the paper if it is published in SAE Transactions.

Society of Automotive Engineers, Inc.

400 COMMONWEALTH DRIVE, WARRENDALE, PA 15096

For permission to publish this paper in full or in part, contact the SAE Publications Division.

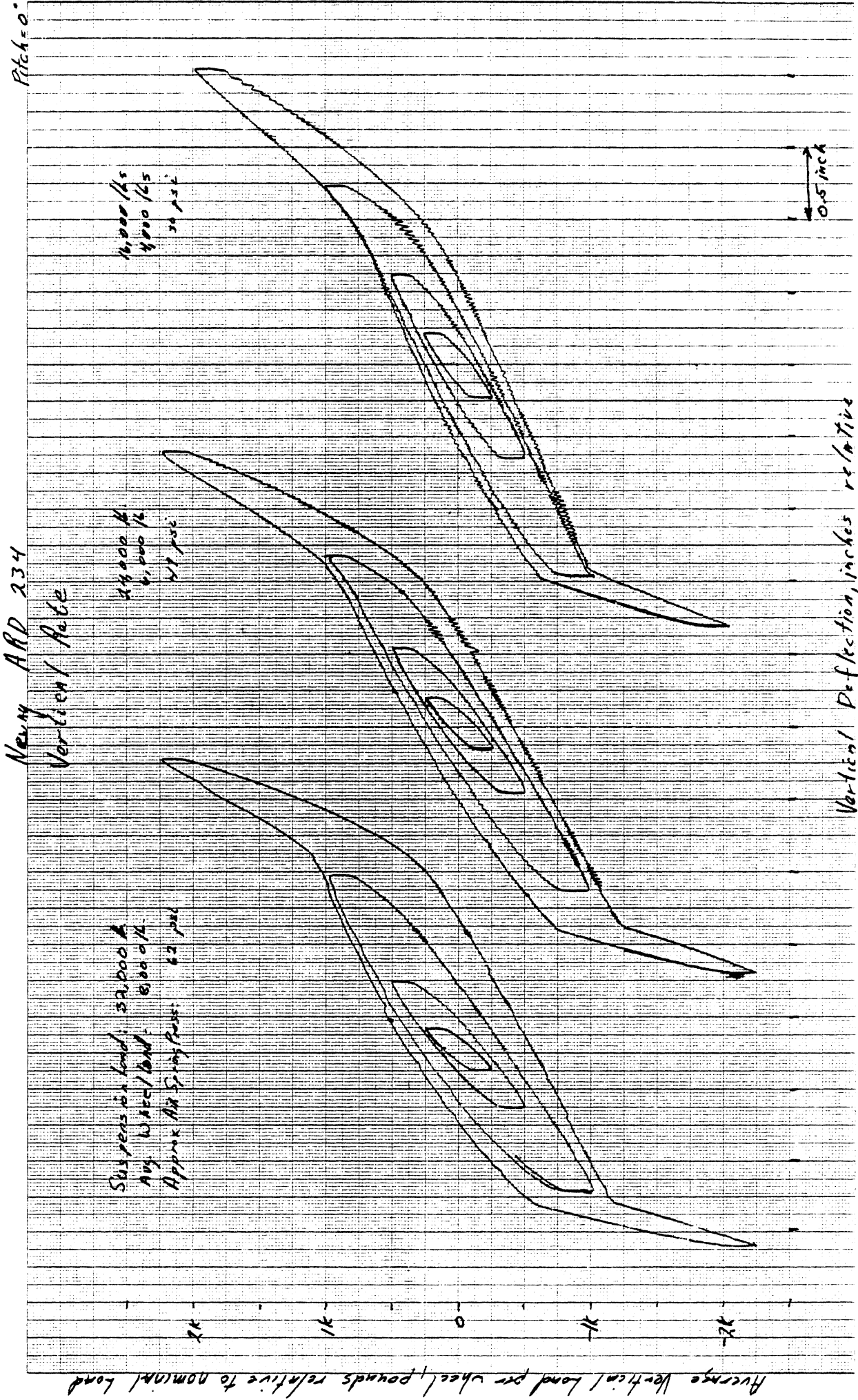
Persons wishing to submit papers to be considered for presentation or publication through SAE should send the manuscript or a 300 word abstract of a proposed manuscript to: Secretary, Engineering Activity Board, SAE.

32 page booklet.

Printed in U.S.A.

ADDITIONAL DATA SETS

1. A Neway air suspension, ARD 234
2. A Freightliner air suspension
3. A Reyco 101F multileaf suspension of the same type as suspension #1 of SAE paper 800906
4. A Freightliner four spring FH-38-A
5. A front suspension installed on a Ford CL-9000 tractor



Pitch = 0°

Heavy ARD 234

Front Axle Roll Rate

Gross Suspension Load 52000 Kg

16,000 Kg

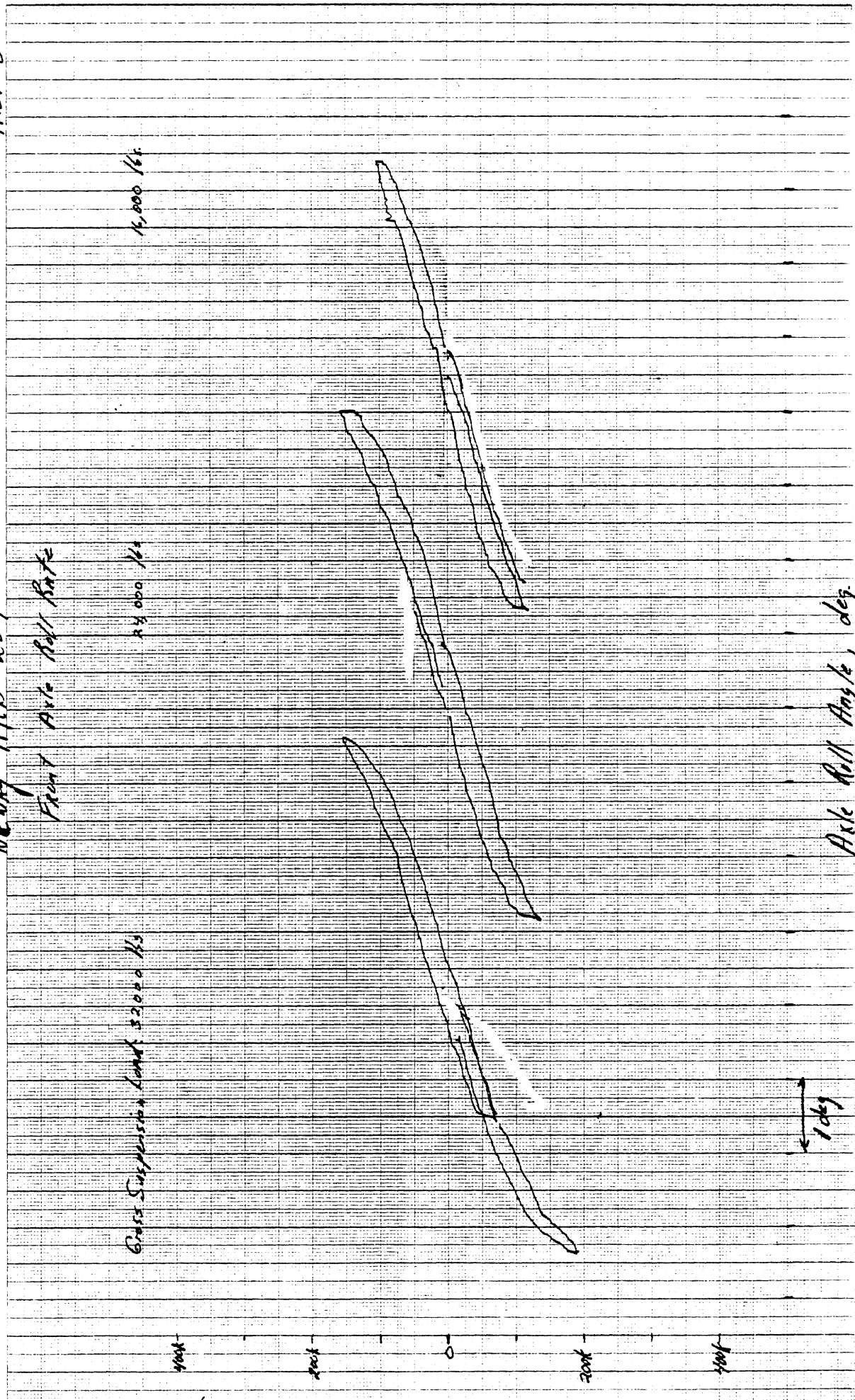
24,000 Kg

Axle Roll Angle, deg.

1 deg

Roll Moment on Axle, in-lb (→ Right Side Compressed)

4000
3000
0
3000
4000



Neway ARP 234

Pitch = 0°

Rear Axle Roll Rate

Gross Suspension Load:
73,000

16,000

24,000

Roll Moment on Axle, in-lb (Right Side Compressed) →

4000

2000

0

2000

4000

1000

Axle Roll Angle, deg.

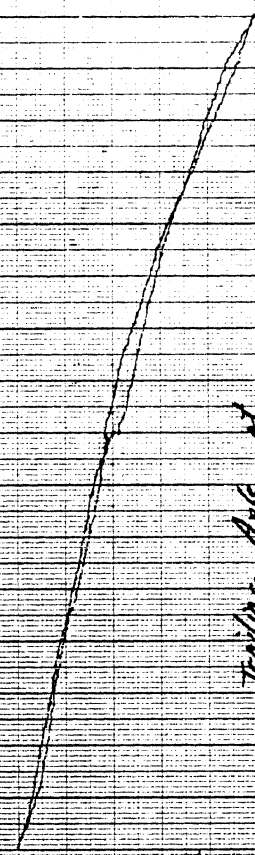
Pitch = 0.

Neway ARD 234

Aligning Moment Compliance Steer

Steer Angle, Degrees (← wheels turned toward right)

5
4
3
2
1
0
1
2
3
4
5



Leading Axle at
Nominal Ride Height

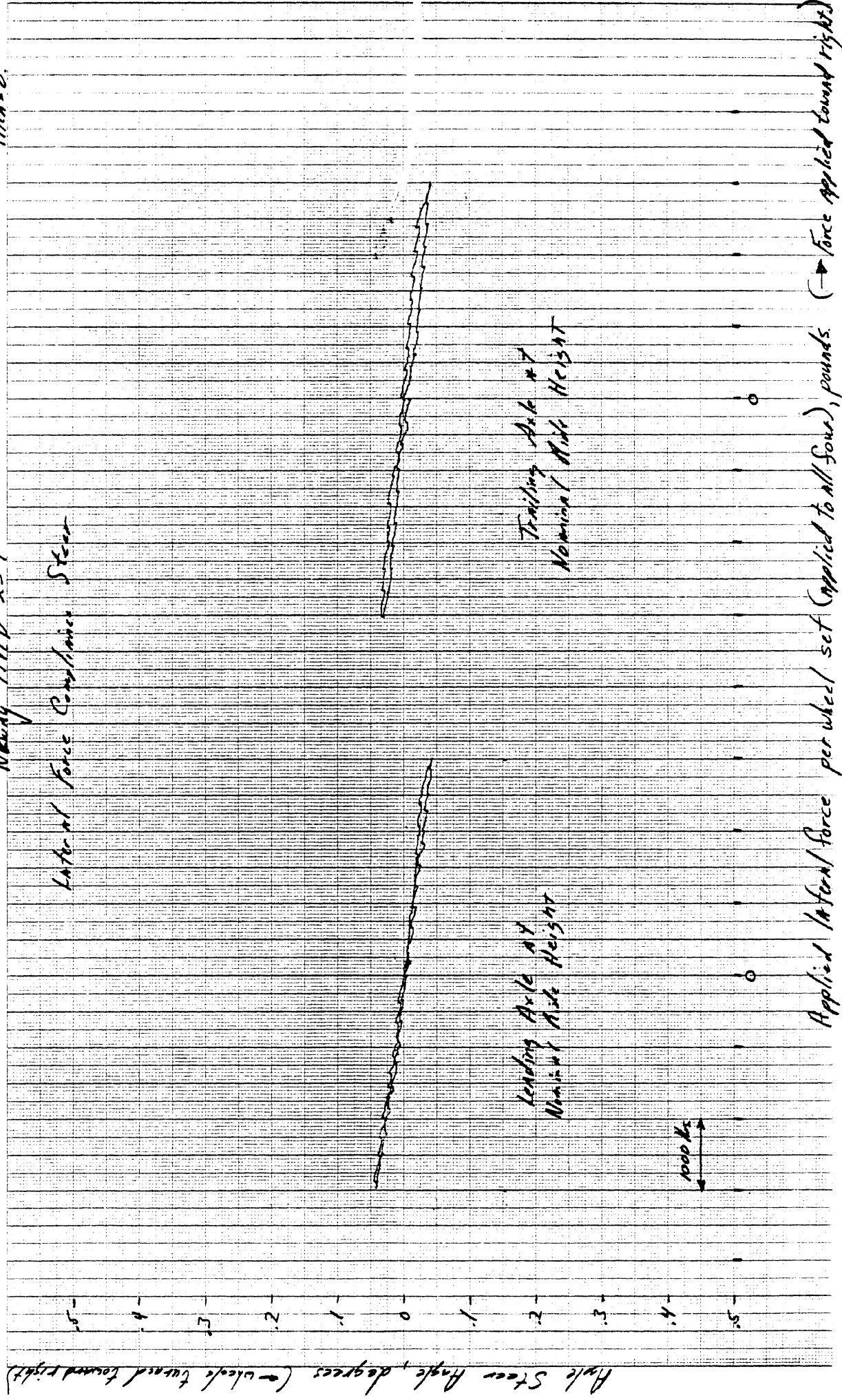
4000 lb-ft

Aligning Moment Applied to each wheelset (Applied to all four), M-lb. (positive →)

Pitch-0.

Neway AHD 234

Lateral Force Constraints Steer



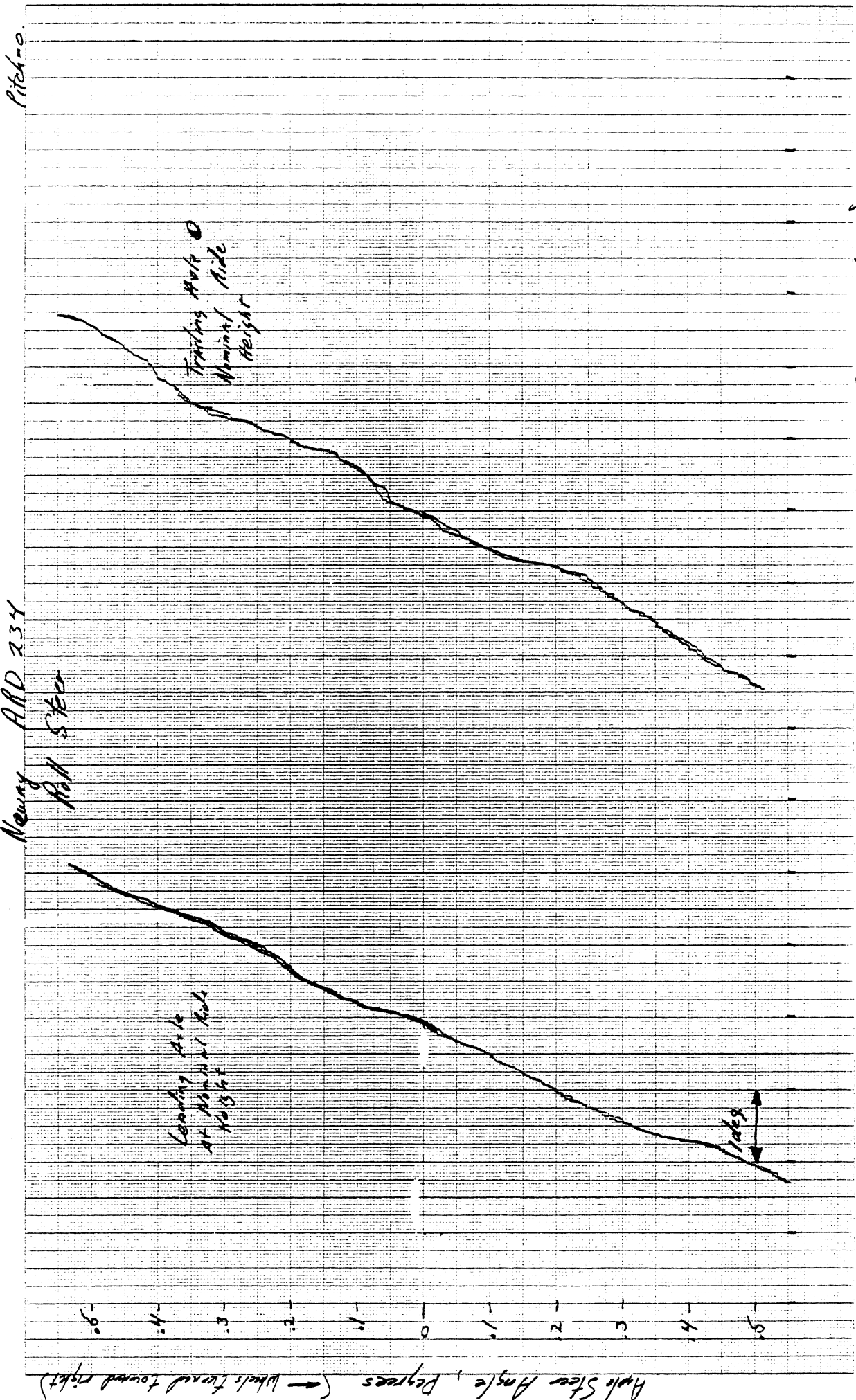
Landing Axle #4
Nominal Ride Height

Trailing Axle #7
Nominal Ride Height

Applied lateral force per wheel set (applied to all four), pounds (- force applied toward right)

Axle Steer Angle, degrees (w/vehicle turned toward right)

1000 lbs



Neway
Roll Steer
ARD 234

Pitch-o

Trailing Side
at Normal
Height

Leading Side
at Normal
Height

1 deg

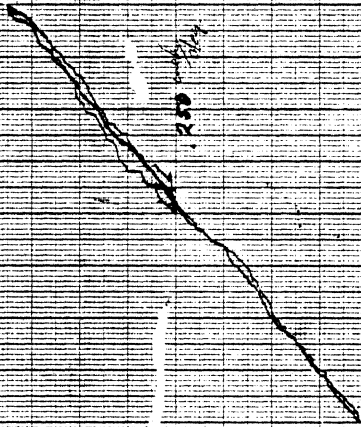
Axle Roll Angle, degrees (Right Side Compressed)

Axle Steer Angle, Degrees (Wheels Turned toward right)

Pitch = 0.

New ARP 234
Roll Center Height

Lateral Deflection of Axle, inches (motion towards right)

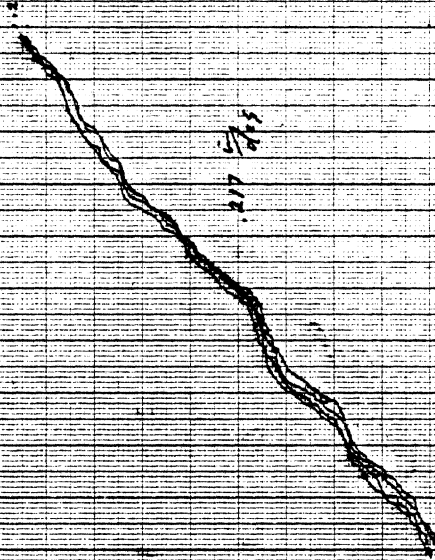
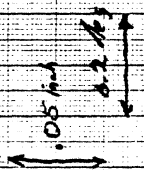


Leading Axle

Lateral p-06 19.87 inches road

$$\frac{50 - 0.64}{50} = 0.9872$$

$$r.c. height = 32.9$$



Trailing Axle

Lateral p-06 21.12 inches ground

$$\frac{50 - 0.55}{50} = 0.989$$

$$r.c. height = 32.9$$

Axle Roll Angle, Degrees (Right side Compressed)

Pitch-o.

Newby ARD 234

Inter axle load transfer

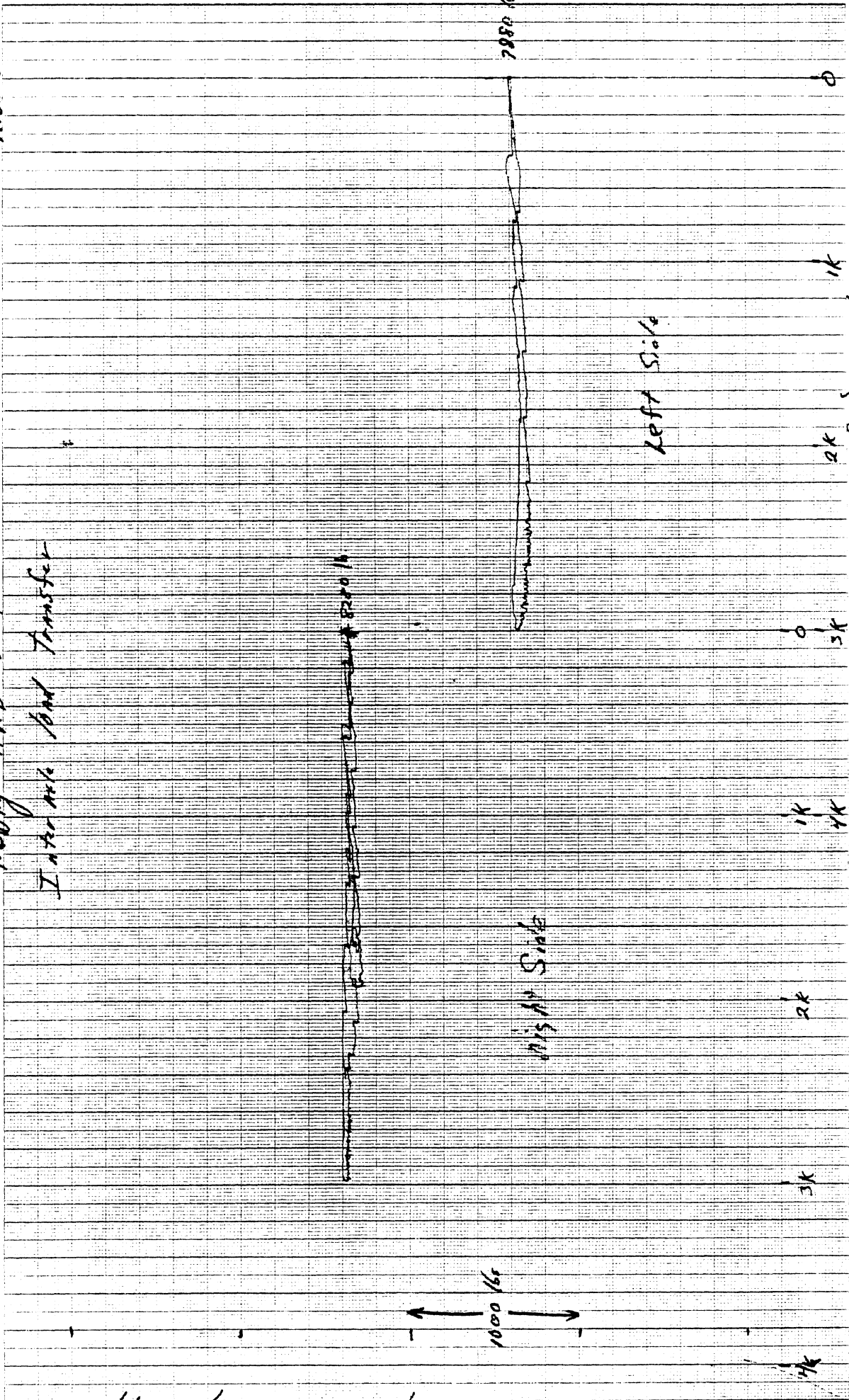
Load Transferred from Leading Wheel to Trailing Wheel, pounds

1000 lbs

Right Side

Left Side

Applied Brake Force per Wheel Set (Applied to All four) pounds.



Pitch=0

Freight per Air Suspension
Vertical Cut

Average Vertical Wheel Load, pounds relative to nominal wheel load

Wheel Suspension Load
Nominal Wheel Load
Nominal Air Suspension Load

20000
15000
10000

20000
15000
10000

20000
15000
10000

Vertical Deflection, inches relative

1.25



Freight lines Air suspension
Vertical load Excess load
Right side

Normal suspension load 30000 lb
Normal wheel load 15000 lb

20000
10000

16000
8000

Per
Excess
Load

Vertical wheel load, leading axle, pounds relative to nominal wheel load

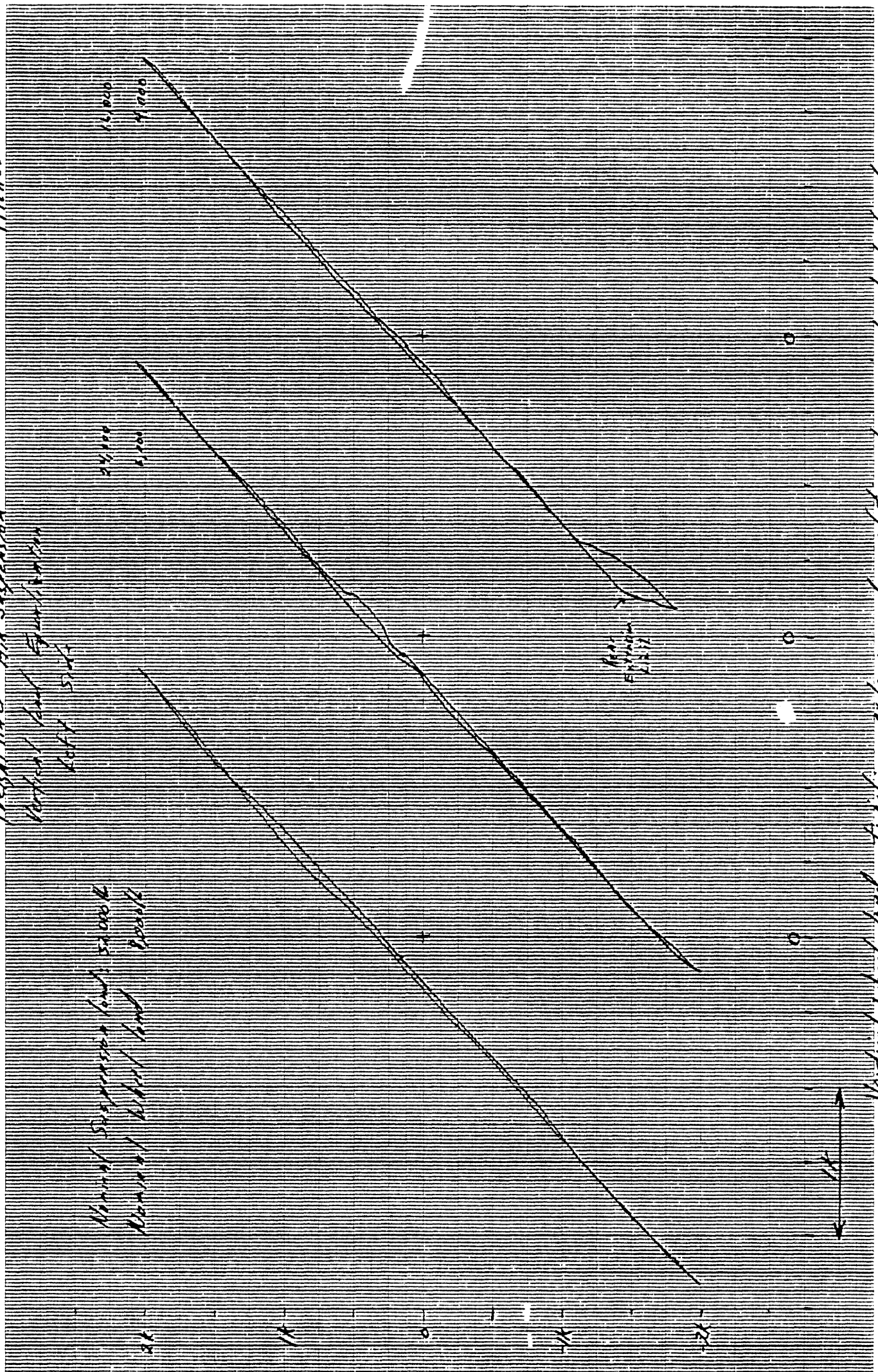
Vertical wheel load, trailing axle, pounds relative to nominal wheel load



Pitch = 0

Freightliner Air Suspension
Vertical Load Distribution
Left Side

Nominal Suspension Load Scale
Nominal Wheel Load Scale



Vertical wheel load, landing axle, pounds relative to nominal wheel load

Vertical wheel load, Trailing axle, pounds relative to nominal wheel load



Freight line Air Suspension Pitch = 1°

Average wheel load, pounds relative to normal wheel load

Normal Suspension Load 33,000
Normal Wheel Load 8,000
Applied Air Spring Pressure 70

25,000
10,000
50

10,000
8,000
55



Vertical Deflection, inches relative

1.25"

Ptd - -1°

Freight line Air Suspension

Load Front Axle - Left Side

Nominal Suspension Load
Nominal Wheel Load

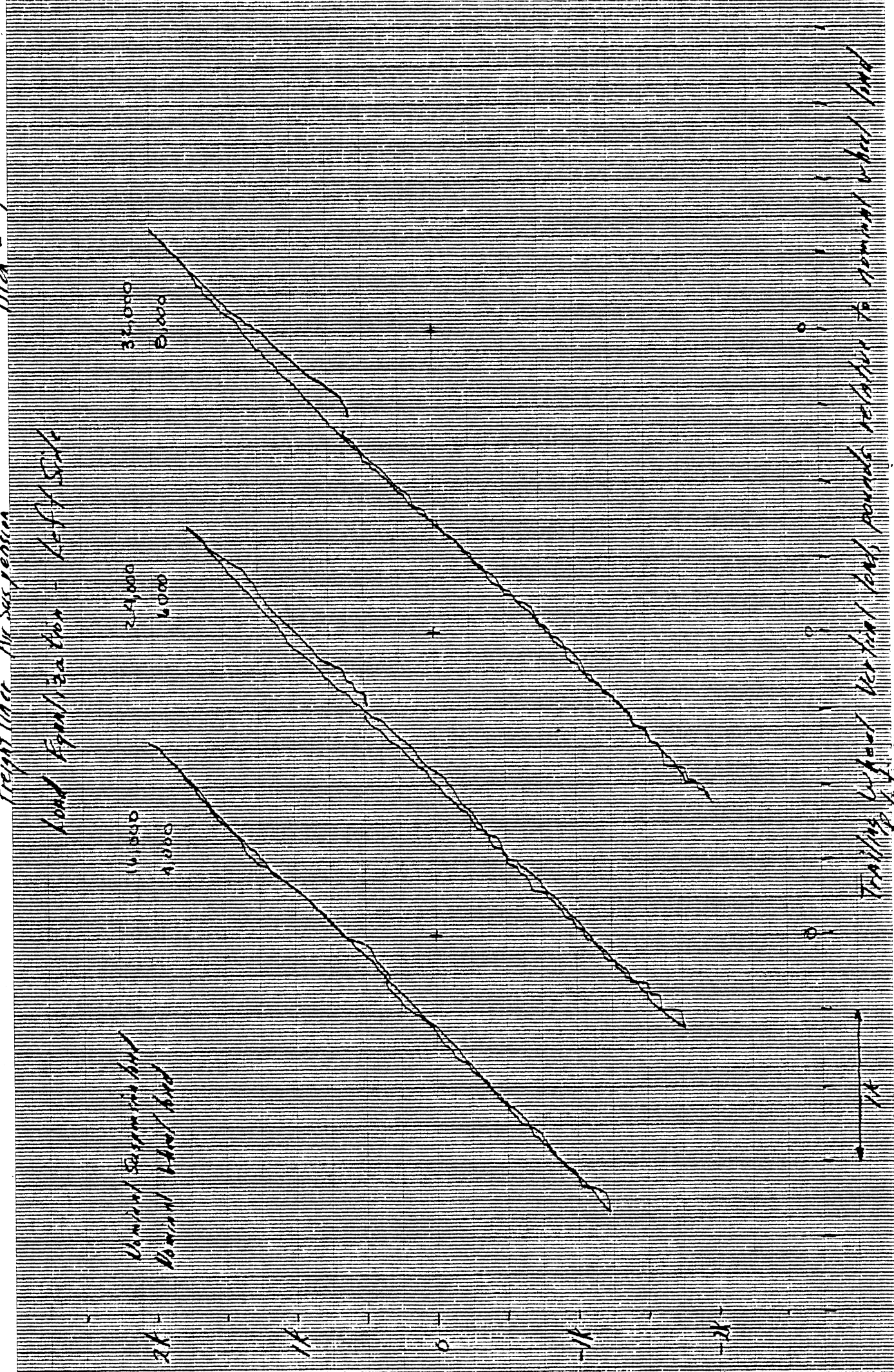
6,000
4,000

24,000
6,000

32,000
8,000

Landing Wheel Vertical load, pounds relative to nominal wheel load

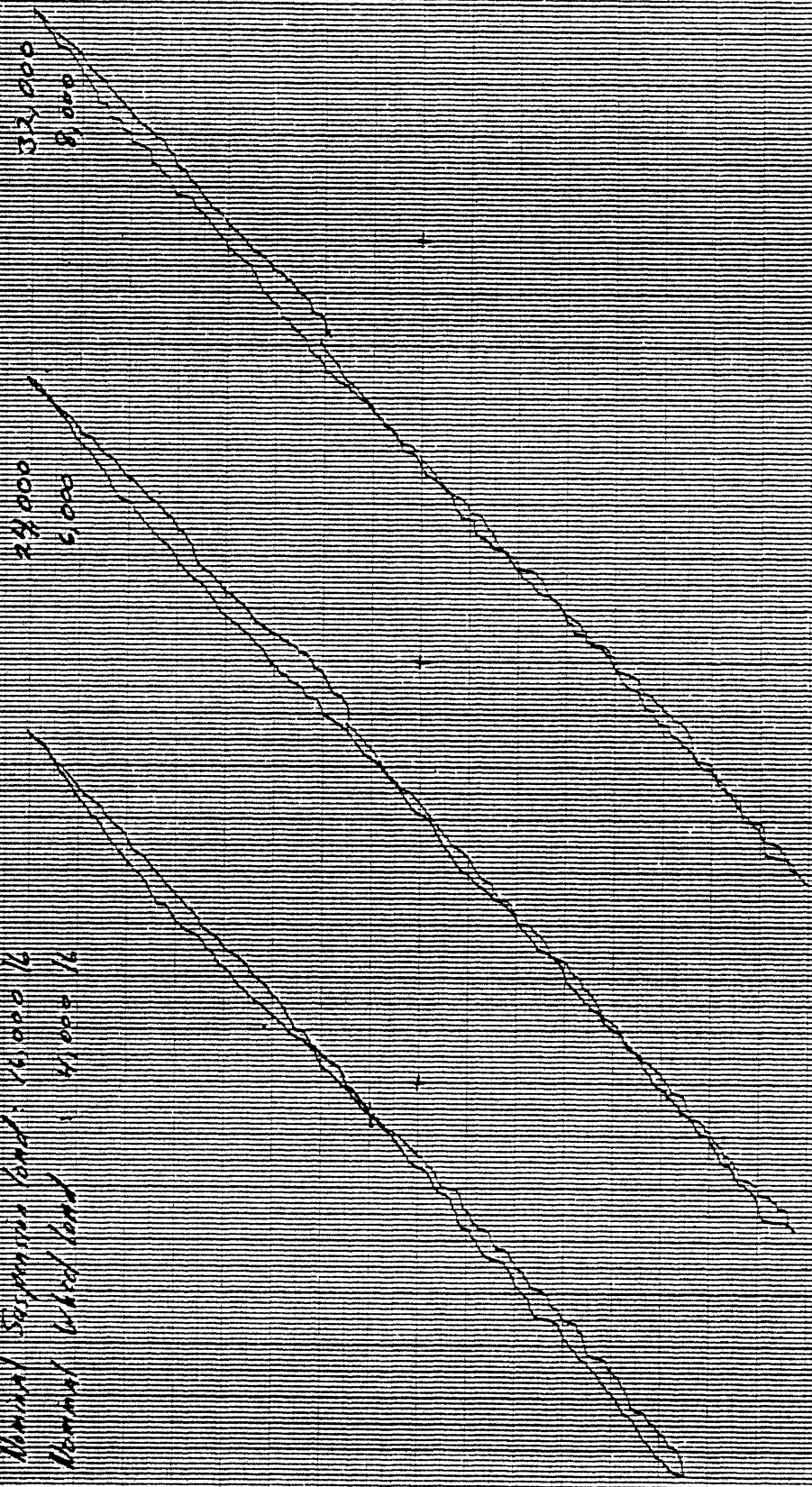
Trailing Wheel Vertical load, pounds relative to nominal wheel load



Pitch = 1°

Freightliner Air Suspension
Load Equalization - Right Side

Nominal Suspension Load: 16,000 lb
Nominal Wheel Load: 4,000 lb



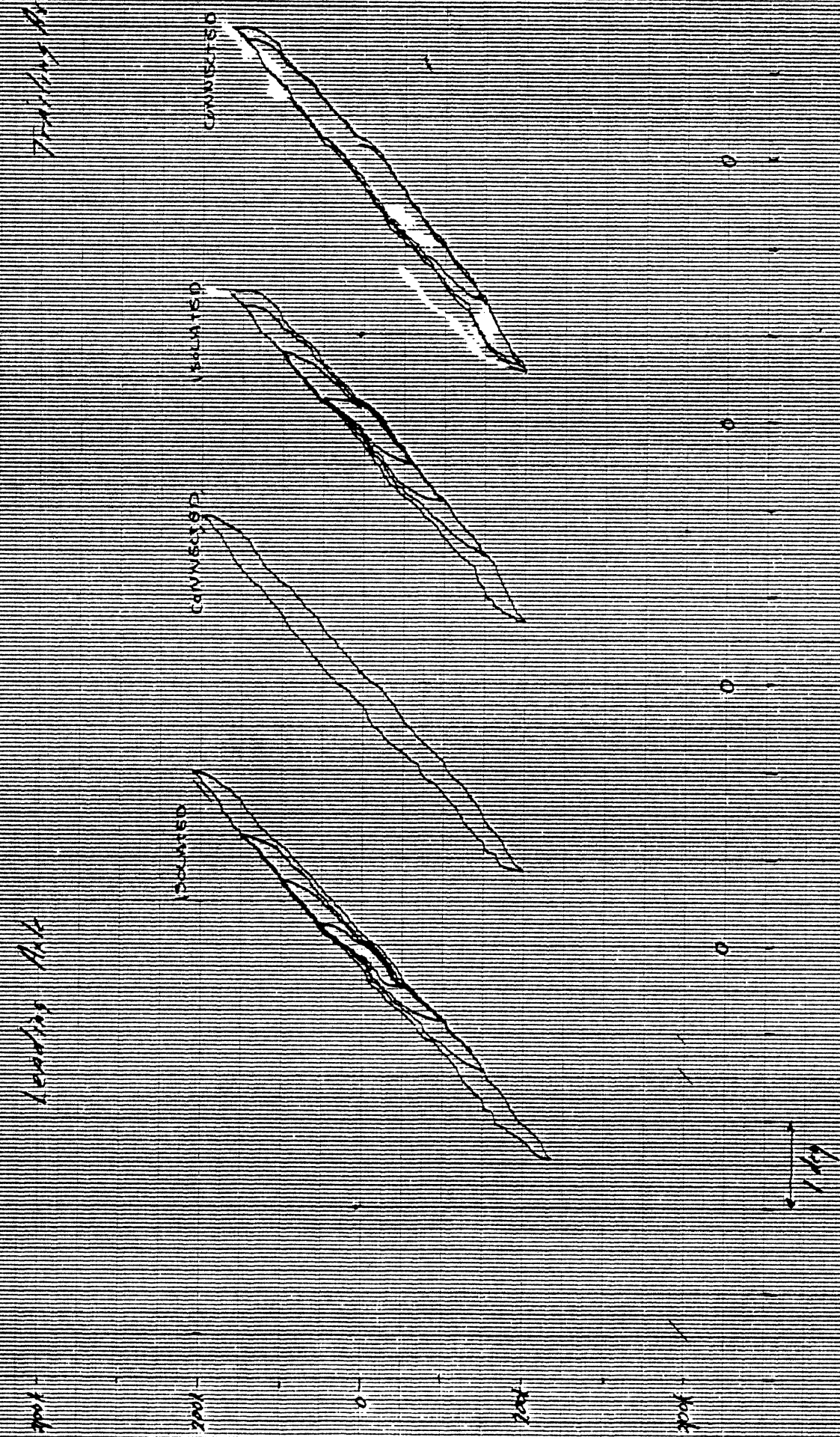
Leading wheel vertical load, pounds relative to nominal wheel load

Trailing wheel vertical load, pounds relative to nominal wheel load

Freight line Air Suspension
Roll Rate at 37,000 ft suspension load

Pitch

Roll Moment on Axle m-16 → Right Side Compressed



Leading Axle

Trailing Axle

Loaded

Connected

Loaded

Connected

Axle Roll Angle, deg

PITCH = 0.

FRIGHTLINER AIR SUSPENSION

ROLL RATE @ 24000 IN SUSPENSION LONG



ROLL MOMENT ON AXLE (IN-LB) (← RIGHT SIDE COMPRESSOR)

1000
0
-1000

LEADING AXLE

TRAILING AXLES

ZIPPED

UNZIPPED

ZIPPED

UNZIPPED

AXLE ROLL ANGLE (deg)



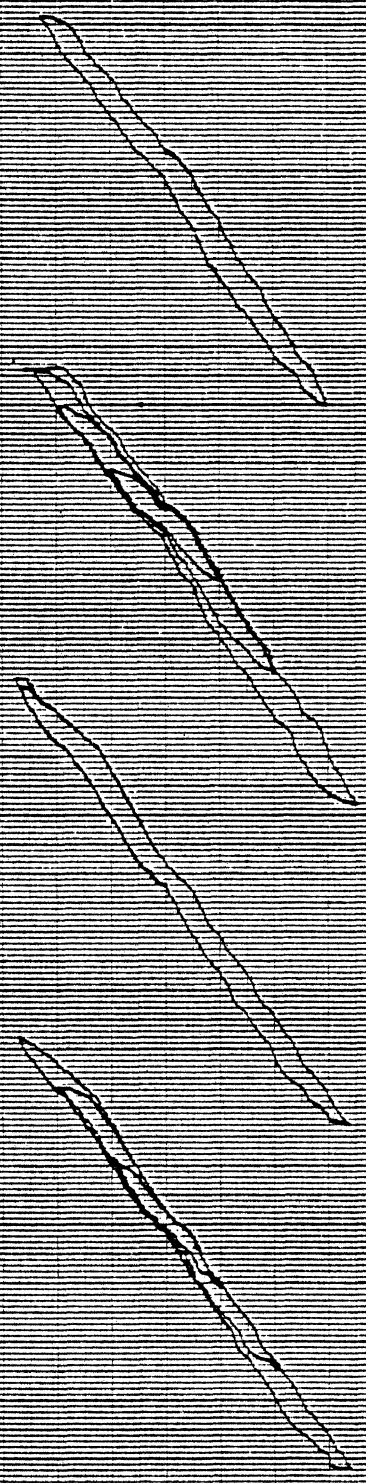
WITCH = 0.

FREIGHTWAGON - AIR SUSPENSION

ROLL RATE @ 16,000 LB SUSPENSION LOAD

ROLL MOMENT ON AXLE (in.-lb) (← RIGHT SIDE COMPRESSED)

1000
500
0
500
1000



← ROLL RATE

AXLE ROLL ANGLE (deg)

Eight line Air Suspension
Roll Steer

Pitch = 0

Measured at 20 K
at 100 K and 100
psi. The suspension
is very sensitive to
side force

Leading Axle



Trailing Axle



Axle Steer angle, deg (steered toward right →)

1 DEG

Axle Roll Angle deg (→ right side compressed)

FREIGHTLINER - AIR SUSPENSION

1/14/70

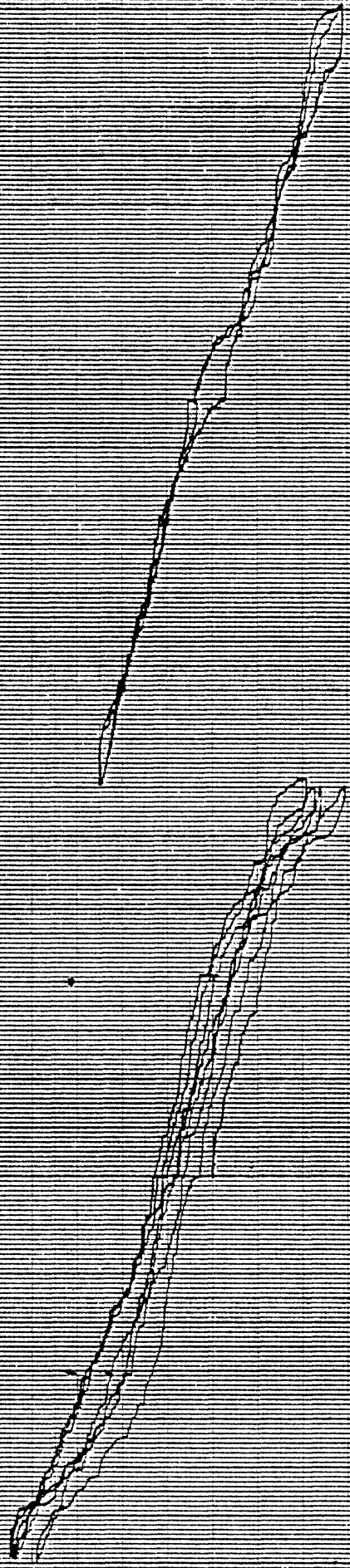
ALIGNING MOMENT COMPLIANCE STEER

MEASURED AT 20 MPH
AT 10 MPH SAME BEHAVIOR
AT 20 MPH DIFFERENT BEHAVIOR
SOLUTION: ADJUSTING STEER
CORRELATED WITH DRIVER

Trucking File

Leading Axis

AXIS STEER ANGLE (deg) (← STEER TO RIGHT)

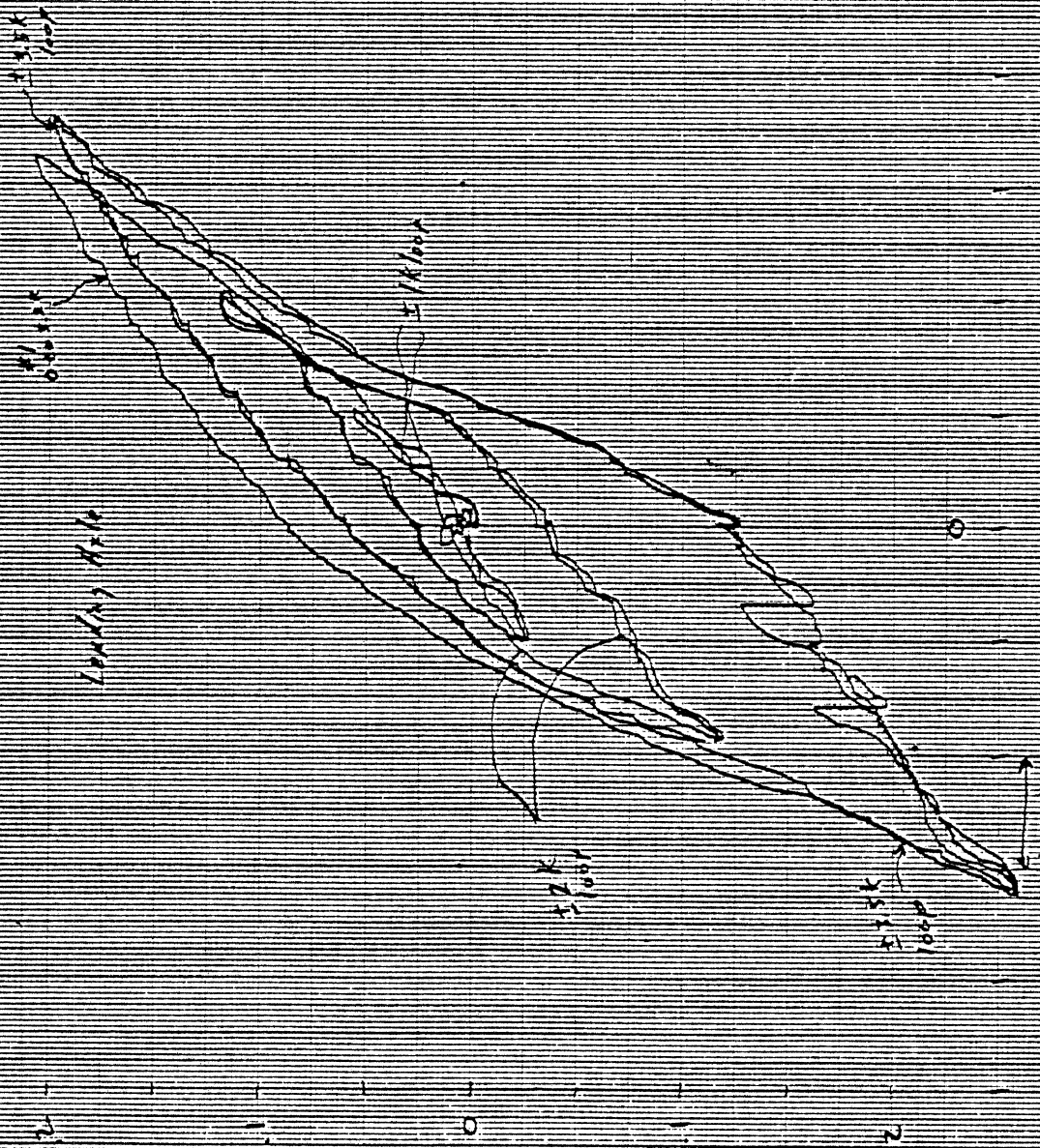


ALIGNING MOMENT PER WHEEL SET (in-lb)
(APPLIED TO ALL WHEEL SETS SIMULTANEOUSLY)

400 in-lb

LATERAL FORCE COMPLIANCE STEER
 FREIGHTLINER - AIR SUSPENSION

38,000 lbs STEERING ONLY



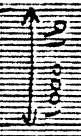
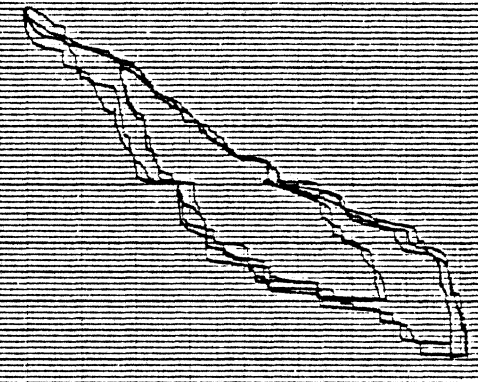
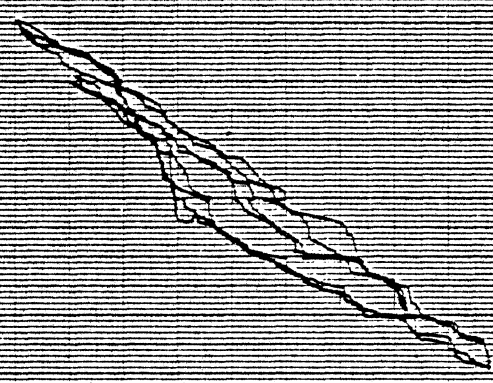
AXLE STEER ANGLE (deg) (STEER TO RIGHT ←)

LATERAL FORCE PER WHEEL SET (lb) (FORCE APPLIED TO RIGHT →)
 (APPLIED TO ALL WHEEL SETS SIMULTANEOUSLY)

FREIGHTLINER - AIR SUSPENSION

LATERAL FORCE COMPLIANCE STEER
16,000 LB SUSPENSION LOAD

AXLE STEER ANGLE (deg) (← STEER TO RIGHT)



LATERAL FORCE PER WHEEL SET (LB) (FORCE APPLIED TO RIGHT →)
(APPLIED TO ALL WHEEL SETS SIMULTANEOUSLY)

FREIGHTLINER - AIR SUSPENSION

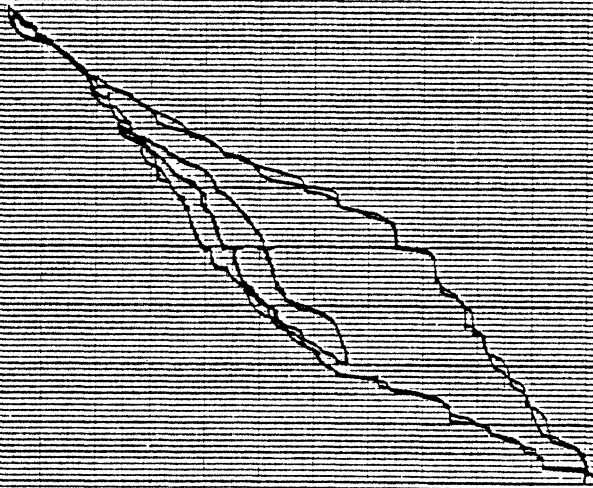
LATERAL FORCE COMPLIANCE STEER

GROSS SUSPENSION LOAD - 24,000 LB

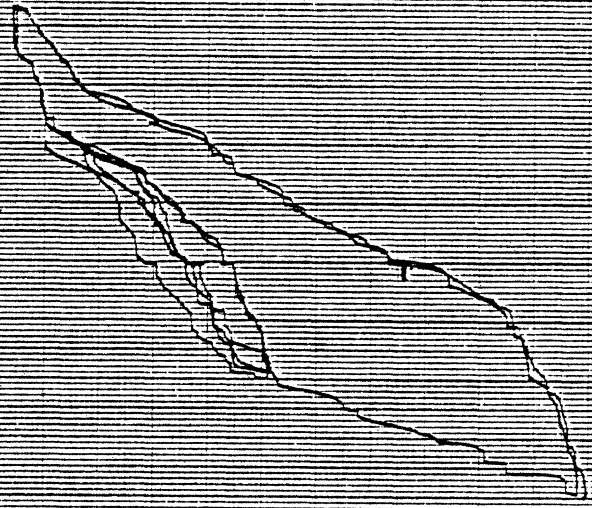
AXLE STEER ANGLE (deg) (← STEER TO RIGHT)



Leading Edge



Trailing Edge

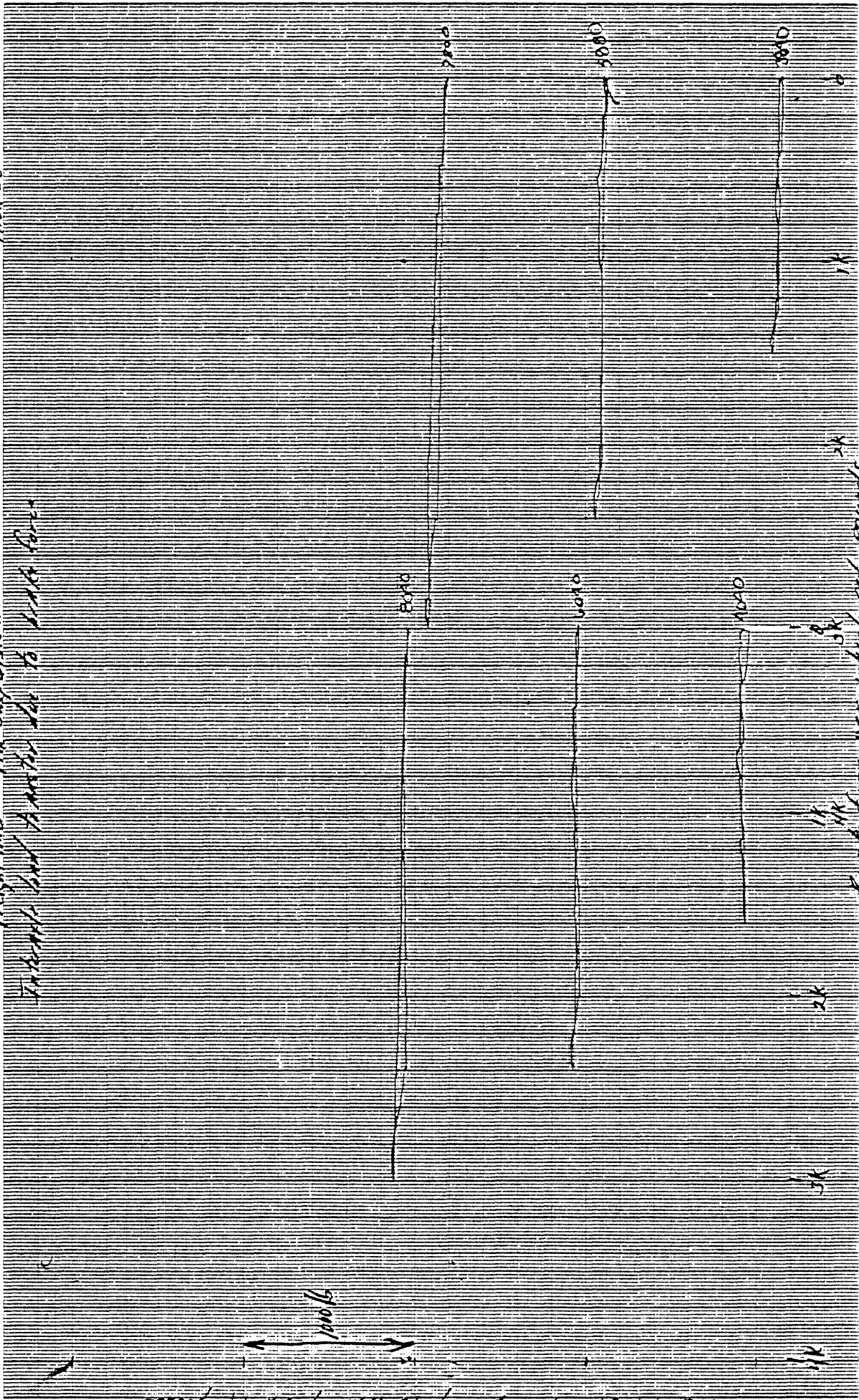


1000 LB

LATERAL FORCE PER WHEEL SET (LB) (FORCE TO RIGHT →)
CHANGED TO ALL WHEEL SETS SIMULTANEOUSLY

Pitch = 0

Fright line Air Suspension
Tire and wheel assembly to deck force



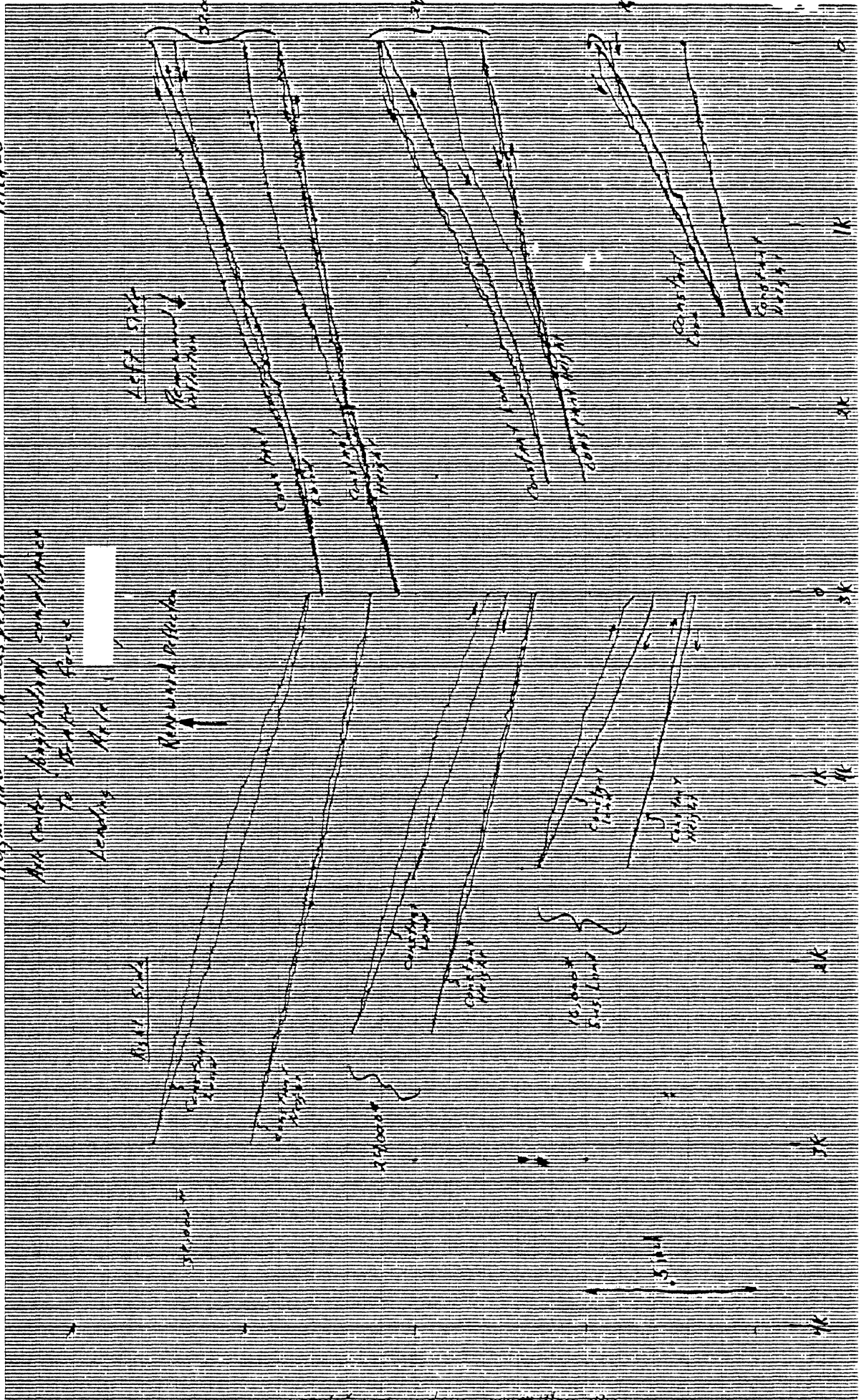
Load Transfer from landing to trailing wheel, pounds

1000
5000
1000
5000
Applied to all four simulated trucks

Axle longitudinal displacement, inches

Pitch

Freight Inc. All Suspension
 All center suspension components
 to Equal Force
 Leaning Axis
 Around Pitch

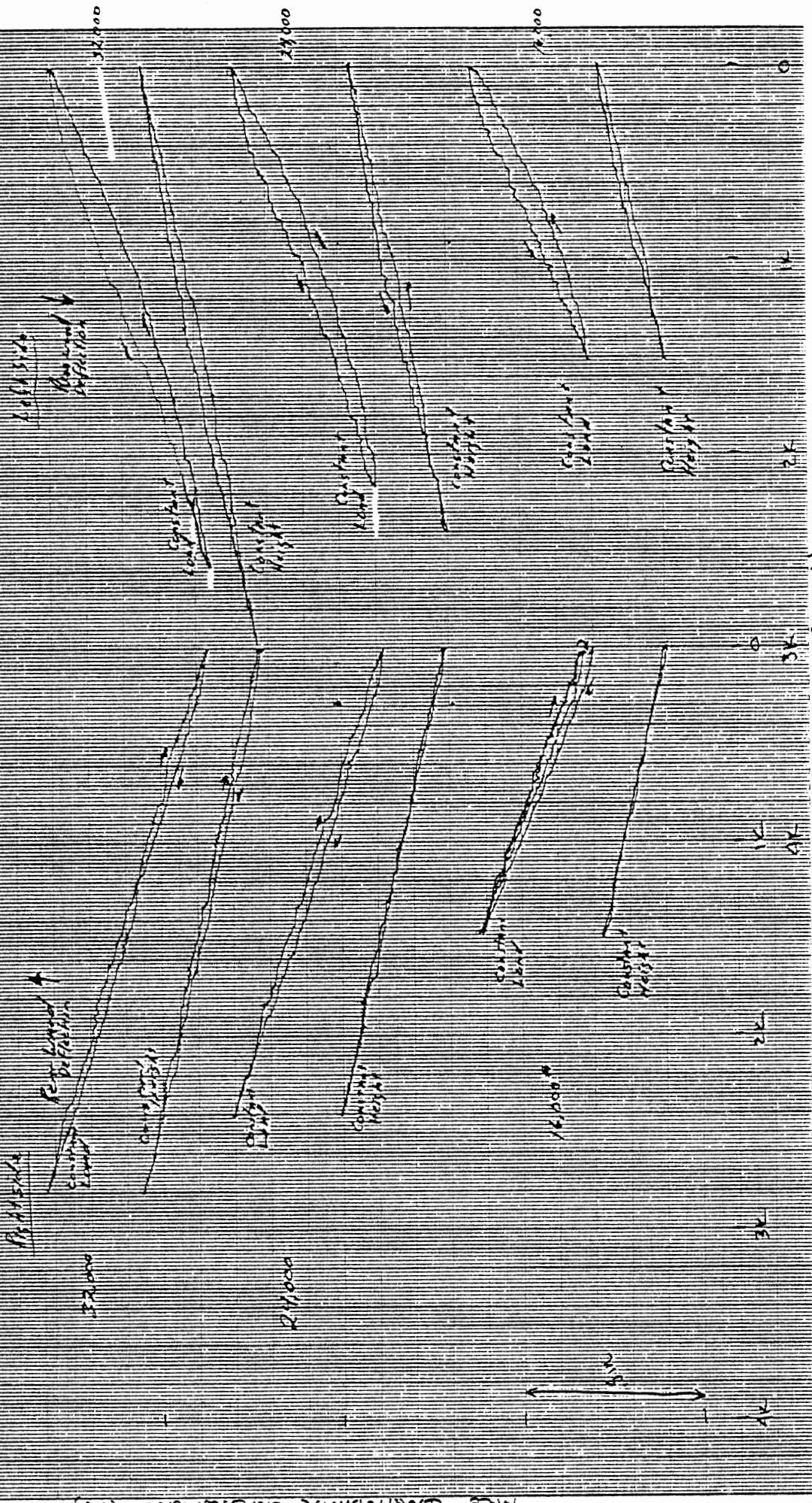


Bank force per wheel set, pounds.

Pitch = 0

FREIGHTLINER - AIR SUSPENSION

ANGLE CENTER LONGITUDINAL COMPLIANCE
TO BRAKE FORCE
TRAINING ANGLE

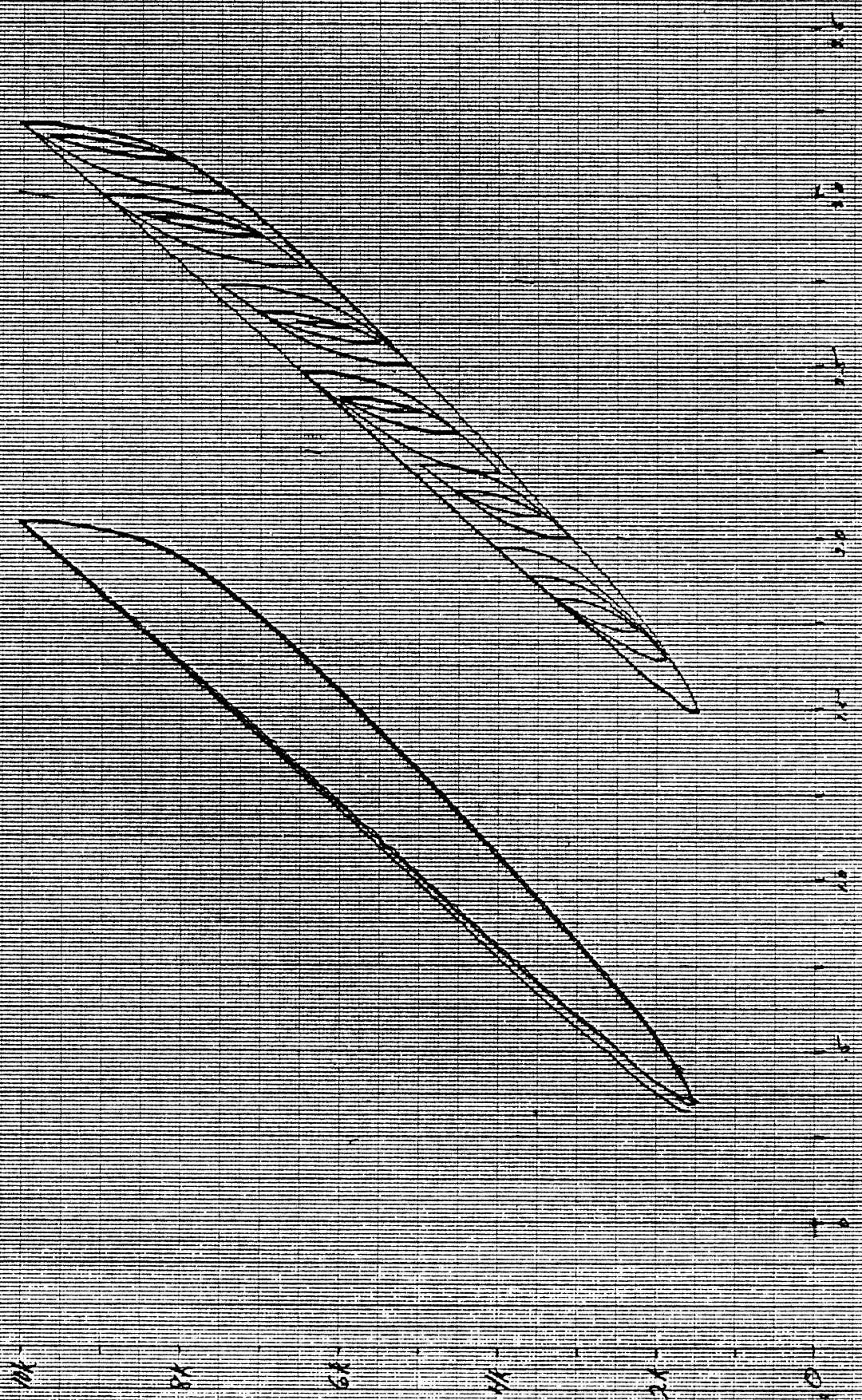


ANGLE LONGITUDINAL COMPLIANCE (in)

BRAKE FORCE PER WHEEL SET (lb)

- Same Traction 101 F multi-leaf Pitch = 0

Vertical Force



Average Vertical Wheel Motion, inches (relative)

Vertical Load per wheel set, pounds (relative)

Plot - 0

Open Tundra
Roll Rate, Landing Axis

10000 ft

25000 ft

One Shorter than 25000 ft

1000

2000

0

1000

2000

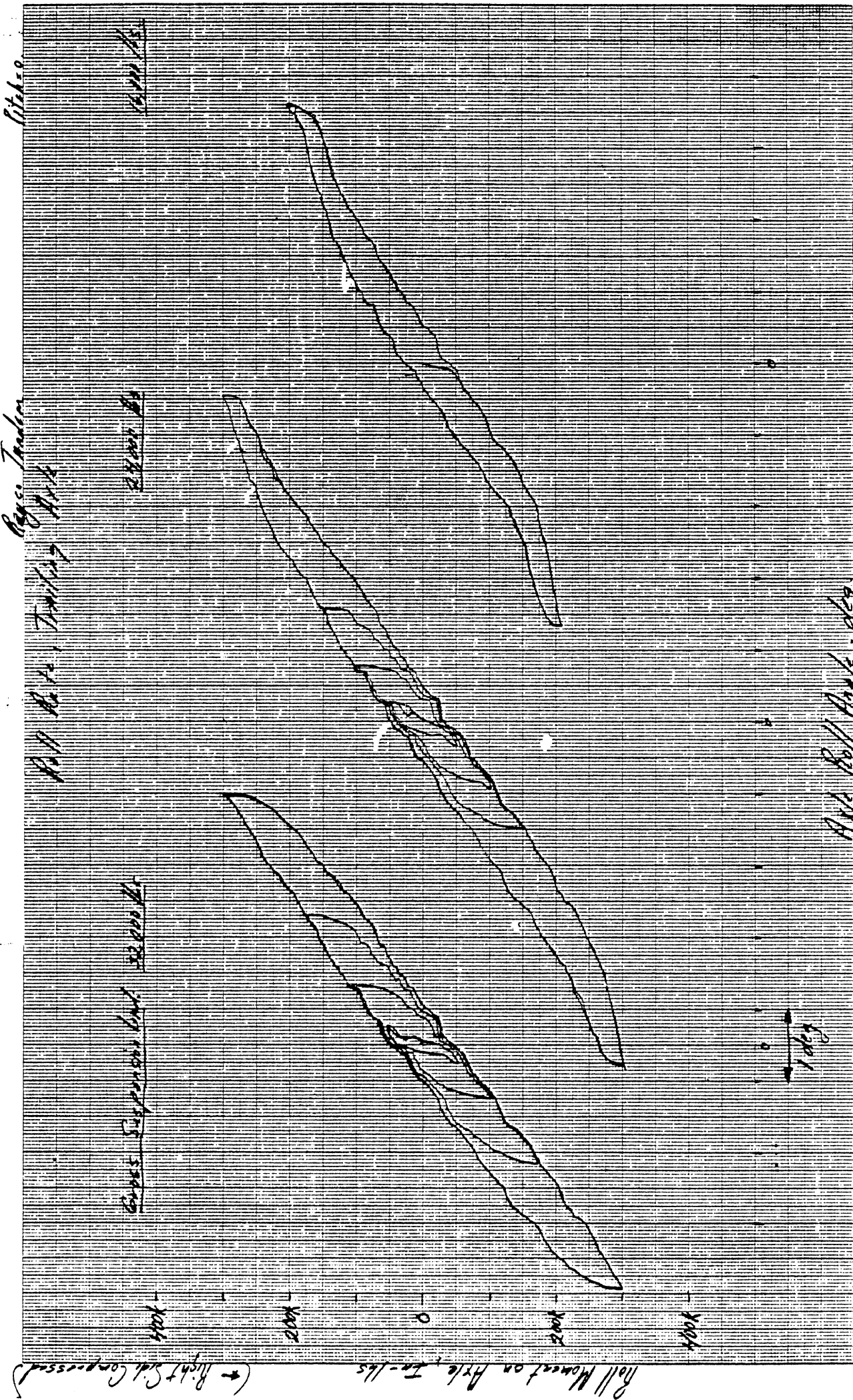
(→ Right Side Expanded)

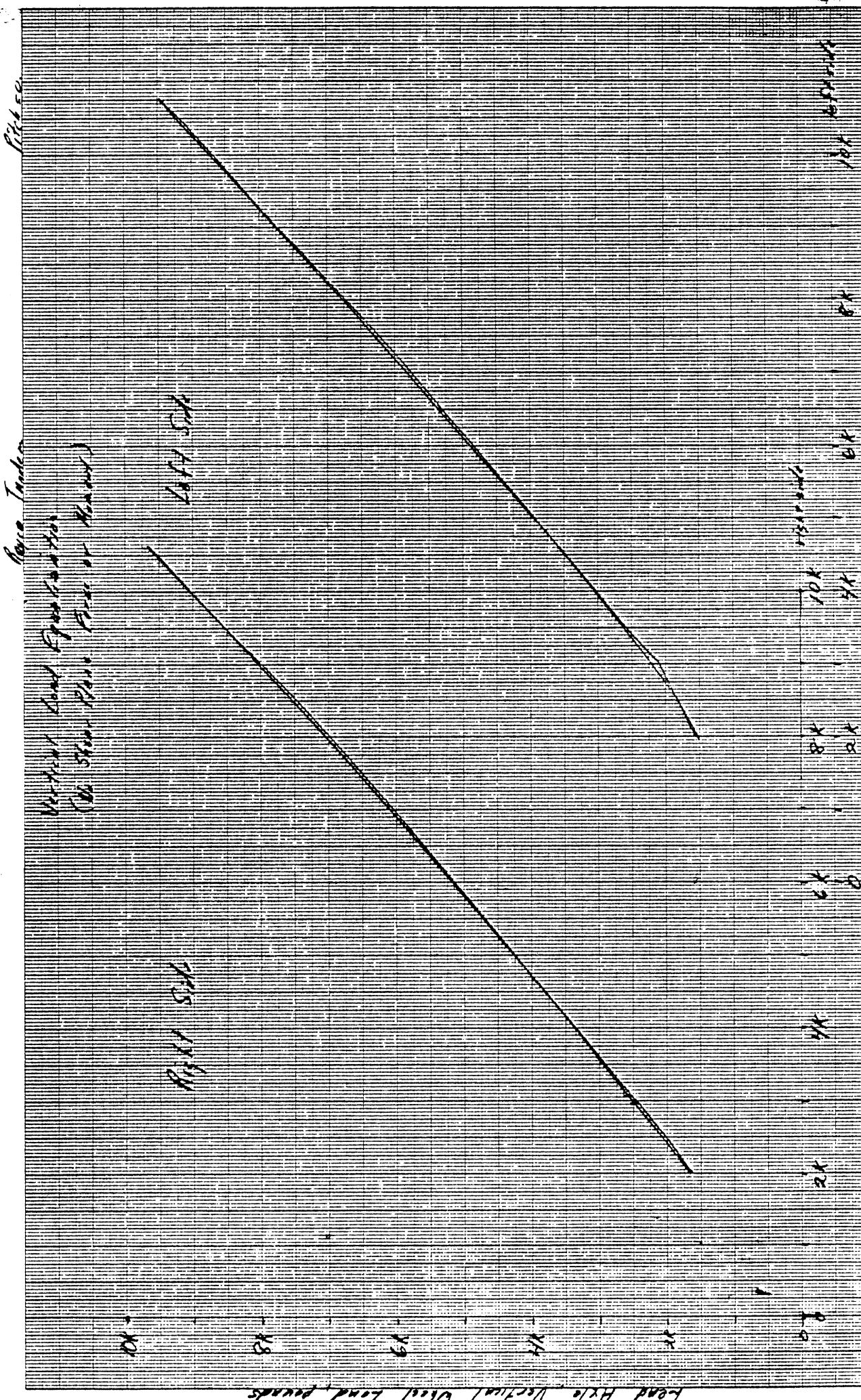
Roll Moment on Axis, In-lbs

Axis Roll Angle, deg

1000







Trailing Axle, Vertical Wheel Load, Pounds

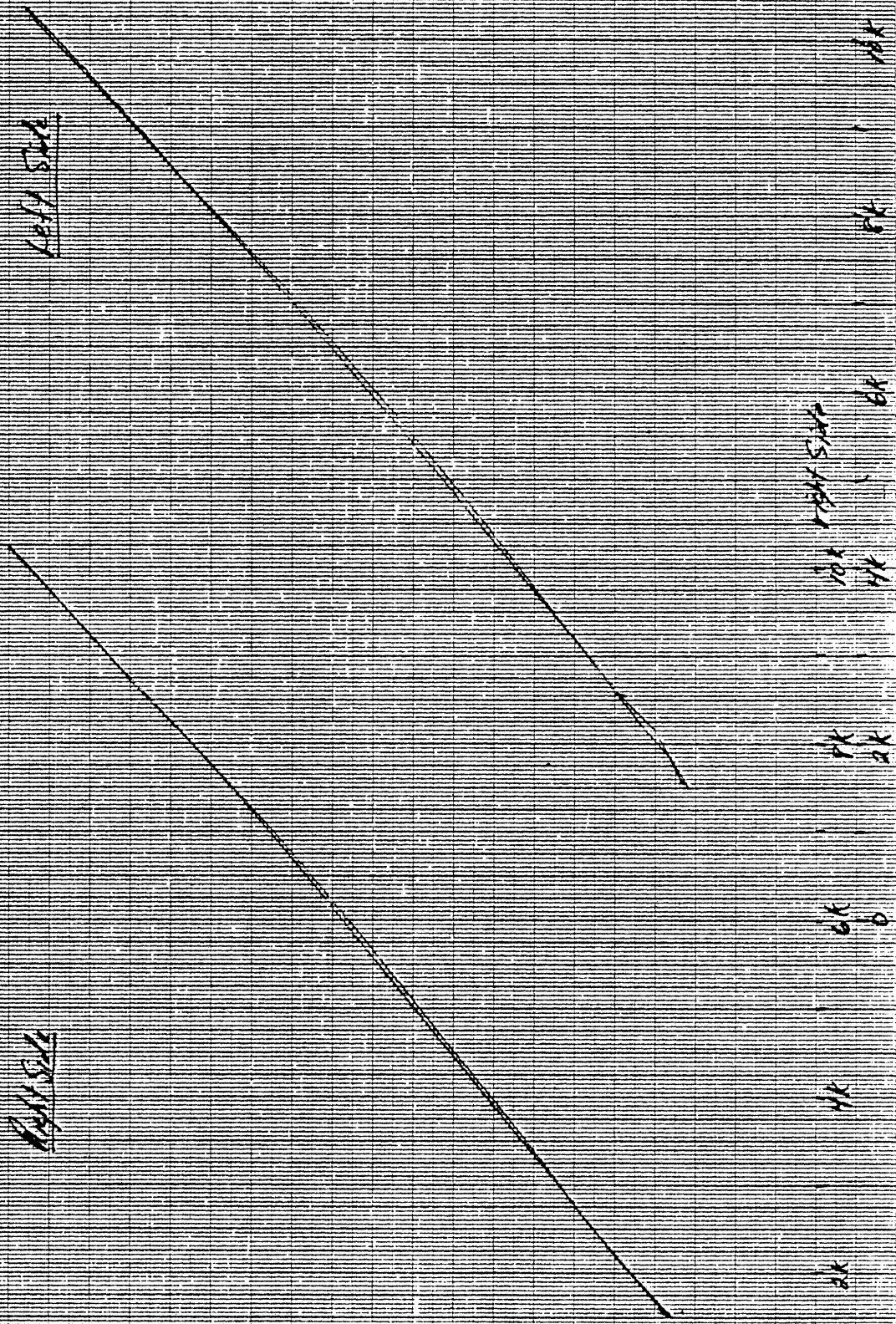
Lead Axle Vertical Wheel Load, pounds

Pitch=20

Rayco Tanker

Vertical Load Equalization
(At Same Time Forces at Rear Axle)

20
25
30
35
40
45
50



40K

50K

Leading Axle Vertical Wheel Load, pounds

Trailing Axle Vertical Wheel Load, pounds.

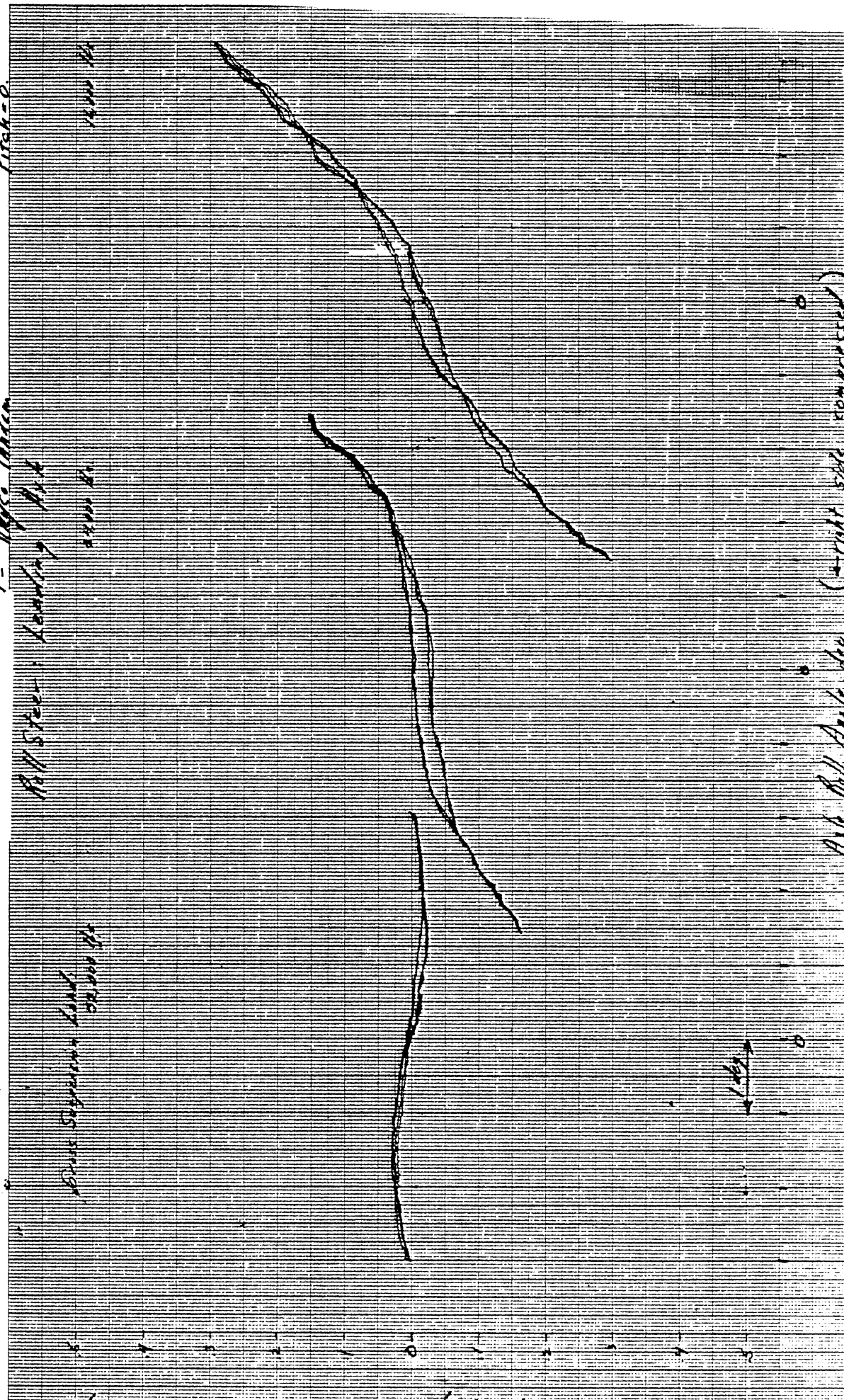
1 - Spgs. Tandem

Pitch = 0

Roll Steer: Landing Pit

Base Springs Land

Roll Steer



(Wind toward right)

Pitkin

Bayco Tundra

111 Steer Trails, Ave

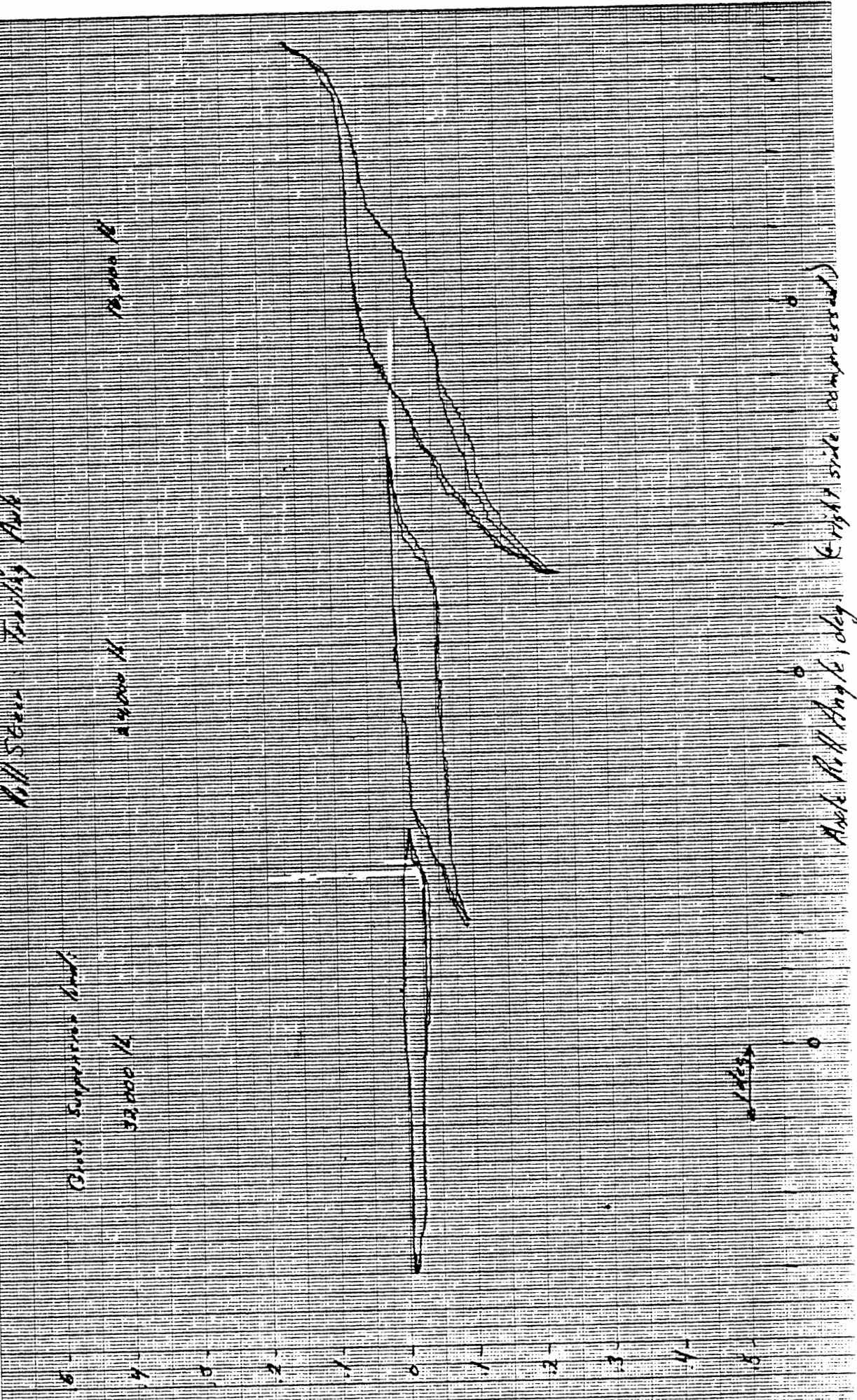
Over Suspension Road

12,000 ft

14,000 ft

32,100 ft

Axle Steer Angle, degrees (→ Wheel toward toward right)



(Right side compressed)

Axle Roll Angle, deg.

Axle Steer Angle, degs. (← Steer toward right)

Case Steer Angle

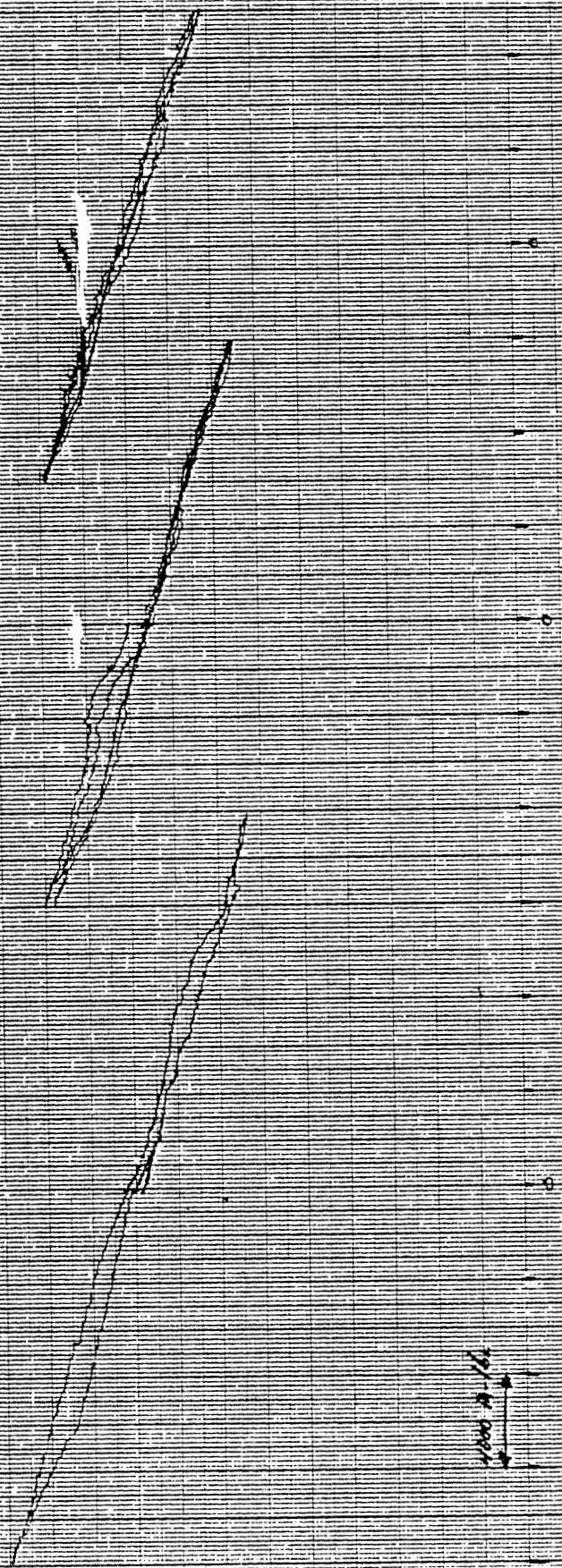
Aluminum Control Steering Landing Pit

Rayco Tumbler

Pittsboro

Wash DC

Wash DC



Aligning Moment per wheel set, ft. lbs. (Capital to 1/4" for same steering)

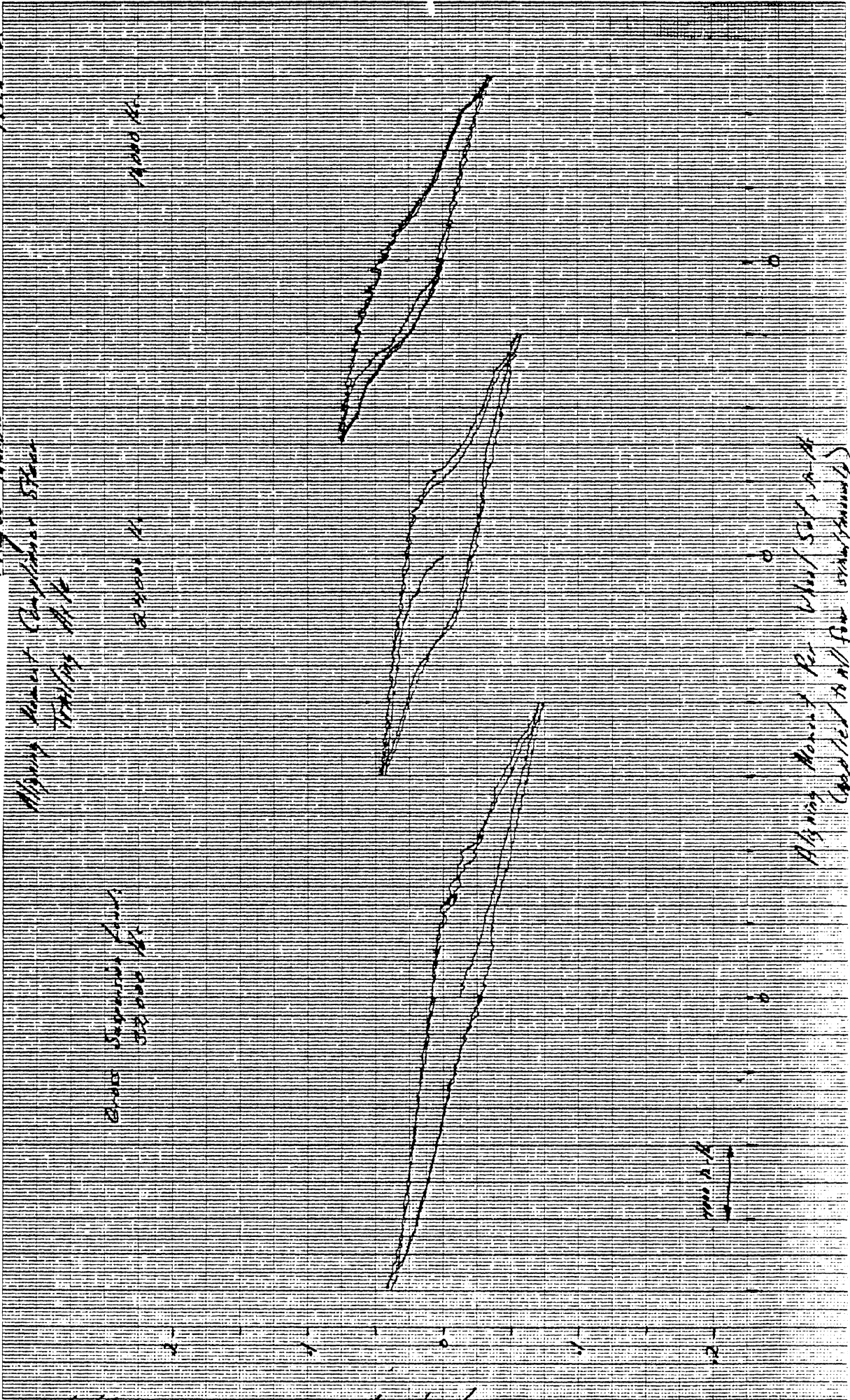
Pitch = 0

1. Rocco Trucks

Aligning Moment (Compensated Steer)
Trailing Hitch

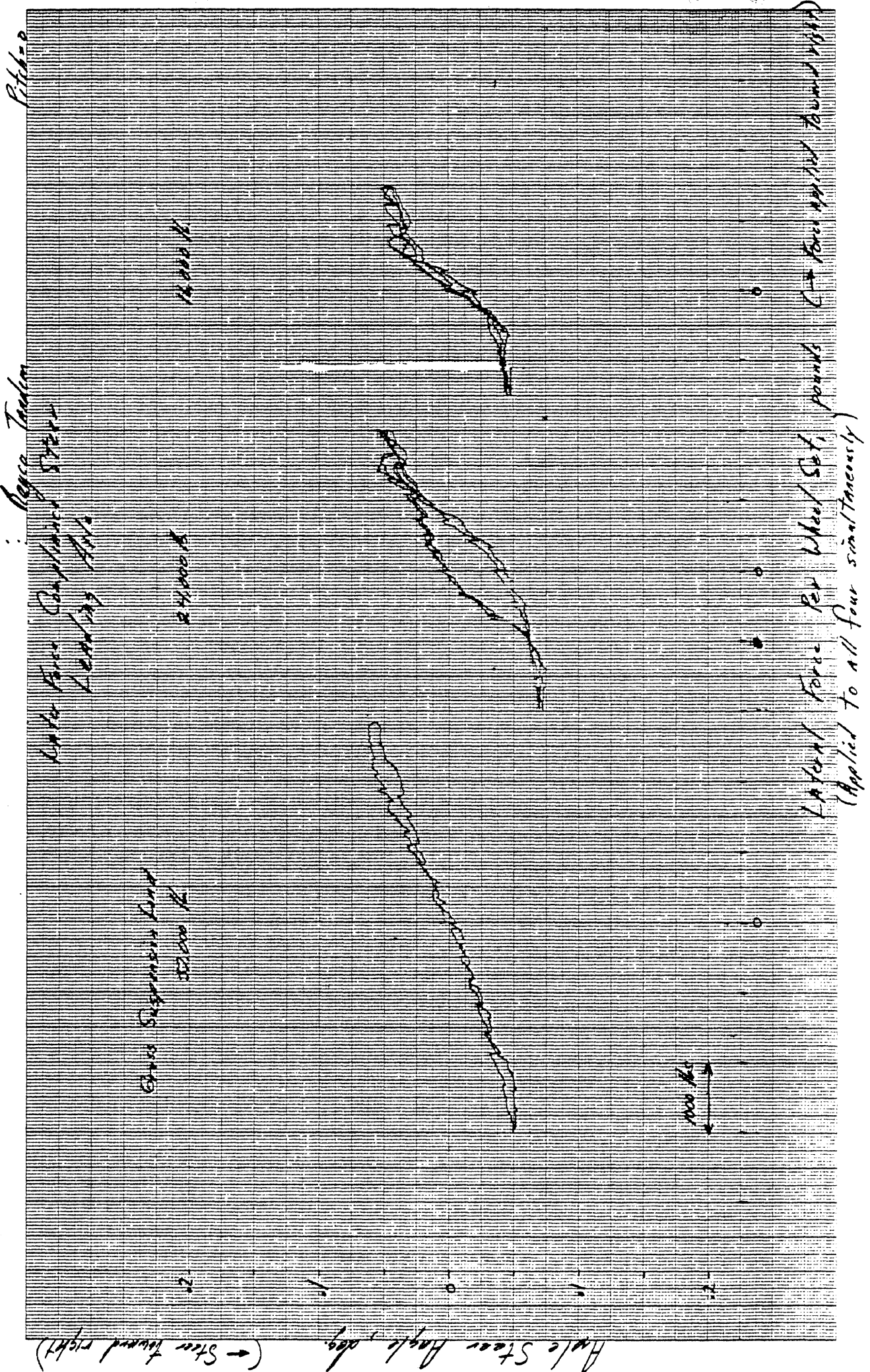
2000 ft
2000 ft

2000 ft



Aligning Moment per Wheel Set is 10 ft
Applied to all four wheels (steering)

Axle Steer Angle, degrees (→ Steered Toward Right)



Pitch

Force Factor

Rate Force Compensated Steer
Leading Axis

22000 lb

24000 lb

26000 lb

Angle Steer Angle, deg. (Steer toward right)

Lateral Force Per Wheel Set, pounds
(Applied to all four simultaneously)

1000 lbs

→ Steer Toward Right

Angle Steer Angle, deg

Plate

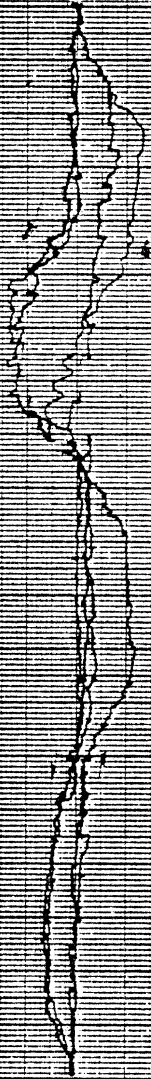
1. Lays Jordan

Latent Force Component of Steer
Training Data

Cross Section, 1/2
32,000 lb

25,000 lb

10,000 lb



1000 lb

Latent Force per wheel set pounds
(Applied to all four simultaneously)

Force applied toward right

Pitch 50.

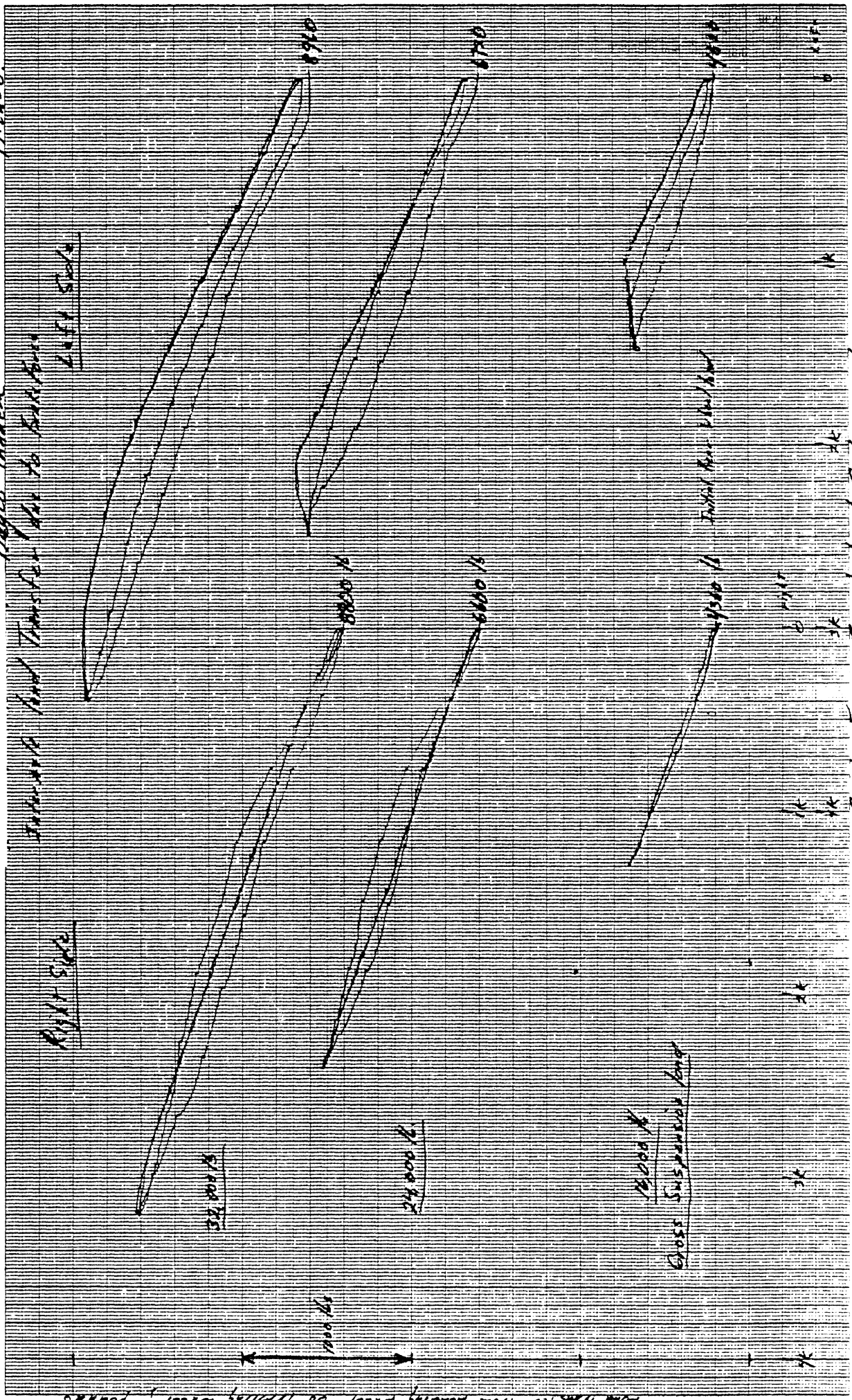
Sevia Trailer

Forward and Transfer due to Suspension

Right Side

Left Side

Load Transfer from leading wheel to trailing wheel, pounds



Brake Force For Wheel Set, pounds
Applied to All Four Simultaneously

Load Transfer from Leading Wheel to Trailing Wheel



Gross Suspension Load

32,500 LBS

Right Side



Front



10,000 LBS



3k

2k

1k

3k

2k

1k

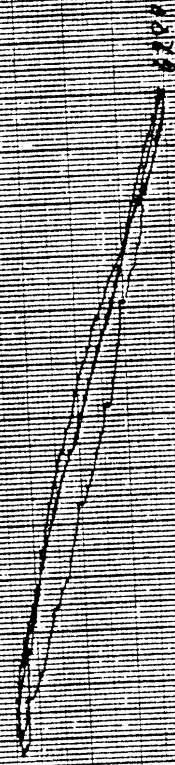
0

0

Pitch = -1°

Rolls Toward
Inside and Thrusts
Due to Brake Force

4000 LBS



also includes
brake wheel load

1500 LBS

2k

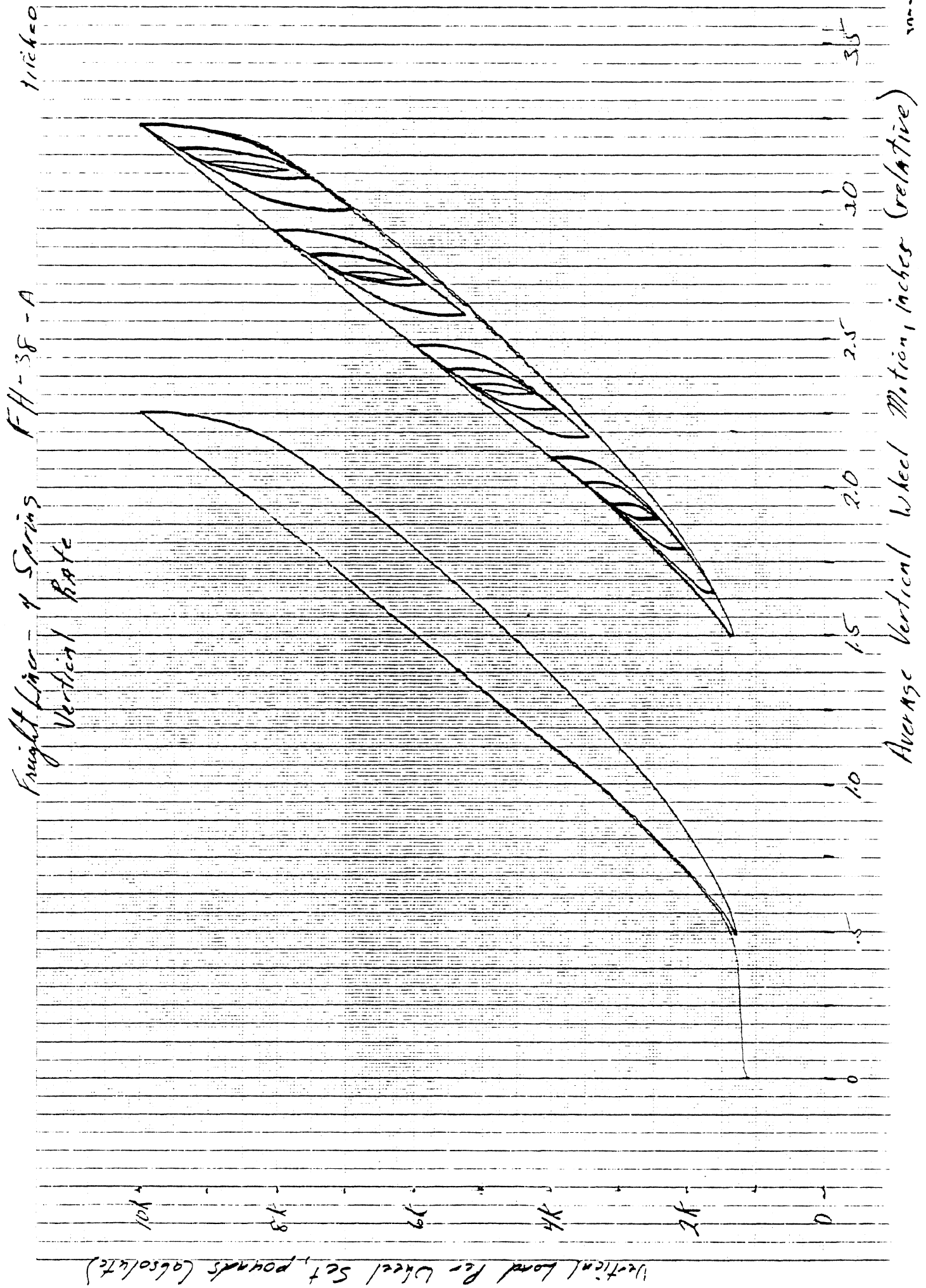
1k

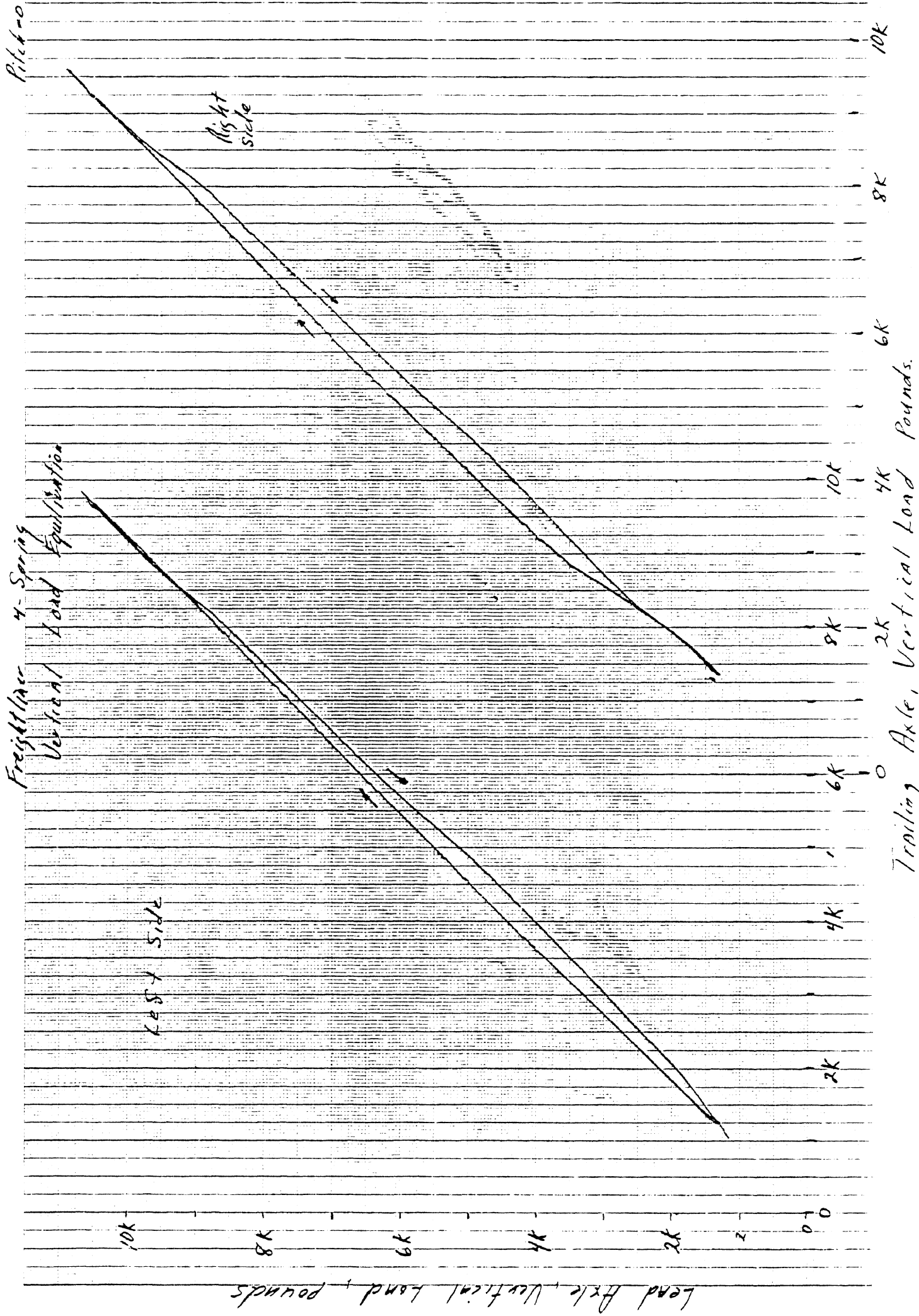
0

0

Brake force per wheel set, pounds
Applied to all four wheels
simultaneously

4307126





Freightliner - 4 Spring
Roll Rate - Trailing Axle

Roll Moment on Axle, Ft-lbs (Right side Comp ←)

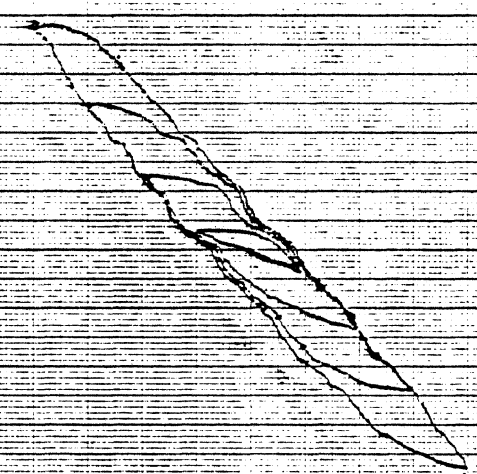
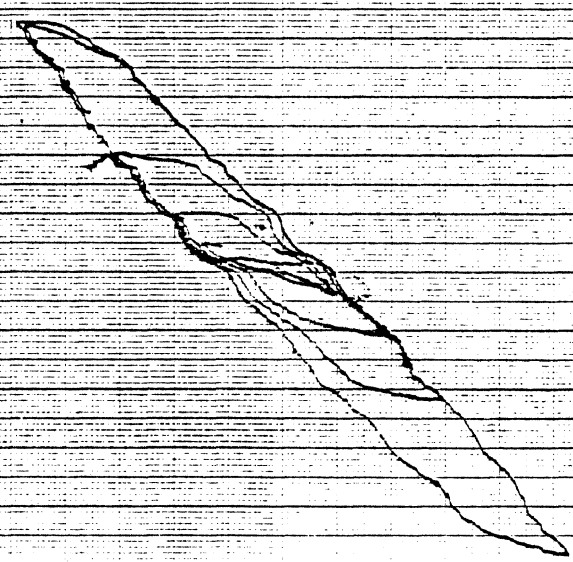
Gross Suspension Load

52,000 lb

24,000 lb

14,000 lb

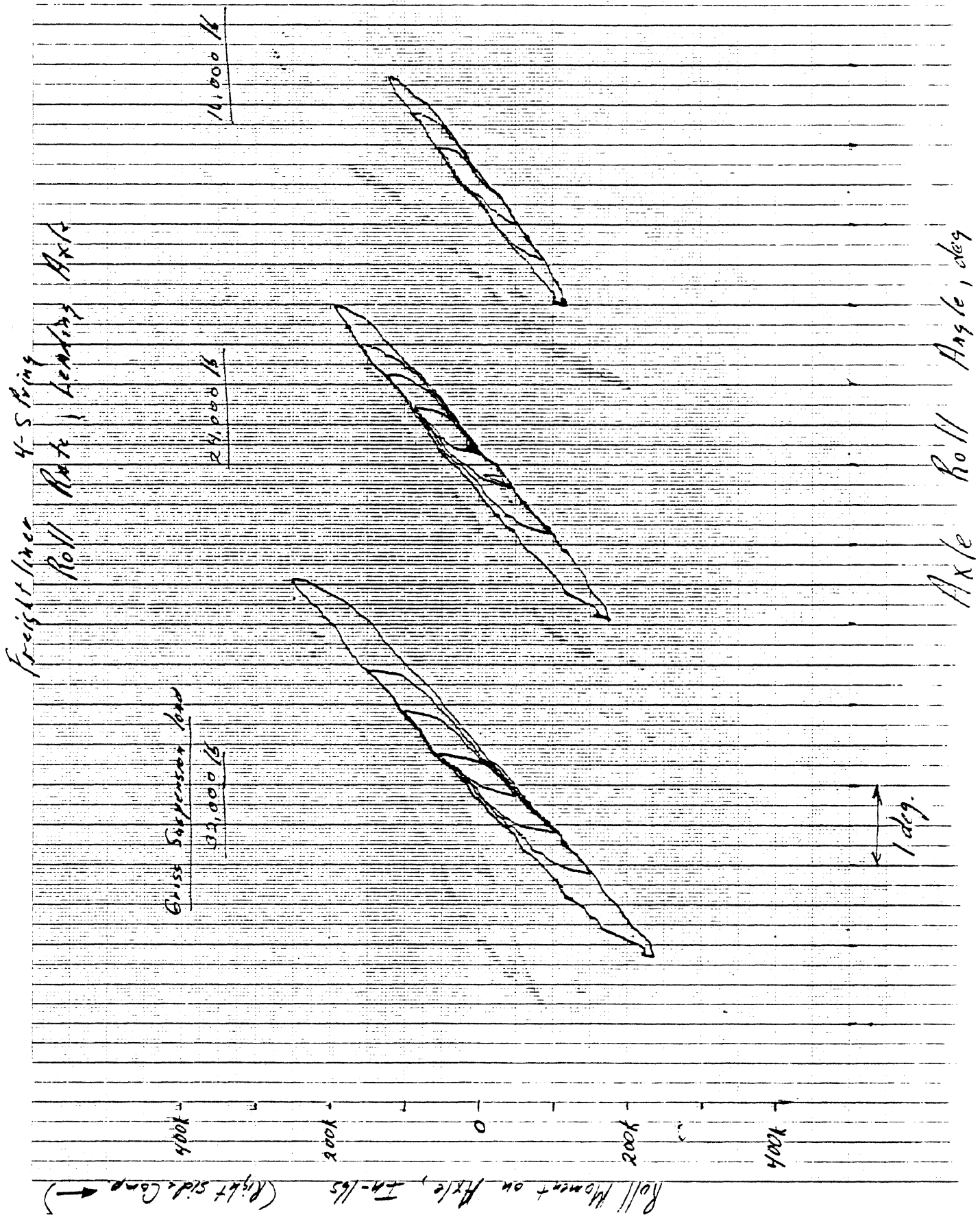
4000
2000
0
2000
4000



1 Deg

Axle Roll Angle, deg.

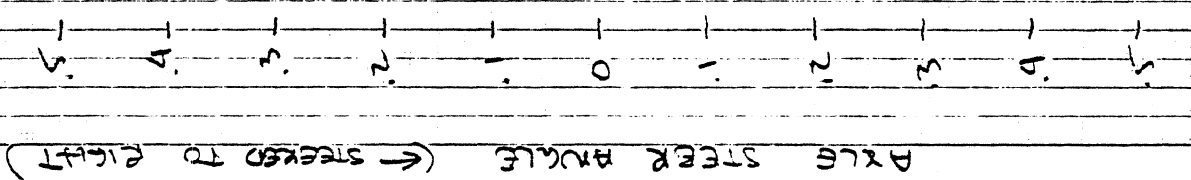
Pitch = 0



PITCH = 0

FREIGHTLINER - 4 SPRING

ROLL STEER - LEADING AXLE



Gross Suspension Load
33,000 lbs

34,000 lbs

16,000 lbs

AXLE ROLL ANGLE (DEG) (← RIGHT SIDE COMPRESSED)

1 DEG

FREIGHTLINER - 4 SPRING
 ROLL STEER - TRAILING AXLE

PITCH = 0

5
4
3
2
1
0
1
2
3
4
5

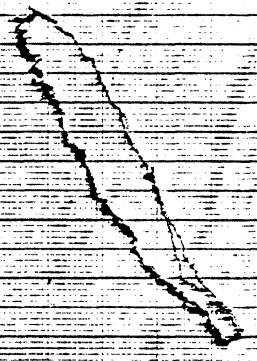
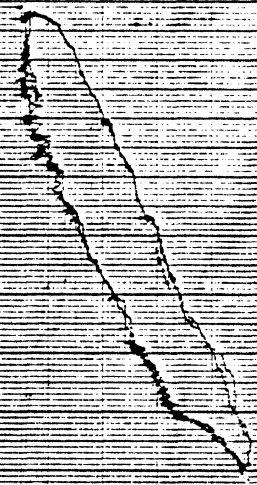
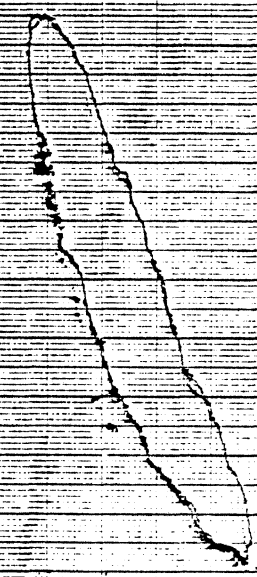
AXLE STEER ANGLE (DEG) (← STEER TO RIGHT)

Gross Suspension Load

52,000 LBS

24,000 LBS

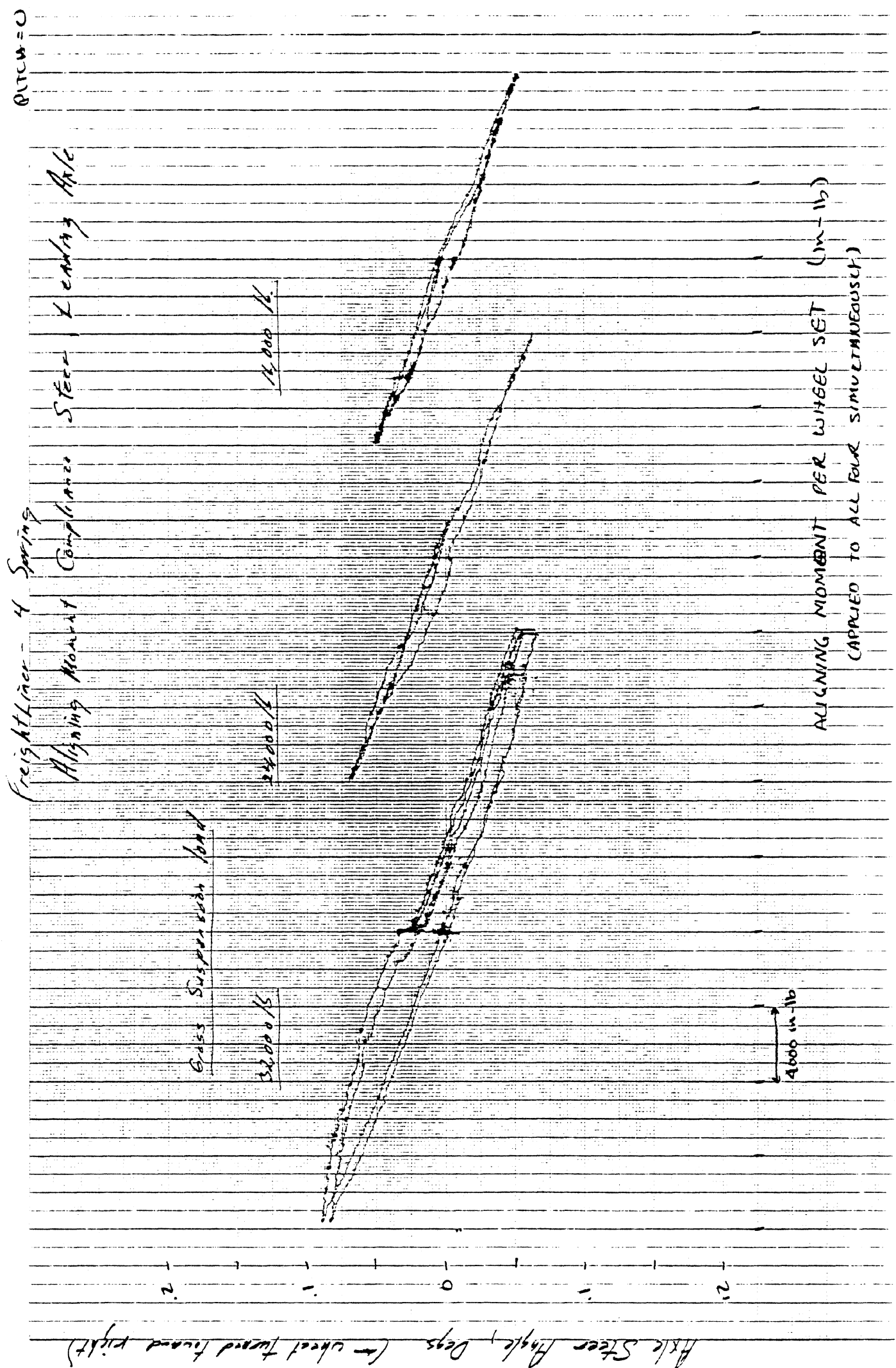
14,000 LBS



1 DEG

AXLE ROLL ANGLE (DEG)

(← RIGHT SIDE COMPRESSED)



PITCH = 0

FREIGHTLINER - 4 SPRING

ALIGNING MOMENT COMPLIANCE STEER

TRAILING ~~TRAILING~~ AXLE

Gross Suspension Load

32,000 lbs.

27,000 lbs.

16,000 lbs.

AXLE STEER ANGLE (DEG) (← STEER TO RIGHT)

2
1
0
1
2

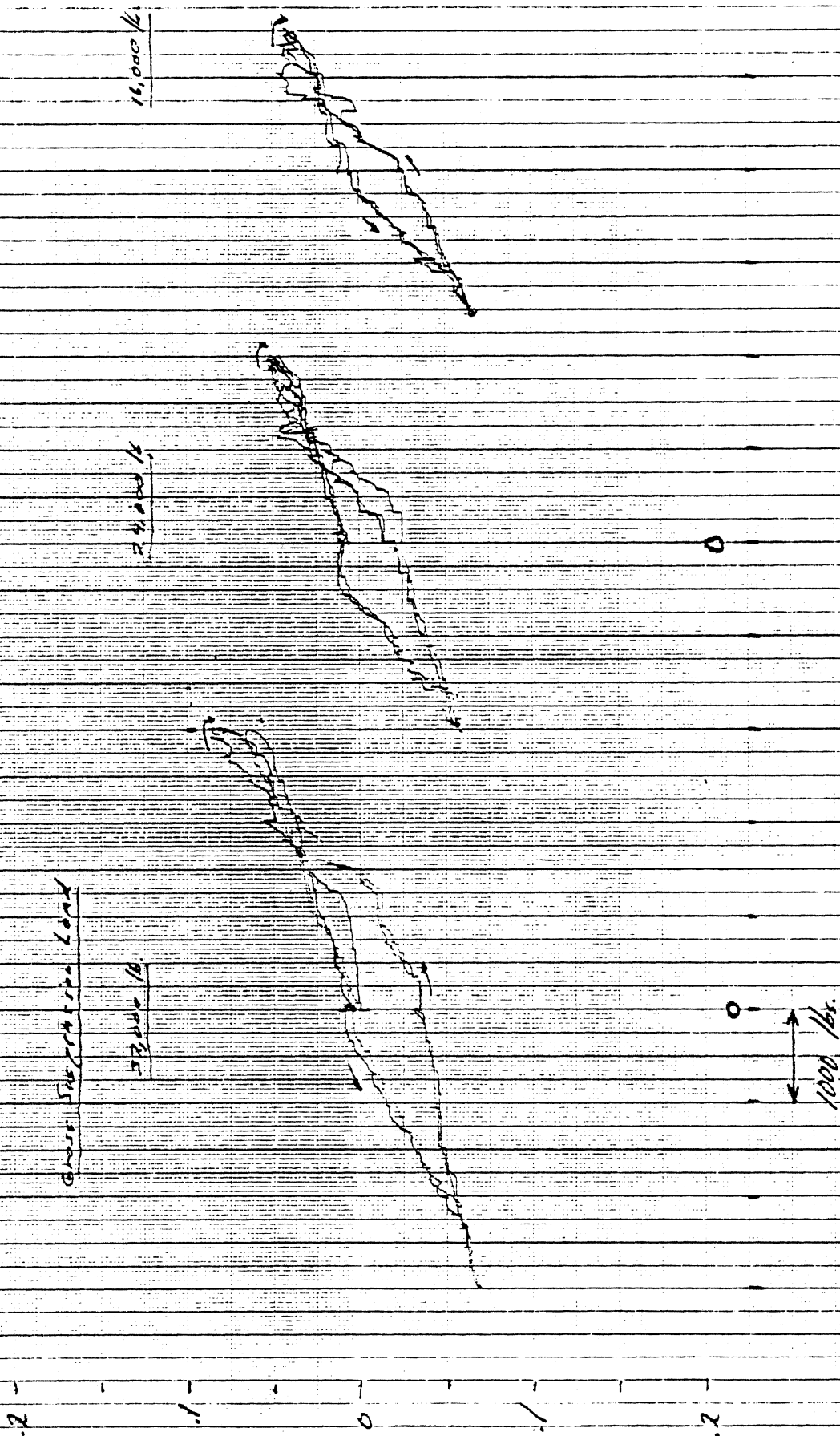


ALIGNING MOMENT PER WHEEL SET
(APPLIED TO ALL FOUR SIMULTANEOUSLY)

4000 in/lb

Pitch=0

Freight liner, H-Spring
Lateral Force Compliance Steer-
Leading Axle



Lateral Force per Wheel Set, pounds (Force applied toward right →)
(Applied to all four simulaneously)

Angle Steer Angle, deg. (Steer toward right →)

Pitch=0

Freight car - 4 Spring
Lateral Force Compliance Steer
Trailing Axle

53000
Great Suspension Load

53000 lb

110000 lb

Axle Steer Angle, deg (Steer toward right →)

2 - 1 - 0 - 1 - 2



1000 lb

Lateral Force Per Wheel Set, pounds (Force applied toward right →)
(Applied to all four simultaneously)

17th-0

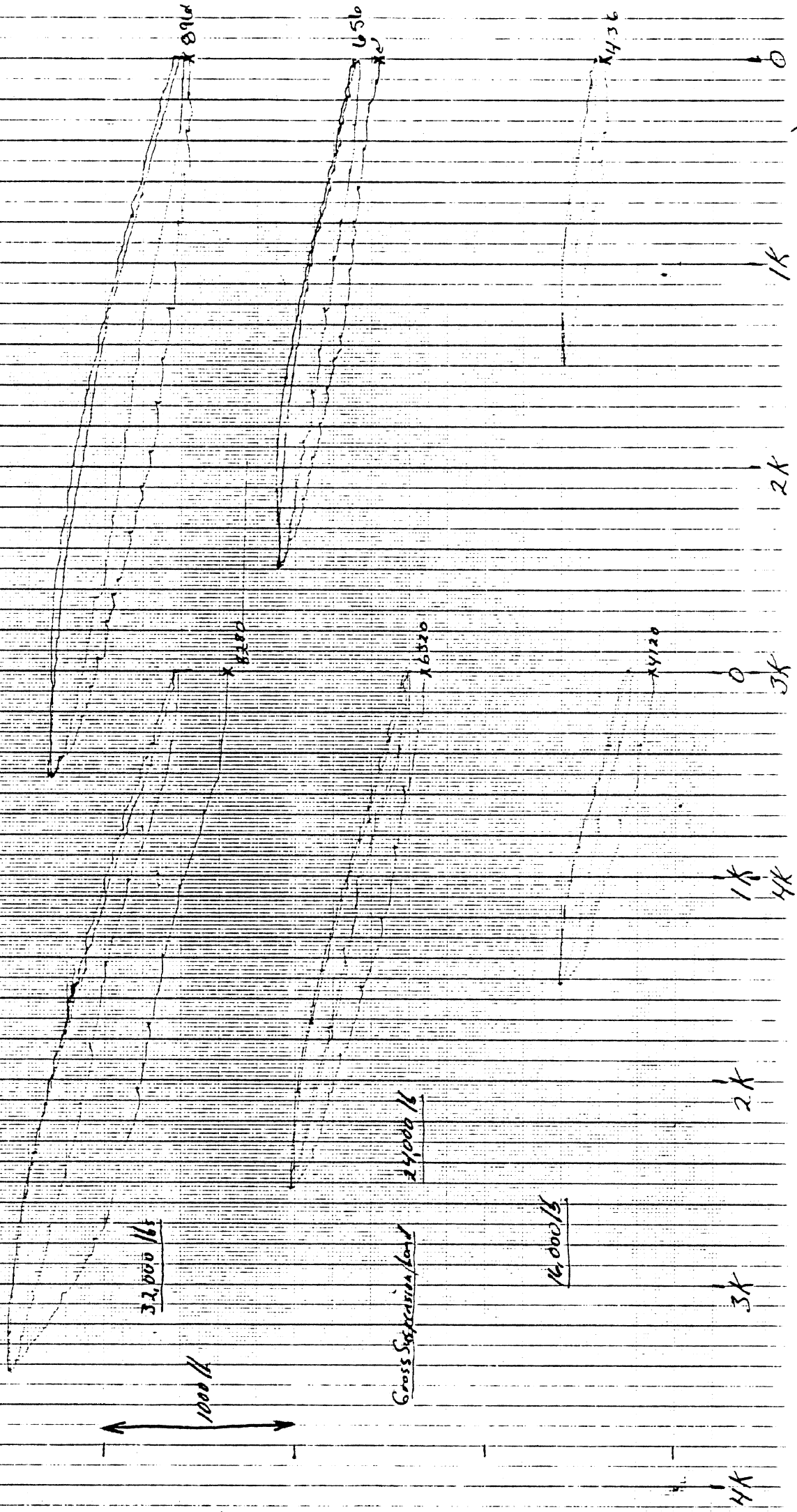
Freightliner - 4 Springs

In turntable load transfer due to Brake Force

Left Side

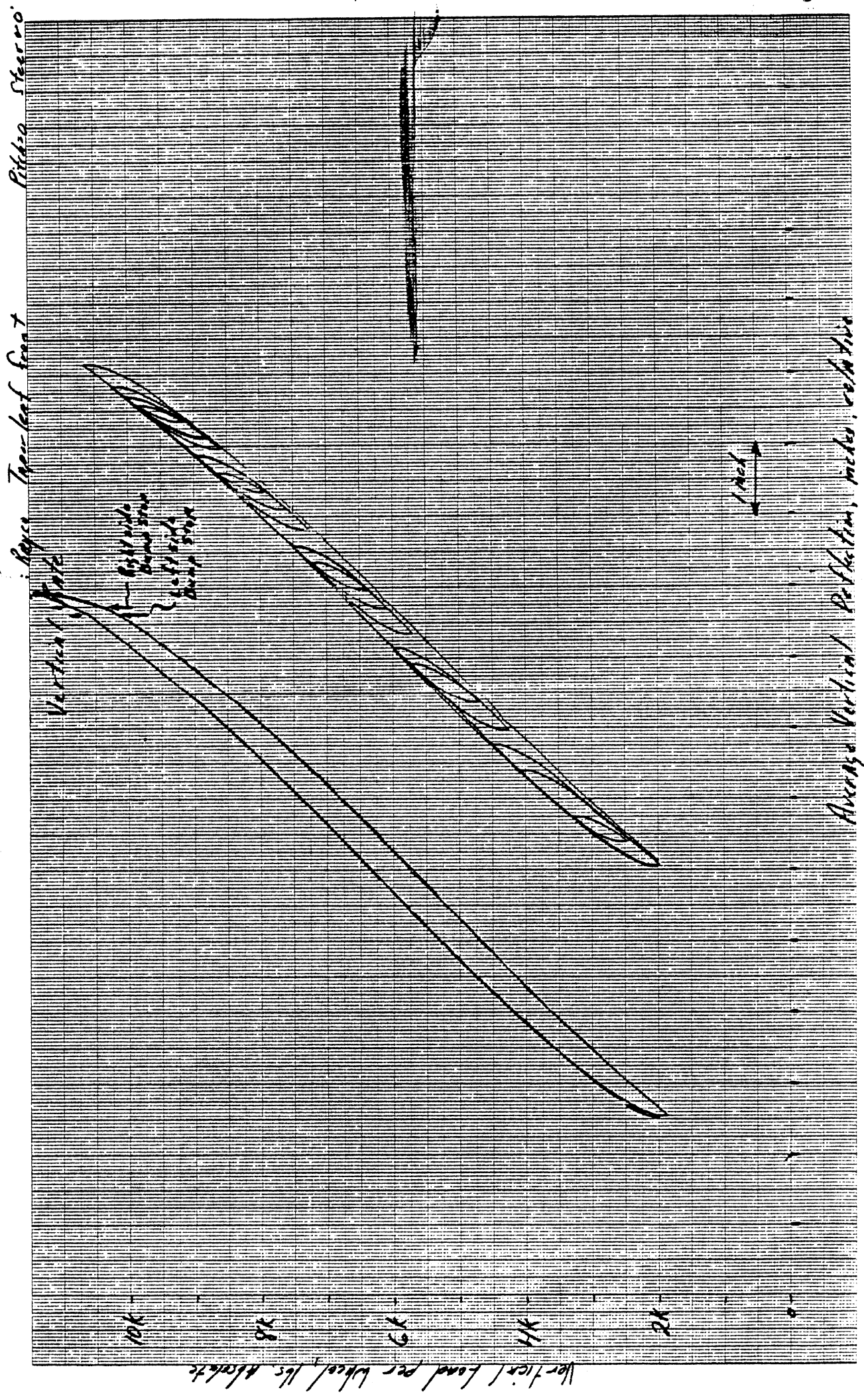
Right Side

Load transfer from leading to trailing wheel



Brake force per wheel set, pounds. (Applied to all four simultaneous ly.)

Front Suspension, Ford CL-9000 Tractor



Vertical load per wheel, lbs. Absolute

Average Vertical Deflection, inches, calculated

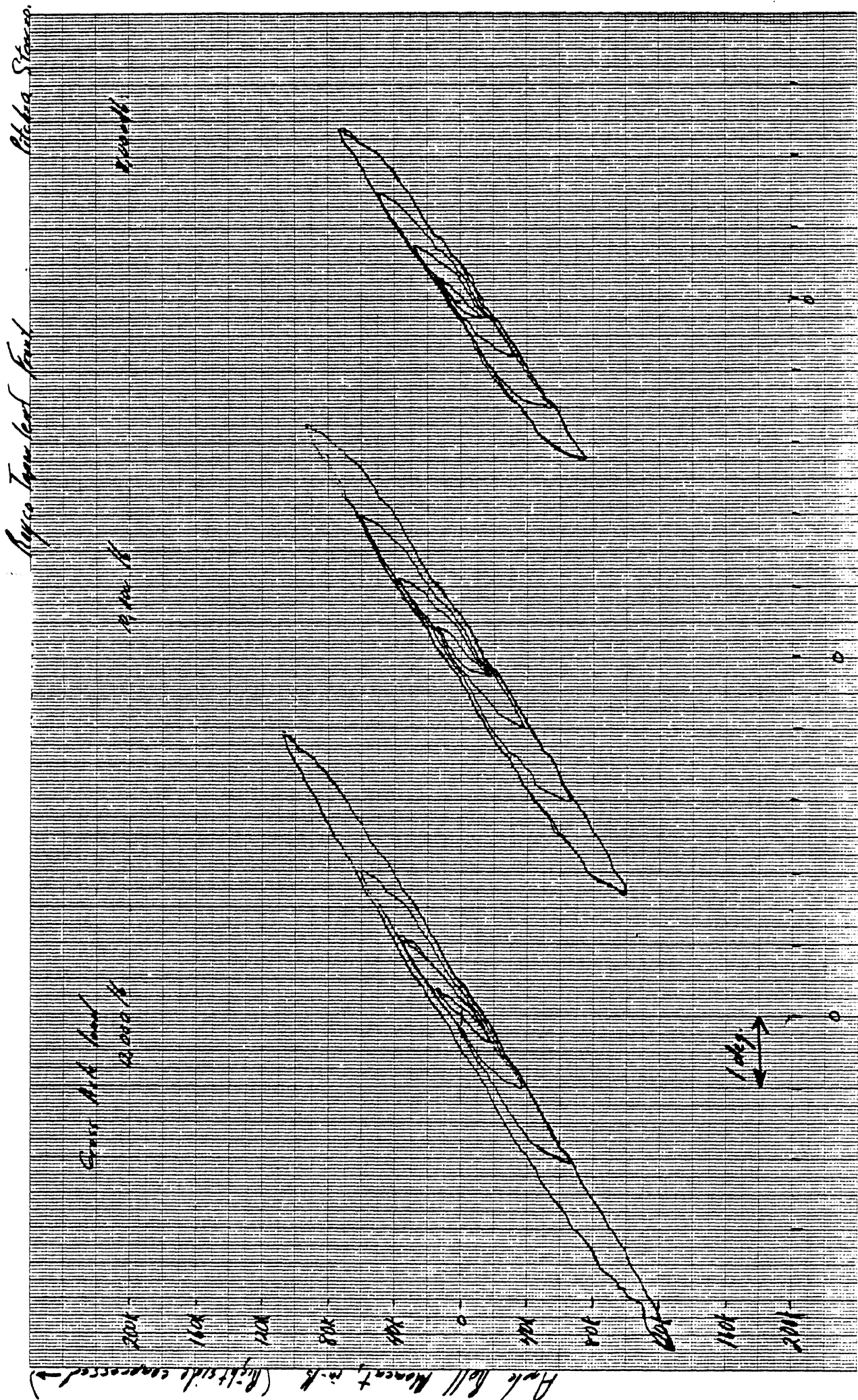
1 inch

Pitman Steerrod

Roll side down

Vertical Force

Roll side up



Alpha Station

Alpha Truss load front

Alpha Station

Case A
20000 lb

Case B

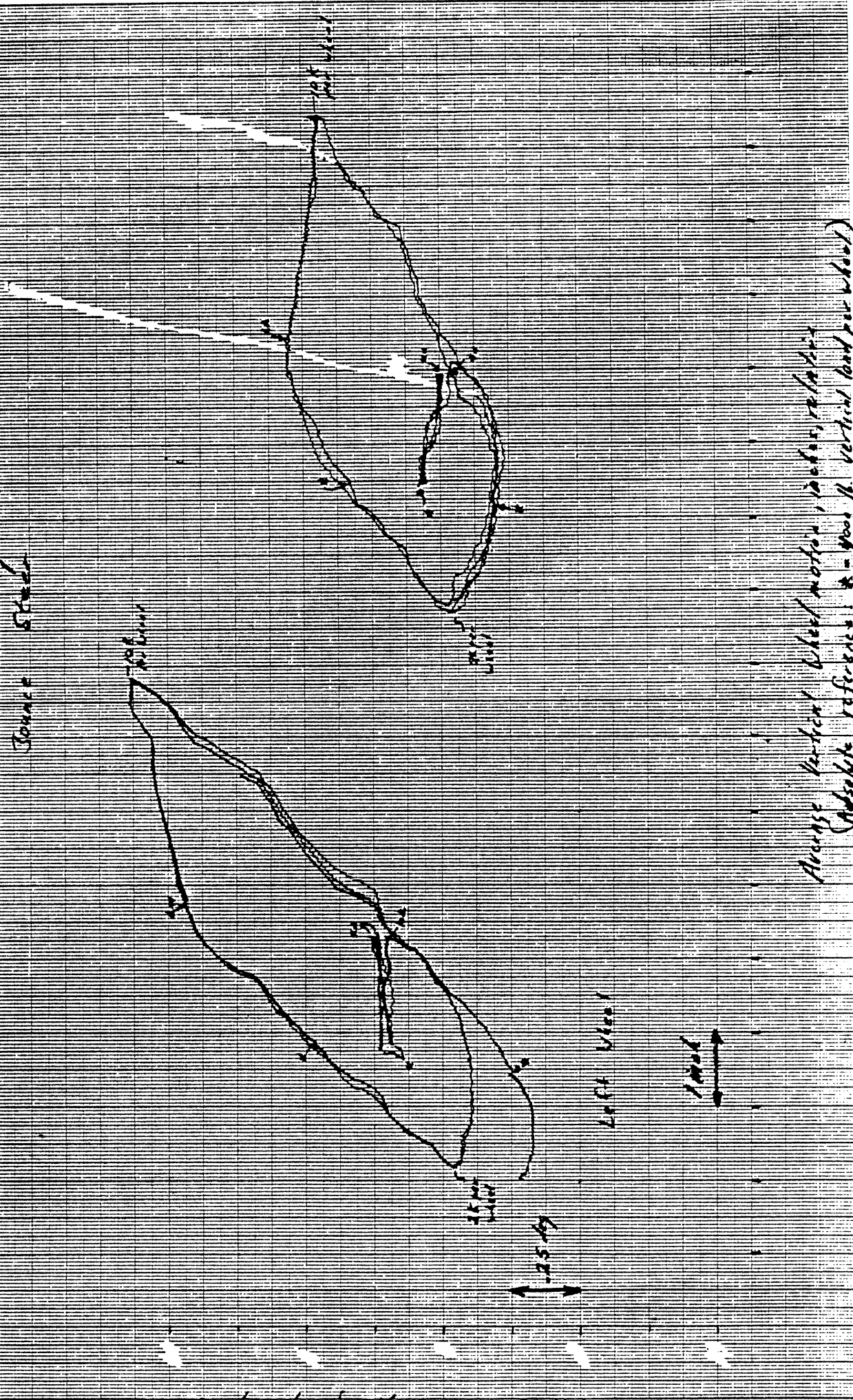
Case C

Axle Roll Moment, m-k (Right side compressed)

Axle Roll Angle, deg.

Philo Street

Upper Town Hall Street



Wheel Steer Angle, depress, relative

Average Vertical Wheel motion, inches, relative
 (Absolute reference: * = 4000 ft. vertical land per wheel)
 XY = 6000

Pitkin Steers

Large Top Leaf Bent

Heavy metal surface steel
Cross the top of the

Left Wheel

Left Wheel

Wheel Steer Angle, degrees (-Steer toward right)



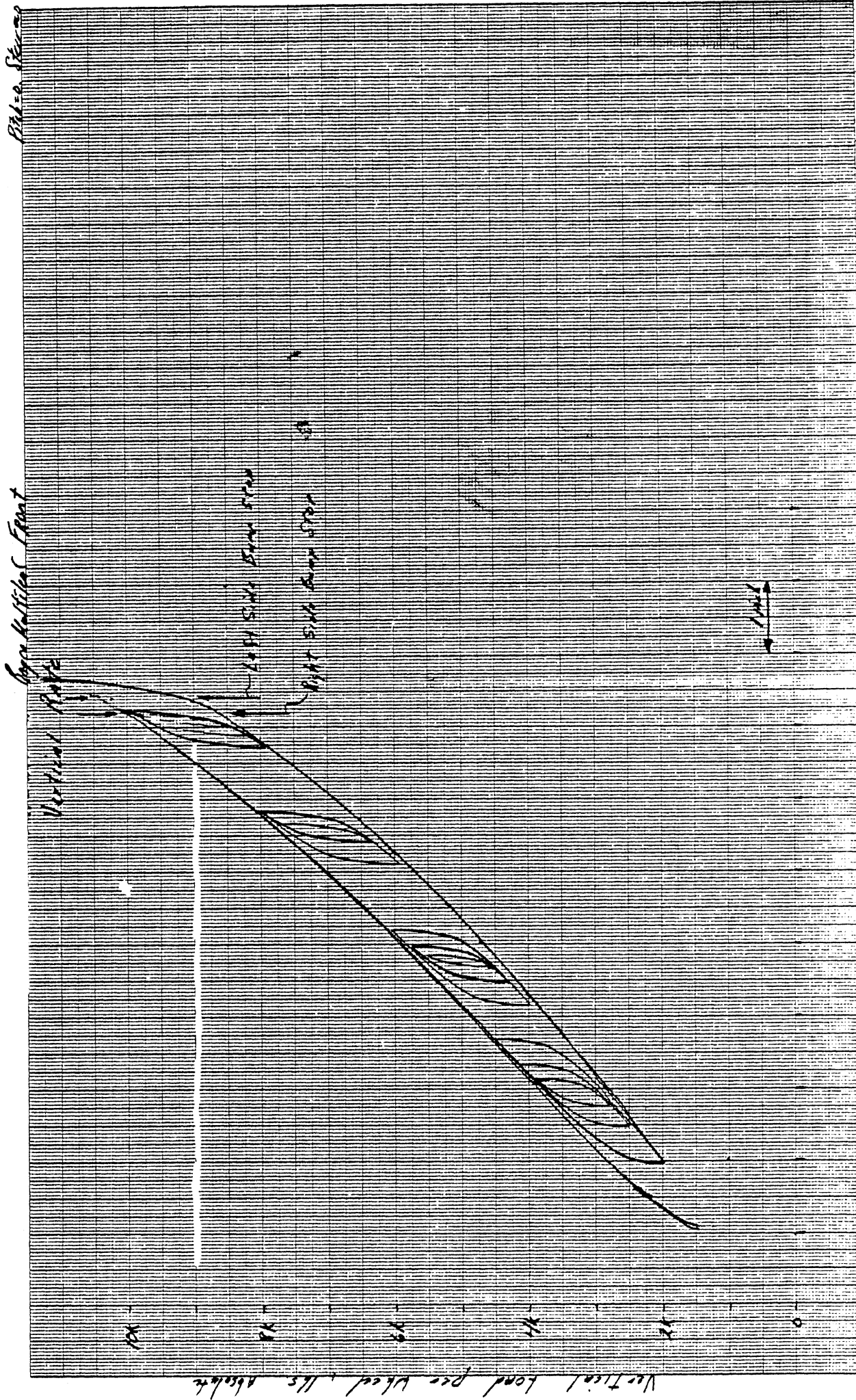
Aligning moment applied per wheel, in lb
Applied to two wheel screw threads

Pitch Steer

Large Multilobed Front



Angle Roll Anst, degrees



A. 2. 2. 2. Vertical deflection, inches, relative

St. Louis

Upper Multilobed Flood

Full Lake

8000 ft

10000 ft

Lower Multilobed Flood

10000 ft

10000 ft

10000 ft

10000 ft

10000 ft

10000 ft

10000 ft

10000 ft

10000 ft

10000 ft

10000 ft

10000 ft

10000 ft

10000 ft

10000 ft

10000 ft

10000 ft

10000 ft

10000 ft

10000 ft

10000 ft

10000 ft

10000 ft

10000 ft

Arctic Roll Moment, cm-165 (Right side compressed)

Arctic Roll Angle, deg

10000

